

**EFFECTS OF CHEMICAL MODIFICATIONS OF
PINEAPPLE LEAF FIBER ON THERMAL
AND MECHANICAL PROPERTIES OF
STYRENIC BASED THERMOPLASTIC
ELASTOMER COMPOSITES**

DARAWAN YUAKKUL

**A thesis submitted in partial fulfillment of the requirements for
the Master of Science degree in Chemistry**

Maharakham University

January 2016

All rights reserved by Maharakham University



**EFFECTS OF CHEMICAL MODIFICATIONS OF
PINEAPPLE LEAF FIBER ON THERMAL
AND MECHANICAL PROPERTIES OF
STYRENIC BASED THERMOPLASTIC
ELASTOMER COMPOSITES**

DARAWAN YUAKKUL

**A thesis submitted in partial fulfillment of the requirements for
the Master of Science degree in Chemistry
Maharakham University
January 2016
All rights reserved by Maharakham University**





The examining committee has unanimously approved this thesis, submitted by Miss Darawan Yuakkul, as a partial fulfillment of the requirements for the Master of Science degree in Chemistry at Mahasarakham University.

Examining Committee

..... *Onanong Cheerarot* Chairman
(Onanong Cheerarot, Ph.D.) (Faculty graduate committee)

..... *S. Saikrasun* Committee
(Assoc. Prof. Sunan Saikrasun, Ph.D.) (Advisor)

..... *T. Amornsakchai* Committee
(Assoc. Prof. Taweechai Amornsakchai, Ph.D.) (Co-advisor)

..... *Yottha Srithep* Committee
(Asst. Prof. Yottha Srithep, Ph.D.) (Faculty graduate committee)

..... *Sayant Saengsuwan* Committee
(Assoc. Prof. Sayant Saengsuwan, Ph.D.) (External expert)

Mahasarakham University has granted approval to accept this thesis as a partial fulfillment of the requirements for the Master of Science degree in Chemistry

..... *Wichian Magtoon*

(Prof. Wichian Magtoon, Ph.D.)
Dean of the Faculty of Science
Mahasarakham University

..... *Pradit Terdtoon*

(Prof. Pradit Terdtoon, Ph.D.)
Dean of Graduate School
TAMUAM 29, 2016



ACKNOWLEDGEMENTS

The author would like to gratefully acknowledge the Center of Excellence for Innovation in Chemistry (PERCH-CIC) and the grant for graduate students, fiscal year 2015, for partial financial support. I am grateful to the Department of Chemistry, Faculty of Science, Mahasarakham University, for providing chemicals, instrumental support and all other facilities.

I would like to express my sincere gratitude and great appreciation to my advisor, Assoc. Prof. Dr. Sunan Saikrasun for his kind supervision, valuable guidance, teaching encouragement, advice, taking care and helpful discussion throughout this research. Sincere gratefulness is also extended to my co-advisor, Assoc. Prof. Dr. Taweechai Amornsakchai for helpful suggestions and comments for completion of this thesis.

The thesis would not have been accomplished if without the help from several people. First of all, I would like to thank Assoc. Prof. Dr. Sayant Saengsuwan, Asst. Prof. Dr. Piyanete Chantiratikul, Dr. Onanong Cheerarot, Dr. Supalak Attharangsana and Asst. Prof. Dr. Yottha Srithep for their valuable suggestions and comments.

I wish to express my sincere appreciation to Miss I-lada Khotpun, Miss Asama Kalapakdee and all of my friends for their excellent assistance, encouragement, sincerity and impression friendship. Everything will always be in my mind.

Finally, I would like to express my sincere gratitude and appreciation to my parents and my family for their encouragement, infinite love and understanding which will be everlasting existed in my mind with greatness and with high regards.

Darawan Yuakkul



TITLE Effects of Chemical Modifications of Pineapple Leaf Fiber on Thermal and Mechanical Properties of Styrenic Based Thermoplastic Elastomer Composites

AUTHER Miss Darawan Yuakkul

DEGREE Master Degree of Science **MAJOR** Chemistry

ADVISORS Assoc. Prof. Sunan Saikrasun, Ph.D.

UNIVERSITY Maharakham University **YEAR** 2016

ABSTRACT

In this work, pineapple leaf fibers (PALFs) were chemically treated by alkaline solution and a silane coupling agent (triethoxy vinyl silane). The elastomeric composite based on styrene-(ethylene butylene)-styrene (SEBS) triblock copolymer and PALFs with and without the presence of maleic anhydride grafted SEBS (SEBS-g-MA) were prepared using melt mixing in an internal mixer, melt blending on a two-roll mill and compression molding. Thermal decomposition, tensile and dynamic mechanical properties of the neat matrix and its composites were evaluated. Among the treated and untreated fibers, the alkali-treated fiber exhibited the highest thermal stability in air. For the composites, the highest thermal stability was observed for the composite containing alkali-treated fibers. The enhancement in mechanical performance of the elastomer matrix was achieved by PALF loadings. The further improvement in tensile stress, over those of SEBS matrix and untreated-fiber composite, was observed for composites containing alkali- and silane-treated fibers. Interestingly, the use of the treated fibers along with SEBS-g-MA compatibilizer remarkably improved the reinforcing performance of the composites as revealed by very high maximum stress ratio (up to \approx 3.25-3.30). The compatibilized composite of alkali-treated fiber showed better reinforcing performance than that of the silane-treated fiber. The dynamic mechanical results related well with the tensile data. The obtained results indicated that both fiber treatments and compatibilizing promotion are mainly necessary factors for elevation of the material reinforcing performance.

Key Words: pineapple leaf fiber; natural fiber; thermoplastic elastomer



ชื่อเรื่อง	ผลของการตัดแปรงเชิงเคมีของเส้นใยจากไบโอสปประรดที่มีต่อสมบัติเชิงความร้อนและสมบัติเชิงกลของวัสดุเชิงประกอบเทอร์มอพลาสติกแบบหยุ่น ประเภทสไตรีนิก		
ผู้วิจัย	นางสาวดารารวรรณ หยวกกุล		
ปริญญา	วิทยาศาสตรมหาบัณฑิต	สาขาวิชา	เคมี
กรรมการควบคุม	รองศาสตราจารย์ ดร.สุนันท์ สายกระสุน		
มหาวิทยาลัย	มหาวิทยาลัยมหาสารคาม	ปีที่พิมพ์	2559

บทคัดย่อ

ในงานวิจัยนี้ได้ทำการแปรงผิวเส้นใยจากไบโอสปประรด (PALFs) ด้วยวิธีอัลคาไลและสารคัพปลิงไซเลน (triethoxy vinyl silane) และนำเส้นใยไปใช้เสริมแรงในวัสดุเชิงประกอบแบบหยุ่น สไตรีน-เอทิลีน บิวทิลีน-สไตรีน (SEBS) ที่เติมและไม่เติมสารเสริมสภาพเข้ากันได้ SEBS-g-MA ทำการเตรียมวัสดุเชิงประกอบ โดยผสมในเครื่อง internal mixer, two-roll mill และ compression molding จากนั้นนำไปวิเคราะห์การแตกสลายทางความร้อน สมบัติการทนต่อแรงดึงและสมบัติเชิงกลพลวัตของเมทริกซ์และวัสดุเชิงประกอบ สำหรับเส้นใย พบว่า การปรับสภาพผิวเส้นใยด้วยวิธีอัลคาไลทำให้เส้นใยมีเสถียรภาพทางความร้อนในบรรยากาศที่เป็นอากาศสูงที่สุด ในกรณีของวัสดุเชิงประกอบ พบว่า วัสดุเชิงประกอบที่เติมเส้นใยที่แปรงผิวด้วยวิธีอัลคาไลมีเสถียรภาพทางความร้อนสูงที่สุดและการเติมเส้นใยช่วยเพิ่มสมรรถนะเชิงกลของวัสดุ นอกจากนี้ วัสดุเชิงประกอบที่เติมเส้นใยที่แปรงผิวด้วยวิธีอัลคาไลและสารคัพปลิงไซเลนยังช่วยทำให้ค่าการความทนต่อแรงดึงสูงกว่า SEBS และวัสดุเชิงประกอบที่มีเส้นใยที่ไม่ผ่านการแปรงผิวเส้นใยที่น่าสนใจคือ การใช้เส้นใยที่ผ่านการแปรงผิวและใช้สารเสริมสภาพเข้ากันได้ SEBS-g-MA จะช่วยเพิ่มประสิทธิภาพการเสริมแรงของวัสดุเชิงประกอบ ซึ่งพบว่า อัตราส่วนความเค้นสูงสุดสูงขึ้น (ประมาณ 3.25-3.30 เท่า) และการเติมสารเสริมสภาพเข้ากันได้วัสดุเชิงประกอบที่มีเส้นใยที่แปรงผิวด้วยวิธีอัลคาไลให้ประสิทธิภาพการเสริมแรงดีกว่าเส้นใยที่แปรงผิวด้วยสารคัพปลิงไซเลน ส่วนผลของสมบัติเชิงกลพลวัตที่ได้มีความสอดคล้องกันกับข้อมูลสมบัติการทนต่อแรงดึง จากผลที่ได้ชี้ให้เห็นว่า การแปรงผิวเส้นใยและการเติมสารเสริมสภาพเข้ากันได้เป็นปัจจัยหลักที่จำเป็นในการช่วยเพิ่มสมรรถนะการเสริมแรงวัสดุ

คำสำคัญ: เส้นใยจากไบโอสปประรด; เส้นใยธรรมชาติ; เทอร์มอพลาสติกแบบหยุ่น



CONTENTS

	PAGE
ACKNOWLEDGEMENTS	i
ABSTRACT (in English)	ii
ABSTRACT (in Thai)	iii
CONTENTS	iv
LIST OF TABLES	viii
LIST OF FIGURES	x
LIST OF ABBREVIATIONS	xiv
CHAPTER 1 INTRODUCTION	
1.1 Background and rational	1
1.2 Research objectives	4
1.3 The scope of research	4
1.4 Expected result obtained from the research	5
1.5 Research place	5
CHAPTER 2 LITERATURE REVIEW	
2.1 Thermoplastic elastomers	6
2.2 Poly[styrene- <i>b</i> -(ethylene- <i>co</i> -butylene)- <i>b</i> -styrene] triblock copolymer (SEBS)	7
2.3 Polymer composites	8
2.3.1 Natural fiber reinforced composites	9
2.3.2 Factors affecting the composite properties	10
2.3.2.1 Plant fiber structure	10
2.3.2.2 Thermal stability of fibers	11
2.3.2.3 Fiber length, loading and orientation	11
2.3.2.4 Presence of voids	11
2.3.2.5 Moisture absorption of fibers	12
2.4 Natural fibers	12
2.4.1 Fiber types	12
2.4.2 Structure and chemical composition	13



CONTENTS (CONT.)

	PAGE
2.4.3 Properties	17
2.4.4 Advantages and limitations of natural fibers	18
2.5 Chemical modification of natural fibers	19
2.5.1 Alkali Treatment	20
2.5.2 Silane Treatment	22
2.6 Pineapple leaf fibers (PALFs)	24
2.6.1 Applications PALFs	27
2.6.2 PALF reinforced polymer composites	27
2.6.2.1 PALF-reinforced Thermoplastics composites	27
2.6.2.2 Hybrid PALF-Reinforced Composites	28
2.6.2.3 PALF-reinforced Rubber and Thermoplastic elastomer composites.....	29
 CHAPTER 3 MATERIALS AND METHODS	
3.1 Materials	30
3.1.1 Dispersed phases	30
3.1.2 Matrix phase	30
3.1.3 Compatibilizer	30
3.1.4 Chemicals	31
3.2 Alkali, Silane and Alkali-Silane treatments	32
3.3 Preparation of elastomer composites	32
3.4 Characterization techniques	34
3.4.1 Fourier Transform Infrared spectroscopy	34
3.4.2 Morphological characterization	34
3.4.3 Thermal decomposition analysis	34
3.4.4 Tensile testing	34
3.4.5 Dynamic mechanical analysis	36
 CHAPTER 4 RESULTS AND DISCUSSION	
4.1 FTIR characterization of fiber surfaces	38



CONTENTS (CONT.)

	PAGE
4.2 Thermal decomposition behavior of the pineapple leaf fiber and composites	40
4.2.1 Effect of fiber treatments on thermal decomposition	40
4.2.2 Effect fiber loadings on thermal decomposition	42
4.2.3 Effect of compatibilizer loading on thermal decomposition for silane treated fiber systems	44
4.2.4 Effect of fiber treatments on thermal decomposition of compatibilized composites	46
4.3 Tensile properties	49
4.3.1 Effect of fiber loadings on tensile properties	49
4.3.2 Effect of fiber treatments on tensile properties of composites	52
4.3.3 Effect of compatibilizer contents on tensile properties of untreated and treated fiber composites systems	55
4.3.4 Effect of compatibilizer loading on tensile properties of untreated- and treated-fiber composites	59
4.3.5 Comparison of different fiber treatment on tensile properties of the compatibilized composites	63
4.3.6 Comparison of stress ratios of the composites.....	65
4.4 Dynamic mechanical properties	68
4.4.1 Effect of fiber loadings on dynamic mechanical properties	68
4.4.2 Effect of fiber treatments on dynamic mechanical properties	71
4.4.3 Effect of fiber treatment and compatibilizer loadings on dynamic mechanical properties	73
4.4.4 Comparison of dynamic mechanical properties for the compatibilized treated-fiber composites	74
4.5 Morphology of composites	76
4.5.1 SEM images of untreated- and treated- PALFs	76
4.5.2 SEM images of the pre-tensile test composites	77



CONTENTS (CONT.)

	PAGE
4.5.3 Pre-tensile test SEM images of fracture surfaces parallel and perpendicular to the fiber direction for PALF/SEBS composites	78
4.5.4 Post-tensile test SEM images of fracture surfaces perpendicular to the fiber direction for PALF/SEBS composites	81
4.5.5 SEM images of pineapple fibers after extraction of the matrix	84
CHAPTER 5 CONCLUSIONS	87
REFERENCES	88
APPENDICES	101
BIOGRAPHY	109



LIST OF TABLES

	PAGE
Table 2.1 Structural compositions of natural fibers	15
Table 2.2 Comparative properties of natural fiber and conventional synthetic fibers	18
Table 2.3 Advantages and limitations of natural fibers	19
Table 2.4 Composition of ground pineapple leaf.	26
Table 3.1 Physical and chemical properties of SEBS (KRATON [®] G1650 Polymer)	31
Table 3.2 Formulations of the composites	33
Table 4.1 Assignments of FTIR bands for untreated-, alkali treated-, silane treated- and alkali-silane treated pineapple leaf fibers	39
Table 4.2 Thermo-oxidative data for the first major weight-loss step of the untreated and treated fibers obtained from non-isothermal TG measurements	42
Table 4.3 Thermo-oxidative data for the first weight-loss step of neat SEBS, PF10 and PF20 obtained from non-isothermal TG measurements	44
Table 4.4 Thermo-oxidative data for the first weight-loss step of SPF10-MA3, SPF10-MA5 and SPF10-MA7 obtained from non-isothermal TG measurements	46
Table 4.5 Thermo-oxidative data for the first major weight-loss step of SEBS, PF10, PF10-MA5, APF10-MA5, SPF10-MA5 and ASPF10-MA5 obtained from non-isothermal TG measurements	48
Table 4.6 Tensile properties of SEBS, PF10 and PF20 in LD and TD	51
Table 4.7 Tensile properties of treated PALF composites in comparison with SEBS and PF10 in LD and TD	54
Table 4.8 Tensile properties of 10 wt% treated PALF with and without compatibilizer composites in comparison with SEBS and untreated fiber system in longitudinal direction	58
Table 4.9 Tensile properties of treated fiber with 5 wt% compatibilizer composites in comparison with SEBS and untreated fiber system....	62



LIST OF TABLES (CONT.)

	PAGE
Table 4.10 Values of stress ratio of untreated- and treated-fiber composites in longitudinal direction	67
Table 4.11 Values of E' at 25°C and 125°C and T_g for the neat SEBS and its composites	70



LIST OF FIGURES

	PAGE
Figure 2.1 Chemical structure of SEBS	7
Figure 2.2 Principle composition of composite materials	8
Figure 2.3 Classifications of natural fibers	13
Figure 2.4 Chemical structure of (a) cellulose (b) lignin and (c) hemicelluloses	16
Figure 2.5 Structure of natural fiber	16
Figure 2.6 Structural organization of the three major constituents in the fiber cell wall	17
Figure 2.7 Typical structure of (a) untreated and (b) alkali treated cellulose fiber ...	21
Figure 2.8 Interaction of silane with natural fibers by hydrolysis process	23
Figure 2.9 Pineapple plant (a) and pineapple leaf fibers (b).....	25
Figure 3.1 Flow charts of the whole experiments.....	37
Figure 4.1 Normalized ATR-FTIR spectra of untreated (PF), alkali treated (APF), silane treated (SPF) and alkali-silane treated (ASPF) PALFs	39
Figure 4.2 Non-isothermal TG (a), DTG (b) and heat flow (c) curves of untreated and treated fibers under heating rate of 10°C/min in air ...	41
Figure 4.3 Non-isothermal TG (a), DTG (b) and heat flow (c) curves of neat SEBS and its composites containing of 10 and 20 wt% untreated PALF under heating rate of 10°C/min in air	43
Figure 4.4 Non-isothermal TG (a), DTG (b) and heat flow (c) curves of SPF10- MA3, SPF10-MA5 and SPF10-MA7 under heating rate of 10°C/min in air	45
Figure 4.5 Non-isothermal TG (a), DTG (b) and heat flow (c) curves of neat SEBS, PF10, PF10-MA5, APF10-MA5, SPF10-MA5 and ASPF10- MA5 under heating rate of 10°C/min in air	47
Figure 4.6 Stress-strain curves of neat SEBS, PF10 and PF20 in longitudinal (a) and transverse (b) direction	50
Figure 4.7 Effect of fiber loadings on secant modulus at 1% strain for the untreated fiber composites in LD and TD	51



LIST OF FIGURES (CONT.)

	PAGE
Figure 4.8 Stress-strain curves of neat SEBS, PF10, APF10, SPF10 and ASPF10 in longitudinal (a) and transverse (b) direction	53
Figure 4.9 Secant modulus at 1% strain of neat SEBS, PF10, APF10, SPF10 and ASPF10 in longitudinal and transverse direction.....	54
Figure 4.10 Effect of compatibilizer contents on stress-strain curves of (a) untreated-, (b) alkali- and (c) silane- treated fiber composite systems in longitudinal direction	56
Figure 4.11 Effect of compatibilizer contents on secant modulus at 1% strain of (a) untreated-, (b) alkali- and (c) silane- treated fiber composite systems in longitudinal direction	57
Figure 4.12 Effect of compatibilizer loading on stress-strain curves in longitudinal (I) and transverse (II) direction of the alkali-treated (a), silane-treated (b) and alkali-silane- treated (c) fiber composites systems	60
Figure 4.13 Effect of compatibilizer loading on secant modulus at 1% strain in longitudinal (LD) and transverse (TD) direction of the alkali-treated (a), silane-treated (b) and alkali-silane- treated (c) fiber composites systems	61
Figure 4.14 Comparison of stress-strain curves for neat SEBS, APF10-MA5, SPF10-MA5 and ASPF10-MA5 in longitudinal (I) and transverse (II) direction	64
Figure 4.15 Comparison of secant modulus at 1% strain for neat SEBS, APF10-MA5, SPF10-MA5 and ASPF10-MA5 in longitudinal (LD) and transverse (TD) direction	64
Figure 4.16 Longitudinal stress ratio (stress of the composites divided by stress of SEBS) in the strain region of 0-500% for the alkali-treated (a), silane-treated (b) and alkali-silane- treated (c) fiber composites systems	66



LIST OF FIGURES (CONT.)

	PAGE
Figure 4.17 Dynamic storage moduli (E') (a) and $\text{Tan } \delta$ (b) as a function of temperature of neat SEBS, PF10 and PF20	69
Figure 4.18 Dynamic storage moduli (E') (a) and $\text{Tan } \delta$ (b) as a function of temperature of neat SEBS, PF10, APF10 and SPF10.....	72
Figure 4.19 Dynamic storage moduli (E') (a) and $\text{Tan } \delta$ (b) as a function of temperature for APF10, APF10-MA5, SPF10 and SPF10-MA5	74
Figure 4.20 Dynamic storage moduli (E') (a) and $\text{Tan } \delta$ (b) as a function of temperature of neat SEBS, PF10, PF10-MA5, APF10-MA5 and SPF10-MA5	75
Figure 4.21 SEM images of untreated fiber (a), alkali treated fiber (b), silane treated fiber (c) and alkali-silane treated fiber (d)	76
Figure 4.22 Pre-tensile test SEM images of fracture surface perpendicular to the fiber direction for (a) neat SEBS, (b) PF10 and (c) PF20.....	77
Figure 4.23 Pre-tensile test SEM images of fracture surface perpendicular (column I) and parallel (column II) to the fiber direction for untreated- and treated-fiber composites	79
Figure 4.24 Pre-tensile test SEM images of fracture surface perpendicular (column I) and parallel (column II) to the fiber direction for untreated- and treated-fiber composites with the presence of 5 wt% SEBS-g-MA	80
Figure 4.25 Post-tensile test SEM images of fracture surface perpendicular to the fiber direction for PF10, APF10 and SPF10 at magnifications of 400 \times (column I) and 2,000 \times (column II)	82
Figure 4.26 Post-tensile test SEM images of fracture surface perpendicular to the fiber direction for PF10-MA5, APF10-MA5 and SPF10-MA5 at magnifications of 400 \times (column I) and 2,000 \times (column II)	83
Figure 4.27 SEM images of pineapple fibers after extraction of the matrix	85



LIST OF FIGURES (CONT.)

	PAGE
Figure 4.28 Scheme of interfacial interactions between SEBS-g-MA and the fiber surface	86
Figure 4.29 Interfacial interactions between SEBS matrix and the fiber surface for the compatibilized silane treated fiber composites	86



LIST OF ABBREVIATIONS

<i>A</i>	Cross sectional area of the specimen
ATR-FTIR	Attenuated total reflectance Fourier transform infrared spectroscopy
CB	Carbon black
cc	Cubic centimeter
cps	Centipoise
DMA	Dynamic mechanical analysis
DTG	Derivative thermogravimetric analysis
<i>E</i>	Secant modulus at 1% strain
<i>E'</i>	Storage modulus
<i>E''</i>	Loss modulus
<i>F</i>	Stress at 1% strain
g	Gram
GPa	Giga pascal
h	Hour
LD	Longitudinal direction
mm	Millimeter
MPa	Mega pascal
NaOH	Sodium hydroxide
NFPCs	Natural fiber reinforced polymer composites
NFRC	Natural fiber reinforced composites
PALF	Pineapple leaf fiber
PE	Polyethylene
PC	Polycarbonate
PP	Polypropylene
psi	Pound per square inch
rpm	Round per minute
s	Second



LIST OF ABBREVIATIONS (CONT.)

SEBS	Poly[styrene- <i>b</i> -(ethylene- <i>co</i> -butylene)- <i>b</i> -styrene] triblock copolymers
SEBS-g-MA	Styrene-ethylene-butylene-styrene grafted with maleic anhydride
SEM	Scanning electron microscope
Tan δ	Loss tangent
TD	Transverse direction
TGA	Thermogravimetric analysis
TPEs	Thermoplastic elastomers
T_d	Peak temperature with the thermal degradation process
T_g	Glass transition temperature
T_m	Melting temperature
T_{max}	Temperature at the maximum weight-loss rate
T_{onset}	Onset degradation temperature
wt	Weight
ΔH_d	Thermal decomposition enthalpy
σ	Tensile strength
α	Conversion extent



CHAPTER 1

INTRODUCTION

1.1 Background and rational

An increase in the global population growth, corroborated with the average individual consumption increase results in very high global consumption levels of raw materials and finished products. Consequently, there is an increasing search for environmentally friendly materials [1]. Such trend and awareness to environmentally friendly behavior and increased demand have progressively driven the primary sector to seek substitutes for materials with polluting attributes [2]. Renewed interest in the utilization of natural materials addresses ecological issues such as recyclability and environmental safety. Currently, synthetic fibers like glass, carbon and aramid are widely being used in polymer-based composites because of their high stiffness and strength properties [3]. However, these fibers have serious drawbacks in terms of their biodegradability, initial processing costs, recyclability, energy consumption, machine abrasion, health hazards, etc. [4]. Thus, adverse environmental impacts alter the attention from synthetic fibers to natural/renewable fibers. The use of natural fibers from annually renewable resources is now popularly. (as reinforcements in polymer matrix.) This provides benefits to the environment with respect to the degradability and utilization of natural materials [3].

Natural fibers like flax, hemp, jute, sisal and pineapple have emerged as a reinforcement alternative in polymer matrices to obtain composites for a wide variety of applications. The advantageous features of these fibers are lightweight, high specific modulus, non-toxic and easy for processing and absorbing CO₂ during their growth [5,6]. However, the main limitations are high moisture absorption with decrease of mechanical properties, occasional poor compatibility with hydrophobic resins, low processing maximum working temperature and seasonality. Pineapple leaf fiber (PALF) is one of the attractive natural fiber due to its superior properties compared to other natural fibers. PALF have a high stiffness (young's modulus 34.5-82.5 GPa and tensile strength 413-1,627 MPa) due to their possess high cellulose content (70-82%) [7,8].



Furthermore, PALFs are smaller, lightweight and biodegradability. It also has the thermal properties and sound insulation as well. The researches on PALFs are successfully used in the reinforcement of polymer such as polyester [9], polyethylene [10], polypropylene [11], natural rubber [12] and bio-plastic [13]. George et al. [14] studied the stress relaxation behavior of PALF reinforced polyethylene composites. They found that the stress relaxation decreased with increasing fiber content due to better reinforcing effect. George *et al.* [14] also reported that properties of fiber reinforced composites depending on many factors like fiber-matrix adhesion, volume fraction of fiber, fiber aspect ratio, fiber orientation as well as stress transfer efficiency of the interface. However, use of PALF is still limitations, due to the polymer matrix are mostly hydrophobic whereas PALFs are hydrophilic. This results in the reduction of efficiency of stress transfer from the matrix to the fiber due to a weak interaction at the interface. Furthermore, PALFs can absorb moisture easily, especially at high temperatures. In order to enhance the effectiveness of interfacial bonding, fiber surface of PALFs needed to be modified with different chemical treatments, reactive additives and coupling agents. Chemical treatments such as the alkalization, acetylation, silanization, benzoylation, peroxide treatment, maleated coupling agents were widely used to modify the fiber surface [15,16]. Chemical modification provides the means of permanently altering the nature of fiber cell walls [17] by grafting polymers onto the fibers [18,19], crosslinking of the fiber cell walls [20], or by using coupling agents [21]. These modifying strategies have been generally reviewed recently [17,22]. The chemical modification may make the fiber cell walls more dimensionally stable, reduces water sorption and increases the interface adhesion between the fiber and matrix.

The alkali wash is one of the possible chemical treatments used to remove amorphous materials, pectin, waxes and other non cellulosic component from the fiber surface [23]. As a result, the fiber surface becomes clean. In other words, the fiber surface becomes more uniform due to the elimination of microvoids and thus the stress transfer capacity between the ultimate cells improves. In addition to this, it reduces fiber diameter and thereby increases the aspect ratio (length/diameter). This increases effective fiber surface area for good adhesion with the matrix [24].

Silanes are recognized as efficient coupling agents extensively used in composites and adhesive formulations [25]. They have been successfully applied in



inorganic filler reinforced polymer composites such as glass fiber reinforced polymer composites [26,27] and mineral filled polymer composites [28,29]. Silanes are also adhesion promoters in many adhesive formulations or are used as substrate primers, giving stronger adhesion [30]. The bifunctional structures of silanes have also been of interest in applying them for natural fiber/polymer composites, since both glass fibers and natural fibers bear reactive hydroxyl groups, and extensive researches have accordingly been carried out to screen the varied silane structures for natural fiber reinforced polymer composites (NFPCs) production.

Lu *et al.* [31] reported that during silane treatment, various type of reactions take place at the surface of the hemp fiber, such as hydrolysis, condensation, hydrogen bonding and covalent bond formation. Silanol molecules react with the hydroxyl group of the fiber resulting in formation of strong covalent bonds to the cell wall. Also the free silanols react with each other forming -Si-O-Si- bond. The vinyl group of the silane molecule couples with the thermoplastic matrix and increases the physical compatibility. Therefore, it could be the polymer matrix, the organo-functional group of the silane molecule (in this case, vinyl) couples with the matrix and increases the strength of bonding. The enhanced covalent bonding added with physical compatibility with the polymer matrix was found to increase the thermal stability of the resultant composites.

Lignocellulosic fibers and rubber can both be obtained from natural resources. Due to their excellent flexibility, elasticity, electrical property, resistance to crack propagation, and other superior mechanical and chemical properties, both natural and synthetic rubbers in vulcanized form are used to produce various rubber products. In the traditional vulcanization process of rubbers, carbon black (CB) and silica are commonly employed as fillers for the benefits of improving strength, stiffness and weather resistance, which lead to a special class of material known as composites [32-34]. However, both CB and silica are non-degradable and consume amount of energy for their production. Therefore, rubber manufacturers are searching for new reinforcing fillers which are renewable, biodegradable, inexpensive, light-weight, and readily available.

The use of natural fibers as fillers or reinforcements to replace CB and silica in the production of rubber composites has attracted much attention. Due to their can be



easily incorporated into rubber compound with other ingredients to fabricate bio-based rubber composites through the standard rubber processing operations. However, the main limitations are the compatibility between rubber and fiber, and their interfacial adhesion, since the properties of the lignocellulosic rubber composites are dominated by the interaction between the filler and matrix [35-37], especially the surface property of the filler is polar and hydrophilic, while the matrix, rubber is generally non-polar and relatively hydrophobic. Numerous surface modifications aiming at improving the miscibility and compatibility between rubber and wood or natural fiber have been carried out recently [38-40]. Generally, the modification strategies fall into two categories, namely physical treatment and chemical treatment.

In this work, PALF-filled reinforced elastomer composites will be prepared. PALFs will be treated using sodium hydroxide (alkali treatment) and triethoxy vinyl silane before compounding. The effects of fiber surface treatments and compatibilizer loading on thermal and mechanical properties of the elastomer will be investigated.

1.2 Research objectives

1. To improve the mechanical properties of PALF reinforced elastomer composites.
2. To study the effects of chemical treatments (alkali and silane treatments) with and without the presence of compatibilizer on mechanical properties of PALF-reinforced elastomer composites.
3. To study the thermal properties of the composites

1.3 The scope of research

In this work, PALFs will be treated using alkali and silane methods. After that, the functional group of the PALF will be characterized by ATR-FTIR. The untreated and treated-PALFs composites will be prepared by melt compounding in an internal mixer. The filler content of 10 wt% will be fixed for each composite without using any compatibilizer. The composites will then be prepared by melt blending on a two-roll mill and then compression-molded into a sheet about 0.5 mm thick. The shape and size



of PALF and fractured surfaces of the composites will be observed with a scanning electron microscope (SEM). The thermogravimetric analyzer (TGA) in air will be performed to study the non-isothermal stability of the composites. Tensile testing will be carried out on a universal testing machine. The dynamic mechanical analysis (DMA) will be performed to obtain dynamic storage modulus (E') and the loss tangent ($\text{Tan } \delta$).

1.4 Expected results obtained from the research.

1. The mechanical properties of treated fiber-containing composites will be enhanced.
2. The further enhancement in mechanical properties will be achieved for the treated fiber-containing composites with the presence of compatibilizer.

1.5 Research Place

SC2 - 206, Department of Chemistry, Faculty of Science, Maharakham University and Science Building 3, Faculty of Science, Mahidol University



CHAPTER 2

LITERATURE REVIEW

2.1 Thermoplastic elastomers

Thermoplastic elastomers form a new class of polymeric materials that have large number of applications because of their unique combination of both mechanical properties and processability. Their modulus level is comparable to that of the reinforced rubber vulcanizate under the using conditions, which covers the range from the low temperature near the glass transition temperature of the rubbery component to the higher temperature approaching the melting or softening point of the plastic component. At the processing temperature, thermoplastic elastomers are in the melt state such that they can be processed with plastic processing equipment. Among the thermoplastic elastomers, the triblock copolymer is a special kind. Typical examples are styrene-*b*-butadiene-*b*-styrene (SBS), styrene-*b*-isoprene-*b*-styrene (SIS), and styrene-*b*-(ethylene-*co*-butylene)-*b*-styrene (SEBS) triblock copolymers [41].

Thermoplastic elastomers (TPEs) have established themselves as important products in the polymer industry, with styrene-based block copolymers occupying the major portion of the TPE market. In their unstabilised form, these materials can undergo degradation and oxidation processes typical of those of conventional thermoplastics. Despite the extensive literature published on the degradation of most thermoplastic and rubber materials, TPE's are relatively newly developed, and consequently research studies on their degradation, is so far limited. Degradation processes in styrene-block copolymers (SBCs) are known to occur in both the polystyrene and elastomer phases [42]. However, the elastomer phase is considered more liable to degradation because its low glass transition temperature (T_g) promotes permeability toward oxygen diffusion. The unsaturated SBCs are considered similar to styrene-butadiene-rubber and natural rubber respectively as regards resistance to oxidation, ozone attack and UV irradiation [43].



2.2 Poly[styrene-*b*-(ethylene-*co*-butylene)-*b*-styrene] triblock copolymer (SEBS)

SEBS is a polystyrene end of the segment to be polybutadiene hydrogenation of ethylene - butylene copolymer block for the middle of the linear three embedded elastic copolymer, a complex system being dependent on the nature of the olefin starting materials, their composition and the manufacturing process [44]. The elastomer block consists of a copolymer of ethylene and butylene, which is derived from a butadiene pre-cursor by hydrogenation. The blocks tend to possess a sharp compositional boundary with pure polystyrene and pure elastomer giving a phase of immiscible domains of polystyrene in an elastomeric matrix. Usually, at less than 50% polystyrene the domains are well-dispersed [45]. SEBS contain unsaturated double bonds, it has good stability and resistance to aging. A typical structure of SEBS is shown in figure 2.1.

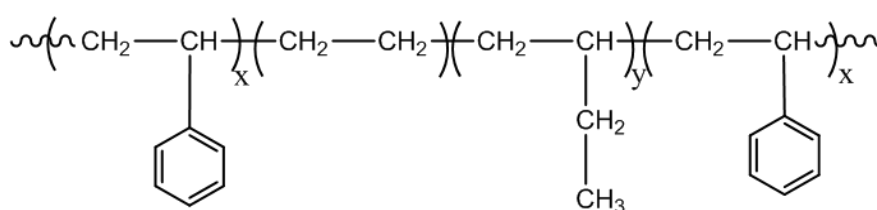


Figure 2.1 Chemical structure of SEBS.

SEBS polymers successfully combine elastomeric properties with low processing costs typical of commodity plastics. The excellent aging resistance of SEBS polymers is due to the absence of carbon-carbon double bonds. By varying the relative ratio of the components (styrene, ethylene and butylene) on SEBS formulations it is possible to obtain a wide variety of elastic and hardness values with different applications in industry. SEBS polymers are commercially available in white color or even in transparent grades. They can be processed at relatively low temperatures and show excellent resistance to intermediate temperatures [46]. The major applications of SEBS are in adhesives, sealants, coatings, footwear industry, automotive parts, and wire insulation, etc.



2.3 Polymer composites

Composites enable the construction of safe automobiles, aircrafts with high range, and extremely light machine components. With this material class the refurbishment of buildings and bridges as well as the manufacturing of medical implants can be accomplished. Composites contribute decisively to the sustainable development within our society [47]. Wherever advancing technology has created a need for combinations of properties no single material can provide, composites are becoming the material of choice. By dispersing fibers or particles of one substance in a matrix, or binder, of another, the designer of a composite can arrive at properties neither material shows on its own (Figure 2.2). Already the need for stiffness and strength combined with low density has led designers of military and commercial aircraft, sports equipment and cars to turn to composites for some components.

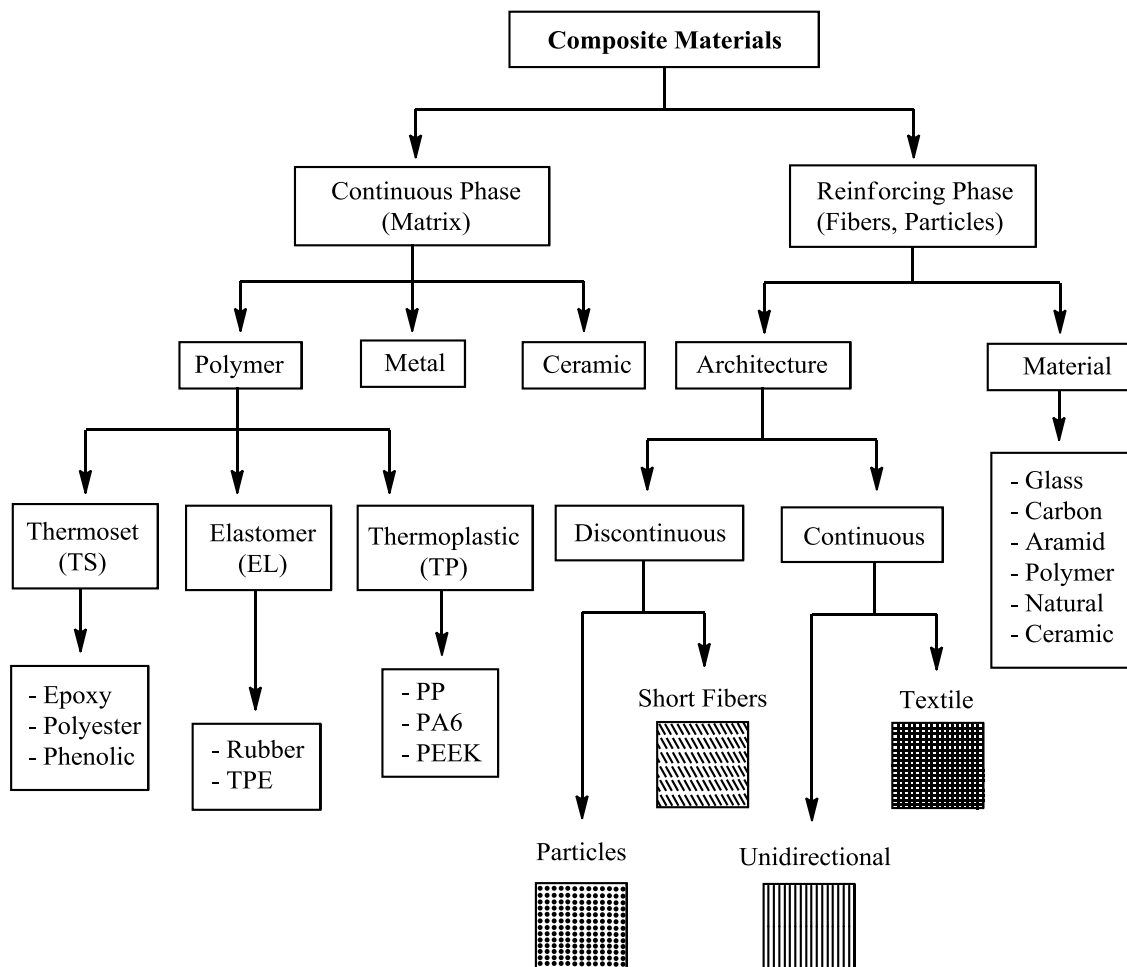


Figure 2.2 Principle composition of composite materials [48].



The relative importance of fibers and matrix on various properties of the composites. The strength and stiffness of the composite remain very much a function of the reinforcing material, but the matrix makes its own contribution to properties. The ability of the composite material to conduct heat and current, for example, is heavily influenced by the conductivity of the matrix. The mechanical behavior of the composite is also governed not by the fibers alone but by a synergy between the fibers and the matrix. The reason is that matrix materials are usually ductile: elastic or plastic. As the broken ends of the fiber pull apart, elastic deformation or plastic flow of the matrix exerts shear forces, gradually building stress back into the fragments. Because of such load transfer the fiber continues to contribute some reinforcement to the composite. The stress on the surrounding intact fibers increases less than it would in the absence of the matrix, and the composite is able to bear more stress without fracturing. The synergy of the fibers and the matrix can thus strengthen the composite and also toughen it, by increasing the amount of work needed to fracture it [47].

However, the properties of an advanced composite are shaped not only by the kind of matrix and reinforcing materials it contains but also by a factor that is distinct from composition: the geometry of the reinforcement. Injection moldable short fiber reinforced thermoplastics represent one kind of composite in which only the concentration of the strengthening fibers is controlled, not their exact dimensions or orientation. For two reasons most high performance composites are therefore strengthened with much longer fibers, usually bundled into continuous yarns. If a composite is to benefit fully from the great strength of the reinforcing material, the reinforcement must be capable of accepting loads that stress it to its breaking point. Otherwise the composite will fail at a load that falls short of the stress the fibers could theoretically sustain; they will simply pull out of the matrix without breaking as the composite disintegrates [47].

2.3.1 Natural fiber reinforced polymer composites

Natural fibers like flax, hemp, jute and sisal have been well recognized as good potential reinforcements for engineering fiber composites. The advantageous features of these fibers are lightweight, high specific modulus, non-toxic and easy for processing and absorbing CO₂ during their growth [5,6]. These benchmarking properties open the wide area of natural fibers in the composite sector and challenge the



replacement of synthetic fibers. However, natural fibers are not a problem-free alternative and they possess certain shortfalls in properties. Their structural compositions (cellulose, hemicelluloses, lignin, pectin and waxy substances) allow moisture absorption from the environment which leads to poor bonding with the matrix materials [7]. Additionally, the chemical structures of the fibers and matrix are different and couplings between these two phases are challenging. This causes ineffective stress transfer throughout the interface of the composites. Therefore, certain chemical treatments on the surface of natural fibers are definitely needed. These treatments are usually based on the use of reagent functional groups that are capable of reacting with the fiber structures and changing their composition. As a result, the tendency of moisture absorption of the fibers is reduced and this facilitates greater compatibility with the polymer matrix [5]. For the fabrication of natural fiber composites, different fiber arrangements such as short-randomly oriented, long-unidirectional and woven fabrics were used. These composites were then investigated by several researchers with respect to their mechanical and thermal properties. Many academic and industrial research activities are ongoing to develop better interfacial bonding properties of the composites. Experimental parameters were tested by using different chemical treatments to achieve stronger fiber surface adhesion to surrounding matrix.

2.3.2 Factors affecting the composite properties

2.3.2.1 Plant fiber structure

The cellulose structure of the fibers is distinguished through crystalline and amorphous regions. Large numbers of strong intra-molecular hydrogen bonds are formed in the crystallite region. This creates cellulose block and makes it difficult for other chemical penetrations. However, dyes and resins are absorbed easily by the amorphous region. The hydrophilic hydroxyl groups present in this region are combined with water molecules from the atmosphere. Hemicellulose, lignin, pectin and waxy substances do normally hold these water molecules. This makes the fiber hydrophilic and polar in character which lowers the compatibility with the non-polar/hydrophobic matrix [49-51]. For the distension of the crystalline region, the elimination of the hydrophilic hydroxyl groups and the removal of surface impurities (waxy substances), natural fiber requires to be chemically modified. Chemical treatments such as



mercerization, acetylation, benzylation, peroxide and coupling agents with or without heat are widely being applied to modify fiber surface and structure.

2.3.2.2 Thermal stability of fibers

Natural fiber generally starts degrading at about 240°C. Structural constituents of the fiber (cellulose, hemicelluloses, lignin, etc.) are sensitive with different range of temperatures. It was reported that, lignin starts degrading at a temperature around 200°C and hemicelluloses and cellulosic constituents degraded at higher temperatures [52]. Thermal stability of the fiber can be enhanced by removing certain proportion of hemicelluloses and lignin constituents by different chemical treatments. The degradation of natural fibers is an important issue in the development of composites in both manufacturing (curing, extrusion or injection moulding) and materials in service [53,54].

2.3.2.3 Fiber length, loading and orientation

The mechanical properties of the composites are depended on several factors such as fiber length, loading and orientation in the matrix. When a load is applied to the matrix, stress transfer occurs by shear at the interface along the fiber length and ends of the fiber. The extent of load transfer is a function of the critical fiber length (aspect ratio), the direction and orientation of fiber and the compatibility between fiber–matrix interfaces. Depending on the fiber orientation at the matrix, three types of composite are prepared. Firstly, longitudinally aligned fiber composites generally have higher tensile strength but lower compressive strength (due to fiber buckling). Secondly, transversely directed fibers undergo very low tensile strength, which is lower than the matrix strength. Finally, randomly orientated short fiber composites have different mechanical properties. This is due to the complexities of load distribution at different direction along the interfaces, consistent mechanical properties of these composites are far more difficult. By controlling factors such as the aspect ratio, the dispersion and orientation of fibers, considerable improvements in the properties can be accomplished [50,52,55].

2.3.2.4 Presence of voids

During the insertion of fiber into the matrix, air or other volatile substances may be trapped inside the composites. After the curing process micro-voids are formed along the individual fiber tows and in the matrix rich regions. This causes



sudden failure of the composites and shows poor mechanical properties. The curing and cooling rate of the composites are also responsible for the void formation [52]. High void content (over 20% by volume) is responsible for lower fatigue resistance, greater affinity to water diffusion and increase variation (scatter) in mechanical properties [56,57]. Composites at higher fiber content display more risk for void formation [57].

2.3.2.5 Moisture absorption of fibers

The lignocellulosic fibers are hydrophilic and absorb moisture. Many hydrogen bonds (hydroxyl groups -OH) are present between the macromolecules in the fiber cell wall. When moisture from the atmosphere comes in contact with the fiber, the hydrogen bond breaks and hydroxyl groups form new hydrogen bonds with water molecules. The cross section of the fiber becomes the main access of water penetration. The interaction between hydrophilic fiber and hydrophobic matrix causes fiber swelling within in the matrix. This results weakening the bonding strength at the interface, which leads to dimensional instability, matrix cracking and poor mechanical properties of the composites [58]. Therefore, the removal of moisture from fibers is an essential step for the preparation of composites. The moisture absorption of fibers can be reduced by eliminating hydrophilic hydroxyl groups from the fiber structure through different chemical treatments [59].

2.4 Natural fibers

2.4.1 Fiber types

Natural fibers are one of abundant and renewable bio-based materials in nature and they can be classified into different types as shown in Fig. 2.3 [60]. The natural fibers can generally be classified according to their origin as bast, leaf, fruit, and seed-hair fibers. The natural fibers that have been reported in literature to reinforce different polymer matrices include wood, cotton, bagasse, rice straw, rice husk, wheat straw, flax, hemp, pineapple leaf, coir, oil palm, date palm, doum fruit, ramie, curaua, jowar, kenaf, bamboo, rapeseed waste, sisal and jute.



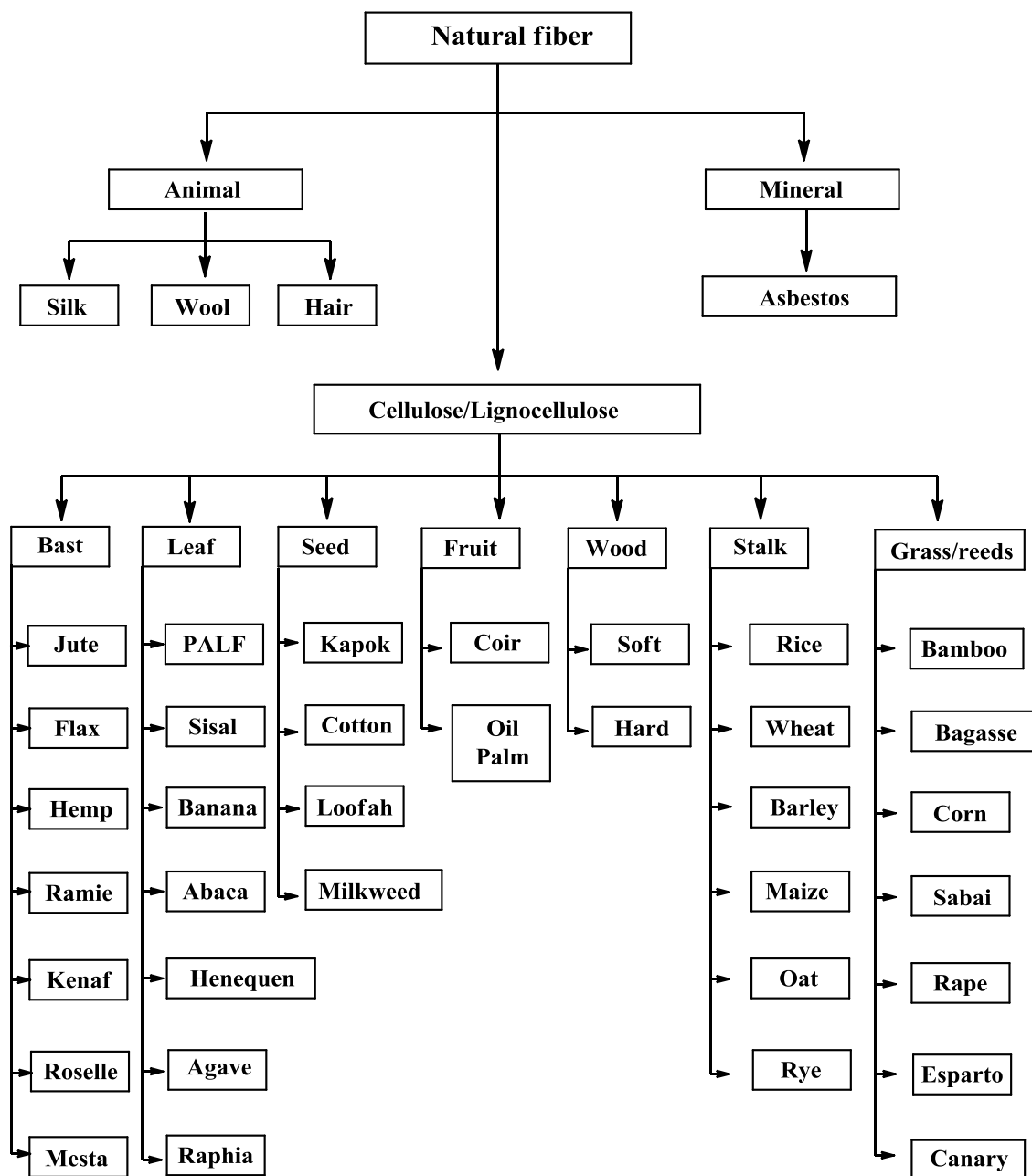


Figure 2.3 Classifications of natural fibers [60].

2.4.2 Structure and chemical composition

Plant based natural fibers are lignocellulosic in nature and are composed of cellulose, hemicelluloses, lignin, pectin and waxy substances. The structural composition of fibers are presented in Table 2.1. Cellulose is considered the major framework component of the fiber structure. It provides strength, stiffness and structural



stability of the fiber. The chemical structure of cellulose (Figure 2.4a) consists of three hydroxyl groups (-OH). Two of them form hydrogen bonds within the cellulose macromolecules (intra-molecular) whilst the rest of the group forms hydrogen bond with other cellulose molecules (intermolecular) [61]. Lignin is amorphous and has an aromatic structure (Figure 2.4b). Hemicellulose occurs mainly in the primary cell wall and has branched polymers containing five and six carbon sugars (Figure 2.4c) of varied chemical structures [62]. Pectin comprises of complex polysaccharides. Their side chains are cross-linked with the calcium ions and arabinose sugars. Additionally, small amounts of organic (extractives) and inorganic (ash) components are present in the fiber structure. Organic extractives are responsible for color, odor and decay resistance whilst inorganic constituents enhance the abrasive nature of the fiber. Figure 2.5 shows a schematic structure of a natural fiber and Figure 2.6 presents the model of the structural organization of the three major structural constituents of the fiber cell wall [63]. In accordance with a specific type of fiber, cellulose microfibrils have their own cell geometry which is a factor responsible for the properties of the fiber [64]. Each fiber cell wall consists of primary and secondary layers of cellulose microfibrils. The fiber structure develops in the primary cell wall and is deposited during its growth. The secondary wall consists of three layers and each layer has a long chain of helical cellulose microfibrils [65]. The cellulose content increases steadily from primary to secondary layers and the hemicelluloses amount are similar in each layer. However, lignin content decreases in this sequence. Hemicellulose molecules are hydrogen bonded with cellulose fibrils and they form cementing materials for the fiber structure. Lignin and pectin are coupled with the cellulose–hemicellulose network and provides an adhesive quality to hold the molecules together. This adhesive quality is the cause for the strength and stiffness properties of the fiber. Secondary thick layer (s2) determines the mechanical properties of the fiber. Generally, fibers with a higher cellulose content and a lower microfibrillar angle (the angle between the fiber axis and cellulose microfibrils) have better strength properties [50,55].



Table 2.1 Structural compositions of natural fibers [55,66].

Fiber	Cellulose (wt%)	Hemicellulose (wt%)	Lignin (wt%)	Waxes (wt%)
Bagasse	55.2	16.8	25.3	–
Bamboo	26–43	30	21–31	–
Flax	71	18.6–20.6	2.2	1.5
Kenaf	72	20.3	9	–
Jute	61–71	14–20	12–13	0.5
Hemp	68	15	10	0.8
Ramie	68.6–76.2	13–16	0.6–0.7	0.3
Abaca	56–63	20–25	7–9	3
Pineapple	70–82	–	9–12	4–7
Sisal	65	12	9.9	2
Coir	32–43	0.15–0.25	40–45	–
Oil palm	65	–	29	–
Curaua	73.6	9.9	7.5	–
Wheat straw	38–45	15–31	12–20	–
Rice husk	35–45	19–25	20	14–17
Rice straw	41–57	33	8–19	8–38



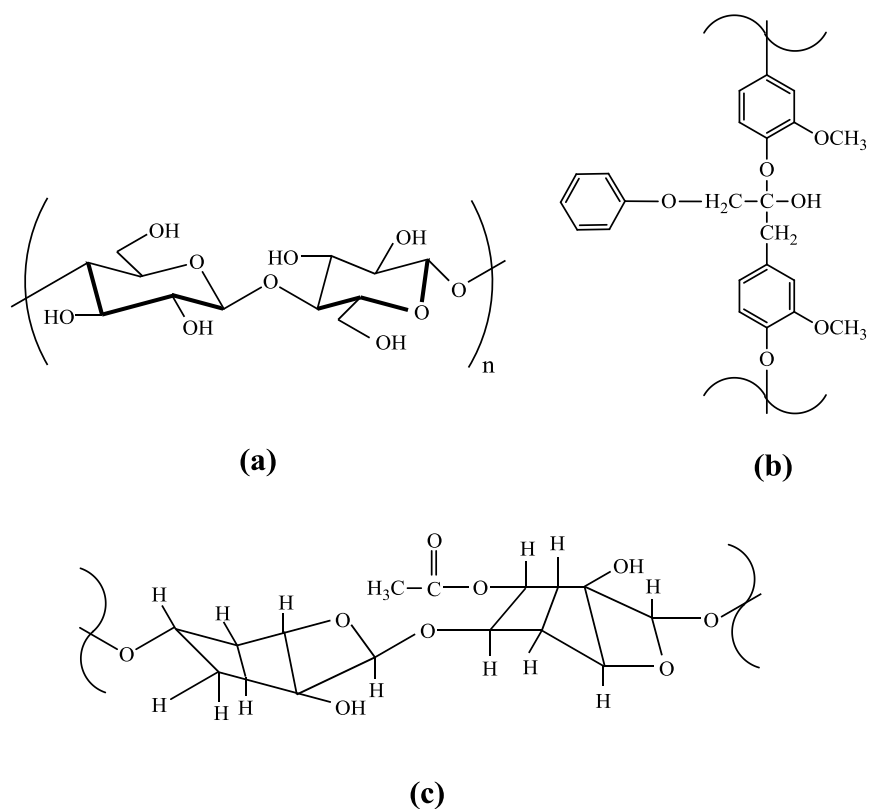


Figure 2.4 Chemical structure of (a) cellulose (b) lignin and (c) hemicelluloses [64].

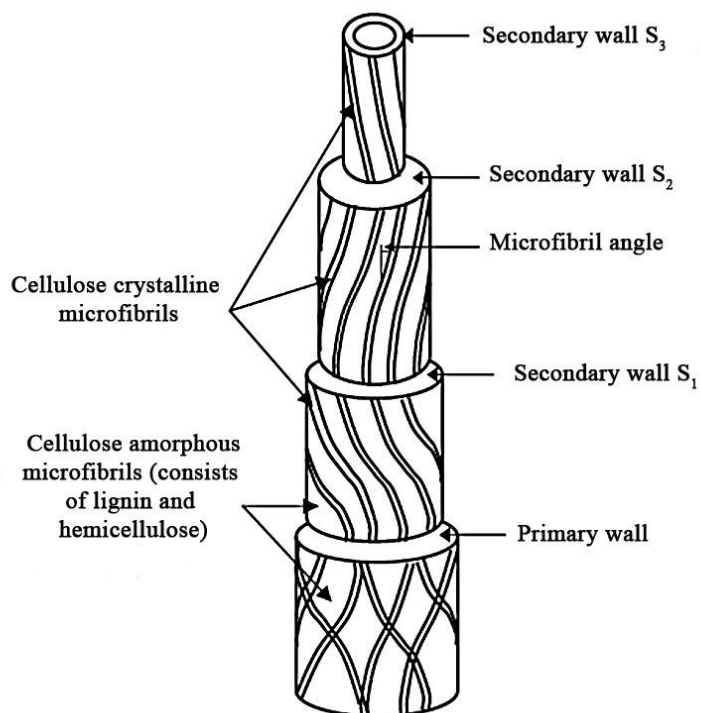


Figure 2.5 Structure of natural fiber [57].

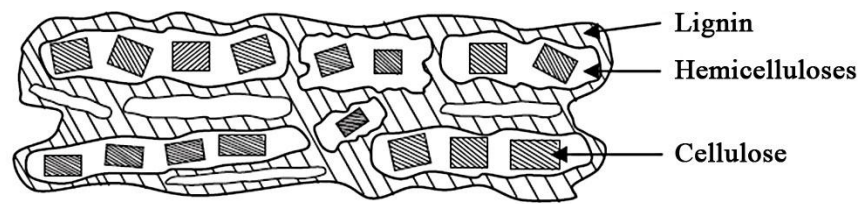


Figure 2.6 Structural organization of the three major constituents in the fiber cell wall [61].

2.4.3 Properties

The properties of natural fibers differ among cited works, because different fibers were used, different moisture conditions were present, and different testing methods were employed. The natural fiber reinforced polymer composites performance depends on several factors, including fibers chemical composition, cell dimensions, microfibrillar angle, defects, structure, physical properties, and mechanical properties, and also the interaction of a fiber with the polymer. In order to expand the use of natural fibers for composites and improved their performance, it is essential to know the fiber characteristics. The range of the characteristic values, as one of the drawbacks for all natural products, is remarkably higher than those of glass-fibers, which can be explained by differences in the fiber structure due to the overall environment conditions during growth. Natural fibers can be processed in different ways to yield reinforcing elements with different mechanical properties. Mechanical properties of natural fibers can be influenced by many factors. Such as either fiber bundles or ultimate fiber is being tested. Table 2.2 [55,66,68-69] presents the important physic-mechanical properties of commonly used natural fibers and conventional synthetic fibers.



Table 2.2 Comparative properties of natural fiber and conventional synthetic fibers.

Fibers	Density (g/cm³)	Tensile strength (MPa)	Young's modulus (GPa)	Elongation at break (%)
Ramie	1.5	400–938	61.4–128	1.2–3.8
Pineapple	1.44	413–1627	34.5–82.5	1.6
Flax	1.5–3	450–1100	27.6	2.7–3.2
Jute	1.3–1.45	393–773	13–26.5	7–8
Hemp	1.14	690	30–60	1.6
Sisal	1.45	468–640	9.4–22	3–7
Cotton	1.5–1.6	287–800	5.5–12.6	7–8
Coir	1.15	131–175	4–6	15–40
Abaca	1.5	400	12	3–10
Bamboo	0.6–1.1	140–230	11–17	–
Oil palm	0.7–1.55	248	3.2	25
Curaua	1.4	500–1150	11.8	3.7–4.3
E-glass	2.5	2000–3500	70	2.5
S-glass	2.5	4570	86	2.8
Aramid	1.4	3000–3150	63–67	3.3–3.7
Carbon	1.7	4000	230–240	1.4–1.8

2.4.4 Advantages and limitations of natural fibers

Natural fibers play an important role in fulfilling the specific requirements of the composites as engineered materials and have received attention from scientists and researchers owing to their advantages over most of the other fillers. Their utilization as reinforcing component in polymer composites is an effective way to produce light weight, low cost, environmentally friendly, hygienic, naturally degradable and CO₂ neutral materials without adversely affecting the rigidity of the composites [70–73]. Furthermore, owing to their susceptibility for living organisms, they are biodegradable and their use in the preparation of composites or hybrid composites does not cause environmental problems which are associated with the disposal of most of the fossil based plastics. The incorporation of these natural fibers in matrix polymers have been found helpful in biodegradation of the composite materials [74–76]. Beside these



aforementioned advantages, their poor compatibility with hydrophobic polymer matrices, higher moisture uptake and their variability in structure makes them less attractive for commercial applications.

Table 2.3 Advantages and limitations of natural fibers [77].

Advantages	Limitations
<ul style="list-style-type: none"> - Low densities and abrasiveness (relatively) - High possible filling levels resulting in high stiffness and high specific properties - Recyclability - High bending resistance - Biodegradability - Non-toxic - Absorbing CO₂ during their growth - Low cost 	<ul style="list-style-type: none"> - High moisture absorption with decrease of mechanical properties - Occasional poor compatibility with hydrophobic resins - Low processing maximum working temperature and seasonality

2.5 Chemical modification of natural fibers

Cellulose fibers, which are strongly polarized, are inherently incompatible with hydrophobic polymers due to their hydrophilic nature. In many cases, it is possible to induce compatibility in two incompatible materials by introducing a third material that has properties intermediate between those of the other two. There are several coupling mechanisms in materials (e.g., weak boundary layers, deformable layers, restrained layers, wettability, chemical bonding, and acid–base effect). The development of a definite theory for the mechanism of bonding using coupling agents in composites is a complex problem. The main chemical bonding theory alone is not sufficient. So the consideration of other concepts appears to be necessary. These include the morphology of the interphase, the acid–base reactions in the interface, surface energy and the wetting phenomena [78].



Chemical modifications of natural fibers aimed at improving the adhesion within the polymer matrix using different chemicals were investigated.

2.5.1 Alkali Treatment

Alkaline treatment or mercerization is one of the most used chemical treatment of natural fibers when used to reinforce thermoplastics and thermosets. The treatment on natural fibers by sodium hydroxide (NaOH) is widely being used to modify the cellulosic molecular structure. It changes the orientation of highly packed crystalline cellulose order and forming an amorphous region. This provides more access to penetrate chemicals. In the amorphous region, cellulose micromolecules are separated at large distances and the spaces are filled by water molecules. Alkali sensitive hydroxyl (OH) groups present among the molecules are broken down, which then react with water molecules (H-OH) and move out from the fiber structure. The remaining reactive molecules form fiber-cell-O-Na groups between the cellulose molecular chains [65]. Due to this, hydrophilic hydroxyl groups are reduced and increase the fibers moisture resistance property. It also takes out a certain portion of hemicelluloses, lignin, pectin, wax and oil covering materials [15,79,80]. As a result, the fiber surface becomes clean. In other words, the fiber surface becomes more uniform due to the elimination of microvoids and thus the stress transfer capacity between the ultimate cells improves. In addition to this, it reduces fiber diameter and thereby increases the aspect ratio (length/diameter). This increases effective fiber surface area for good adhesion with the matrix [81]. Mechanical and thermal behaviors of the composite are improved significantly by this treatment. If the alkali concentration is higher than the optimum condition, the excess delignification of the fiber can take place, which results in weakening or damaging the fibers [15,82]. The chemical reaction of the fiber-cell and NaOH is represented in Scheme 2.1. Figure 2.7 presents the schematic view of the cellulose fiber structure, before and after an alkali treatment. Treated fibers have lower lignin content, partial removal of wax and oil cover materials and distension of crystalline cellulose order.



Scheme 2.1



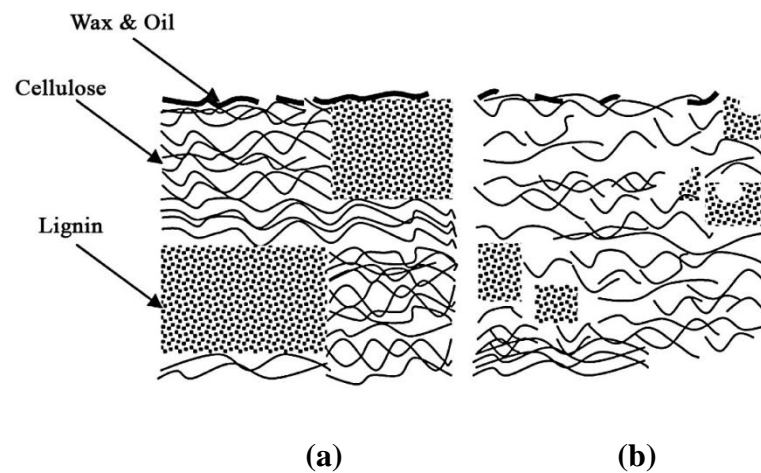


Figure 2.7 Typical structure of (a) untreated and (b) alkalinized cellulose fiber [61].

The effects of alkali treatment of pineapple leaf fiber on the performance of the pineapple leaf fiber/PLA composites have been shown [82]. It was found that alkali-treated fiber reinforced composite offered superior mechanical properties compared to untreated fiber reinforced composites. This study also suggested that the appropriate modification of fiber surfaces significantly contributes to improving the interfacial properties of the biocomposites. Since improvement of the interfacial adhesion increases the impact performance, surface properties of fibers can be greatly modified in terms of different treatments as characterized by an increased surface energy, which improves wettability of the fiber when compounding with a PLA matrix. DMA showed that treated fiber composites have a higher storage modulus, which indicates greater interfacial bond strength and adhesion between the matrix resin and the fiber. The alkalinized fiber composites have high storage modulus values, which correspond with their high flexural modulus.

Jute fibers were subjected to alkali treatment with a solution containing 5% NaOH for 0, 2, 4, 6 and 8 h at 30°C [80]. The modulus of the jute fibers improved by 12%, 68% and 79% after 4, 6 and 8 h of treatment, respectively. The tenacity of the fibers improved by 46% after 6 and 8 h treatment and the percentage of breaking strain was reduced by 23% after 8 h treatment. For 35% of the composites with fiber treated for 4 h, the flexural strength improved by 20% from 199.1 to 238.9 MPa. The flexural modulus improved by 23% from 11.89 to 14.69 GPa and the laminar shear strength increased by 19% from 0.238 to 0.283 MPa.



2.5.2 Silane Treatment

The surface energy of fibers is closely related to the hydrophilic nature of the fiber. Some investigations are concerned with methods to decrease hydrophilicity. Silane coupling agents may contribute hydrophilic properties to the interface, especially when amino-functional silanes, such as epoxies and urethanes silanes, are used as primers for reactive polymers. The primer may supply much more amine functionality than can possibly react with the resin in the interphase. Those amines, which could not react, are hydrophilic and therefore responsible for the poor water resistance of bonds. An effective way to use hydrophilic silanes is to blend them with hydrophobic silanes such as phenyltrimethoxysilane. Mixed siloxane primers also have an improved thermal stability, which is typical for aromatic silicones.

Silane is a multifunctional molecule which is used as a coupling agent to modify fiber surfaces. The composition of silane forms a chemical link between the fiber surface and the matrix through a siloxane bridge. It undergoes several stages of hydrolysis, condensation and bond formation during the treatment process of the fiber. Silanols form in the presence of moisture and hydrolysable alkoxy groups (hydrolysis). During condensation process, one end of silanol reacts with the cellulose hydroxyl group (Si–O–cellulose) and other end reacts (bond formation) with the matrix (Si–Matrix) functional group. This co-reactivity provides molecular continuity across the interface of the composite. It also provides the hydrocarbon chain that restrains the fiber swelling into the matrix

In general, interaction of silane coupling agents with natural fibers may mainly proceed through following steps [83,84]:

- 1) Hydrolysis (Figure 2.8a): The silane monomers are hydrolyzed in the presence of water and catalyst (normally acid or base) liberating alcohol and yielding reactive silanol groups.

- 2) Self-condensation (Figure 2.8b): During the hydrolysis process, the concomitant condensation of silanols (aging) also takes place. The condensation should be minimized at this stage to leave the silanols free for being adsorbed to the hydroxyl groups in the natural fibers. For the bulking treatment of fibers, the condensation should also be controlled in order to retain a small molecular size of monomers or oligomers to diffuse into the cell walls. The condensation rate of silanols is controllable by adjusting

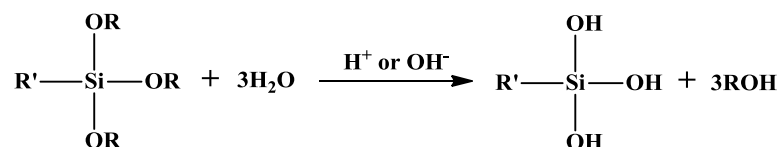


the pH of the hydrolysis system. An acidic pH environment is usually preferable to accelerate the hydrolysis rate of silanes but slow down the condensation rate of silanols.

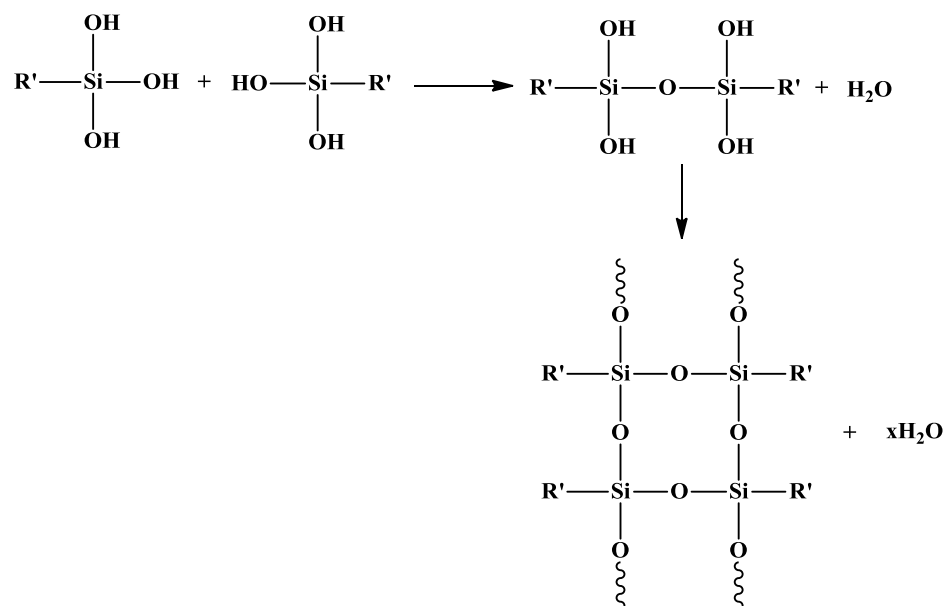
3) Adsorption (Figure 2.8c): The reactive silanol monomers or oligomers are physically adsorbed to hydroxyl groups of natural fibers by hydrogen bonds on the fiber surfaces (surface coating) and/or in the cell walls (cell wall bulking), which depends on the molecular size of silanol monomers/oligomers formed. The free silanols also adsorb and react with each other thereby forming a rigid polysiloxane structures linked with a stable $-\text{Si}-\text{O}-\text{Si}-$ bond.

4) Grafting (Figure 2.8d): Under heating conditions, the hydrogen bonds between the silanols and the hydroxyl groups of fibers can be converted into the covalent $-\text{Si}-\text{O}-\text{C}-$ bonds and liberating water. The residual silanol groups in the fibers will further condense with each other. The bonds of $-\text{Si}-\text{O}-\text{C}-$ may not be stable towards hydrolysis; however, this bond is reversible when the water is removed at a raised temperature.

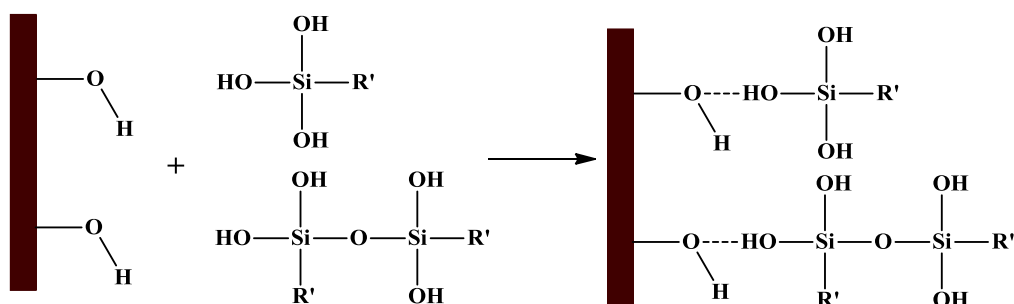
a) Hydrolysis :



b) Self-condensation :



c) Adsorption :



d) Chemically grafting :

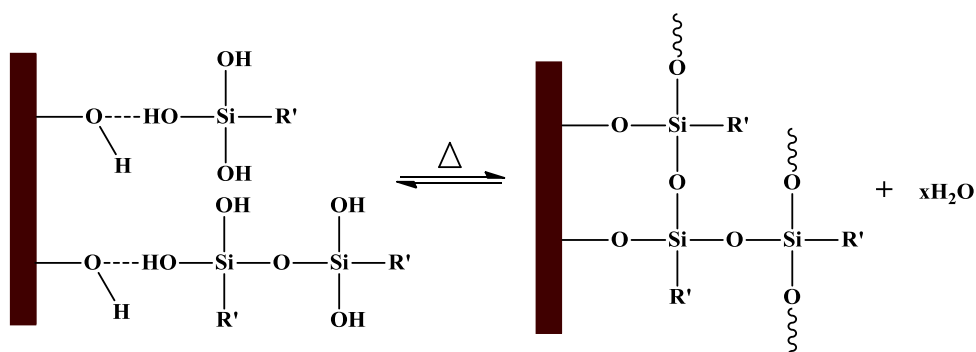


Figure 2.8 Interaction of silane with natural fibers by hydrolysis process.

The surface of the kenaf fiber was modified using a silane coupling agent (3-methacryloxypropyl triethoxysilane) to promote adhesion with the PS matrix [85]. The fiber–matrix adhesion increased through a condensation reaction between alkoxy silane and hydroxyl groups of kenaf cellulose. Due to the fiber modification, kenaf/PS composites exhibited higher storage modulus and lower $\tan \delta$ than those with untreated fiber indicating a greater interfacial interaction between the matrix resin and the fiber.

2.6 Pineapple leaf fibers (PALFs)

PALF are obtained from the leaves of pineapple plant (*Ananas cosomus*) from the family of Bromeliaceae [86] as shown in Figure 2.9. Mwaikambo stated that pineapple plants are largely grown in tropical America, Africa, and Far-East Asian countries [87]. Thailand and Philippines are the biggest pineapple fruit producers in the world. The Food and Agriculture Organization (FAO) has reported that most of the



world pineapple fruit production in 2001 amounting to about 13.7 million tons of fresh fruits are produced in Asia. Pineapple leaves from the plantations are being wasted as they are cut after the fruits are harvested before being either composted or burnt. Ahmad et al. concluded that the practices of decomposing and burning the leaves in situ did not contribute to the improvement of plantation yield [88,89]. Additionally, burning of these beneficial agricultural wastes causes environmental pollution.



(a)



(b)

Figure 2.9 Pineapple plant (a) and pineapple leaf fibers (b) [86].

PALF, which is rich in cellulose, relatively inexpensive and abundantly available has the potential for polymer-reinforced composite. PALF at present is a waste product of pineapple cultivation. Hence, without any additional cost input, pineapple fibers can be obtained for industrial purposes. Among various natural fibers, PALFs exhibit excellent mechanical properties. These fibers are multicellular and lignocellulosic. The main chemical constituents of pineapple fibers are cellulose (70–82%), lignin (9–12%) and ash (1.1%). The superior mechanical properties of PALFs are associated with their high cellulose content.

The compositions and content of ground pineapple leaf based on the shape of ground materials are shown in Table 2.5. Total recoverable solid or WGL constituted approximately 12.85% weight of fresh leaf. Approximately 21% of WGL is PALF and the rest is NFM. Interestingly, the amounts of PALF and NFM compare very well to that of the two major components of plants, cell wall and cell content usually determined in forage analysis [90]. They are generally determined in terms of neutral detergent fiber (NDF) and neutral detergent soluble (NDS), respectively. Thai pineapple leaf has been reported to contain NDF and NDS as respectively approximately 39.4% and 60.6% of dry leaf [91]. NDF represents the amount of structural components such



as cellulose, hemicellulose, lignin, silica and cell wall protein while NDS represents the amount of carbohydrate, protein, lipid, pectin, etc. within the plant cell [92]. It should be noted that the values for NDF and NDS for Thai pineapple leaf are quite different from the 64.9% and 35.1% found in Hawaiian pineapple leaf [93].

Table 2.4 Composition of ground pineapple leaf [94].

Composition	Designation	Percentage ^a	Percentage ^b
Total solid (whole ground leaf)	WGL	12.9 ± 6.4	100
Fibrous material (pineapple leaf fiber)	PALF	2.8 ± 0.1	21.4 ± 1.4
Non-fibrous material	NFM	10.1 ± 0.6	78.6 ± 1.4

^a Weight percentage of dried materials based on fresh leaf. Fresh leaf contains approximately 85% water.

^b Weight percentage of dried materials based on dried leaf.

PALF is a high textile grade commercial fiber, generally extracted by water retting. Pineapple leaf contains only 2.5-3.5% fiber, covered by a hydrophobic waxy layer, which remains beneath the waxy layer [95]. Pineapple leaf fiber is graded in between jute and cotton or jute and ramie. It has all textile properties and is capable of blending with jute, cotton, ramie and some other synthetic fibers [96,97]. So pineapple leaf fiber can capture an important position among natural fibers as potential commercial grade textile fiber, but there is need of its assured supply to processing industry in sufficient quantities.

Thailand, like many agricultural countries, has access to various kinds of natural fiber. Any kind of natural fiber can be used to produce natural fiber reinforced composites (NFRC), and indeed almost everything has been studied. However, for widespread use, the fiber availability and its properties are the main factors determining selection. A fiber that is abundantly available and is used very little is PALF. Thailand is currently the world's largest pineapple producer [94] with about 240,000 acres under cultivation [94]. After harvesting, a large amount of pineapple leaf waste approximately 20,000–25,000 tons/acre, remains causing various problems for farmers. Pineapple is also grown in many other countries worldwide, such as Brazil, Philippines, Costa Rica, Malaysia, Indonesia and Hawaii, in total on about 2.1 million acres.



2.6.1 Applications PALFs

PALF have been traditionally used for making threads and textile fabrics in many countries. In the Philippines, PALF have been used for commercial products such as dresses, table linens, bags, mats and other clothing items [86]. The consumption of pineapple's leaves are used to produce the textile fiber employed as a component of wall paper and furnishings, amongst other uses due to PALF is rich in cellulose, relatively inexpensive and abundantly available. Furthermore, it has the potential for polymer reinforcement. At present PALF are a waste product of pineapple cultivation and therefore these relatively inexpensive pineapple fiber can be obtained for industrial purposes [78]. PALF are also being utilized as textile materials in Indonesia, while works on using PALF for this application have just started in Malaysia [98]. The use of chemically treated PALF in making industrial textiles, V-belt cord, conveyor belt cord, transmission cloth, air-bag tying cord, and shoe laces was reported in Basu *et al.* [99]. PALF can be blended with polyester fibers to replace jute for making needle-punched nonwovens for technical textiles [100]. The spinning, weaving and processing of PALF were examined in Kumar *et al.* [101], where the authors reported the use of PALF in making carpets and urged further studies on chemical processing, dyeing behavior, strength losses and fiber degradation of PALF. PALF were blended with polyester fibers and silk, resulting in esthetically pleasing fabric and nonwovens [102]. The use of PALF to reinforce composites, the main focus of this review, shall be explained in the coming sections. Using PALF as textiles involves elaborate processes to increase the fiber fineness, blendability and dyeing-ability. PALF dresses are known to be very costly understandably due to tedious manual processes involved. In contrast, the use of PALF as reinforcements in polymer composites may not involve such processes.

2.6.2 PALF reinforced polymer composites

2.6.2.1 PALF-reinforced thermoplastics composites

Thermoplastics, especially commodity resins like polyethylene (PE) and polypropylene (PP), account for majority of the matrices used with PALF. Understandably, these commodity resins are inexpensive, widely available and recyclable. Processing methods of natural fiber reinforced thermoplastic composites include melt mixing and injection molding [103-106], sandwiching with compression molding [11,107,108], melt mixing and compression molding [109,110], extrusion and



compression molding [111]. Mixing natural fibers with thermoplastic matrices must be carried out at less than 200°C as most natural fibers lose their strength at temperature of 160°C [14].

George *et al.* [14] studied stress relaxation behavior of pineapple fiber-reinforced polyethylene composites. They found stress relaxation to be decreased with an increase of fiber content due to better reinforcing effect. It is also reported by George *et al.* [112] that properties of fiber-reinforced composites depend on many factors like fiber–matrix adhesion, volume fraction of fiber, fiber aspect ratio, fiber orientation as well as stress transfer efficiency of the interface. Luo and Netravali [107] found an increase in the mechanical properties of “green” composites prepared from PALFs and poly(hydroxybutyrate-*co*-valerate) resin (a biodegradable polymer) with the fibers in the longitudinal direction. However, the researchers reported a negative effect of the fibers on the properties in the transverse direction.

The use of PALF as reinforcement to improve mechanical properties of polycarbonate (PC) has been investigated [113]. The study focused on the tensile and flexural behaviors of PALF–polypropylene composites as a function of volume fraction. It follows that relatively soft polymeric surface of PC can easily scratch, and notch sensitivity at lower temperatures limits PC in some applications. The tensile modulus and tensile strength of the composites were found to be increasing with fiber content in accordance with the rule of mixtures. The flexural modulus gives higher value at 2.7% volume fraction. The flexural strength of the composites containing 5.4% volume fraction was found to be higher

2.6.2.2 Hybrid PALF-reinforced composites

Hybrid biocomposites are formed by incorporating two or more fibers into a single matrix resulting in an apparent synergistic improvement in composite properties and favorable balance between the inherent advantages and disadvantages of individual components [114]. Mishra *et al.* [115] evaluated the mechanical properties of PALF/glass fiber reinforced polyester composites and observed improvement in tensile, flexural and impact strengths of the composites through incorporation of a small amount of glass fiber indicating positive hybrid effects. An optimum glass fiber loading of 8.6 wt% was noted. The PALF/glass fiber reinforced polyester composites also showed significant reduction in water uptake compared to unhybridized samples.



Thermophysical properties of PALF/glass fiber reinforced polyester composites were also studied in Idicula *et al.* [116]. Varying hybrid effects may be calculated for the mean values of thermal conductivity, diffusivity, specific heat and density obtained.

2.6.2.3 PALF-reinforced rubber and thermoplastic elastomer composites

Lignocellulosic fibers can be easily incorporated into rubber compound with other ingredients to fabricate bio-based rubber composites through the standard rubber processing operations, such as compress moulding, injection moulding and extrusion [117]. Although these composites provide good strength and dimensional stability during fabrication, the main issues, namely the compatibility between rubber and fiber, and their interfacial adhesion, should be and are yet to be addressed, since the properties of the composites are dominated by the interaction between the filler and matrix [118-120].

Kalapakdee *et al.* [121] studied the effect of fiber content and compression molding temperature on *mechanical* properties of PALF reinforced santoprene composites in two directions (longitudinal and transverse). It found that the composites exhibit clear anisotropy in mechanical properties. Modulus at low strain, tensile strength, hardness, and tear strength in the longitudinal direction all increase with increasing PALF content. Compression temperature also affects modulus and tear strength but not tensile strength.

Wisittanawat *et al.* [122] evaluated the effect of fiber content and bonding agent on mechanical properties of PALF reinforced nitrile rubber composite. It found that, PALF has a very high potential for reinforcement of nitrile rubber. it were improves mechanical properties of nitrile rubber composites in term of tensile strength, modulus and tear strength. Bonding agent improves interfacial adhesion between PALF and NBR and leads to even better mechanical properties, especially those measured at failure such as tensile and tear strengths. The tensile and tear strengths of nitrile rubber were improved using silica filler combined with the advantages of short fiber reinforcement [123]. The addition of silica initially lowers the early part of the stress-strain curve but prolongs breaking to greater strains. Further addition of silica raises the early part of the stress-strain curve back to and above that of the lower silica contents. Moreover, the elongation at break was found to significantly increase with silica loading.



CHAPTER 3

MATERIALS AND METHODS

3.1 Materials

3.1.1 Dispersed phases

Pineapple leaf fibers (Smooth Cayenne cultivar) dispersed phase used in this work was obtained from cultivation areas in Kok Kwai District, Ban Rai, Uthai Thani Province, Thailand. The preparation of PALFs was adopted from the previous research [94]. The leaves were washed to remove soil and dirt. The leaves were cut to a length of 6 mm and then milled using dish mill with two circular plates of 150 mm diameter under the revolution speed of about 7700 rpm. The discs were separated by projecting teeth, between which the substances are ground. The chopped pineapple leaves were fed into the hopper at the top of the mill and continuously milled for 10 s. The milled materials were cleaned with water and air dried at room temperature for 3 days. The dried milled materials (dry crumb) were then ground with a high speed grinder (Hao Peng, China) using a rotating speed of 25,000 rpm for 30 s and yielded a loose powder or a whole ground leaf. The material at this stage consists of fibrous and non-fibrous materials. The fibrous materials or PALFs were separated using steel wire sieve (mesh number 60).

3.1.2 Matrix phase

The polymer used as matrix phase was styrene-(ethylene-butylene)-styrene (SEBS) triblock copolymer (Kraton G1650) consisting a styrene/rubber weight percent ratio of 29/71. The SEBS polymer matrix was purchased from Toyota Tsusho (Thailand) Co.



Table 3.1 Physical and chemical properties of SEBS (KRATON[®] G1650 Polymer) [124].

Properties	Typical Value	Units	Test Method
Physical State	Solid	-	-
Color	Clear or White	-	-
Odor	Essentially odorless	-	-
Solubility (in water)	Insoluble	-	-
Specific gravity	0.91	gm/cc	ASTM D4025
Hardness	72	Shore A (10s)	ASTM 2240
Tensile strength	5000	psi	ASTM D-412
Styrene / Rubber ratio	29/71	-	n/a
300% Modulus	800	psi	ASTM D-412
Elongation at break	500	%	ASTM D-412
Solution Viscosity	8000	cps	BAM 922
Glass Transition Temperature (T_g)	- 42	°C	Measured by Rheovibron
Melting Temperature (T_m)	175	°C	-

3.1.3 Compatibilizer

The compatibilizer used in this work is a block copolymer of styrene-ethylene-butylene- styrene grafted with maleic anhydride (SEBS-g-MA) produced by Sigma-Aldrich[®], USA. This polymer was purchased from S.M. Chemical Supplies Co., Ltd. (Thailand). From the Sigma-Aldrich[®] product literature, the compatibilizer contains about 2 wt% maleic anhydride and has a melt flow rate of 22 g/10 min. All materials were dried in a vacuum oven at 70°C for at least 12 h before use.

3.1.4 Chemicals

NaOH pellets were obtained from Carlo Erba Reagents (Italy). Silane was obtained from Acros Organics (New Jersey, USA). Acetic acid was supplied by BDH Laboratory Supplies (England) and ethanol was supplied by Analar Normapur[®] (Ecuador).



3.2 Alkali, Silane and Alkali-Silane treatments

PALFs were treated using 5 wt% of NaOH solution. The PALFs were immersed in the NaOH solution, stirred continuously for 10 min, soaked for 6 h at room temperature, and washed with distilled water until the pH became neutral, respectively. After that, the alkali-treated PALFs were air dried at room temperature for 24 h and then dried in oven at 80°C for 24 h and stored in a desiccator prior to composites preparation. The alkali-treated PFs were designated as APF.

For silane treatment, the 10 wt% silane solution (weight percentage compared to the fiber) were dissolved for hydrolysis in 50v/50v ethanol/water mixture. The pH of silane solution was adjusted to 4 by adding acetic acid. The fibers were immersed in the silane solution and stirred continuously for 10 min. The fibers were soaked in the solution for 6 h at room temperature and then washed with distilled water until the pH became neutral. The silane-treated fibers were dried and stored under the same conditions as APF. The silane-treated fibers were designated as SPF.

For alkali-silane treatment, PALFs were treated with 5% NaOH solution for 6 h, washed in distilled water until the pH value reached 7.0, and then treated with a silane coupling agent (triethoxy vinyl silane) under the same conditions as SPF. Finally, The alkali-silane treated fiber were dried in oven at 80°C for 24 h and stored in a desiccator. The alkali-silane treated fibers were designated as ASPF.

3.3 Preparation of elastomer composites

SEBS based elastomer composites were prepared in three steps. First, SEBS, treated or untreated PF and SEBS-g-MA were melt mixed on an internal mixer using a rotor speed of 60 rpm at 175°C for 30 min. Next, the composites were mixed on a two roll mill for 10 min. The temperature of the front and back rollers of the two roll mill were 182°C and 175°C respectively. For the last step, the composites were compression molded to form a sheet of about 1 mm thickness at a temperature of 175°C for 7 min, cooled for 7 min and pressure of 500 psi. All formulations of the composites are summarized in Table 3.2.



Table 3.2 Formulations of the composites.

Sample	Materials					
	SEBS (wt%)	PALF (wt%)				SEBS-g-MA (wt%)
		Untreated (PF)	Alkali treated (APF)	Silane treated (SPF)	Alkali-Silane treated (ASPF)	
SEBS	100	–	–	–	–	–
PF10	90	10	–	–	–	–
PF20	80	20	–	–	–	–
PF10-MA3	87	10	–	–	–	3
PF10-MA5	85	10	–	–	–	5
PF10-MA7	83	10	–	–	–	7
APF10	90	–	10	–	–	–
APF10-MA3	87	–	10	–	–	3
APF10-MA5	85	–	10	–	–	5
APF10-MA7	83	–	10	–	–	7
SPF10	90	–	–	10	–	–
SPF10-MA3	87	–	–	10	–	3
SPF10-MA5	85	–	–	10	–	5
SPF10-MA7	83	–	–	10	–	7
ASPF10	90	–	–	–	10	–
ASPF10-MA3	87	–	–	–	10	3
ASPF10-MA5	85	–	–	–	10	5
ASPF10-MA7	83	–	–	–	10	7



3.4 Characterization techniques

3.4.1 Fourier Transform Infrared spectroscopy

To study the surface properties of the PALFs after treatments, the functional groups of the fibers was characterized by Attenuated Total Reflection-Fourier Transform Infrared (ATR-FTIR) spectroscopy (Spectrum GX-1, Perkin Elmer). The scan was conducted in the range of 4000-650 cm^{-1} at resolution of 4 cm^{-1} . The number of scans was set to 32.

3.4.2 Morphological characterization

The morphological characterization of elastomer composites was performed by scanning electron microscope (SEM) (JEOL; JSM- 6460LV, Tokyo, Japan) operated with an accelerating voltage of 15 kV. Prior to examination, the elastomer composites were immersed in liquid nitrogen for 10 min and then fractured. The specimens were sputter-coated with gold for enhanced surface conductivity.

3.4.3 Thermal decomposition analysis

Thermal decomposition analysis was carried out using TA instruments, SDT Q600 (Luken's drive, New Castle, DE). The neat and composite samples of 8-10 mg were loaded in alumina crucible and then non-isothermally heated from ambient temperature to 700°C at heating rate of 10°C/min. The TG was performed in air with the flow rate of 100 mL/min. The TG data were recorded online in TA instrument's Q series explorer software. The analyses of TG data were done using TA Instrument's Universal Analysis 2000 software (version 3.3B).

3.4.4 Tensile testing

The measurement of tensile properties for the polymer matrix and its composites was performed on an Instron mechanical tester (model 5569, Instron, Canton, MA) at room temperature, set at a grip length of 25 mm. crosshead speed of 50 mm/min and a full scale load of 1 kN. The stress is engineering stress which was calculated from the original cross section area of the sample. Test pieces were punched out from molded sheets with the long axis either parallel or perpendicular to the fiber orientation axis (termed longitudinal direction and transverse direction, respectively). The stress-strain curves and the secant modulus and tensile strength were reported. The



average value of five measurement was determined. The equations used for calculation of tensile properties are expressed as follows:

(a) Secant modulus at 1% strain

$$E = \frac{F}{A} \times 100 \quad (3.1)$$

E = secant modulus at 1% strain

F = stress at 1% strain

A = cross sectional area of the specimen

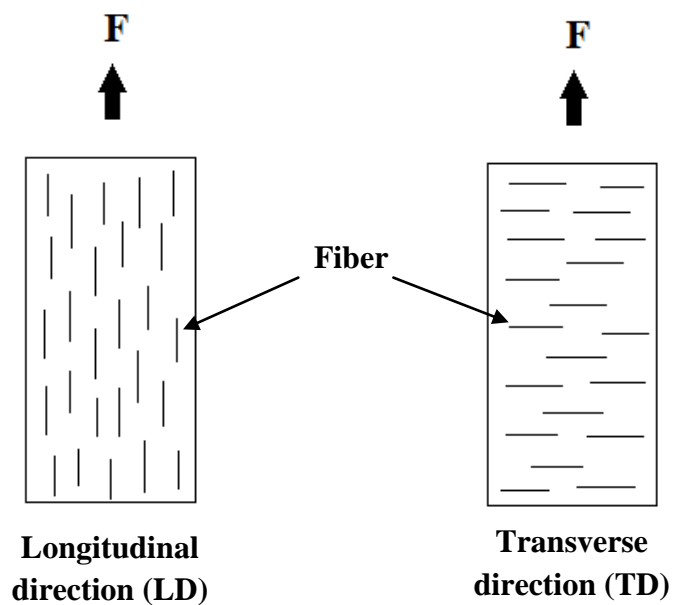
(b) Tensile strength

$$\sigma = \frac{F}{A} \quad (3.2)$$

σ = tensile strength

F = stress at the breaking point

A = cross sectional area of the specimen



3.4.5 Dynamic mechanical analysis

Dynamic mechanical properties were measured using TA instrument Q800 dynamics mechanical analyzer (DMA) (Luken's drive, New Castle, DE, USA), were measured longitudinal direction. The glass transition temperature (T_g), storage modulus (E'), loss modulus (E'') and $\tan \delta$ were measured. The tension mode was applied at an oscillating frequency of 10.0 Hz. The maximum force and maximum amplitude were set at 0.1 N and 15 μm , respectively. The measurements were carried out from -100 to 140°C with a heating rate of 5°C/min.

The whole experiments can be summarized as shown in Figure 3.1



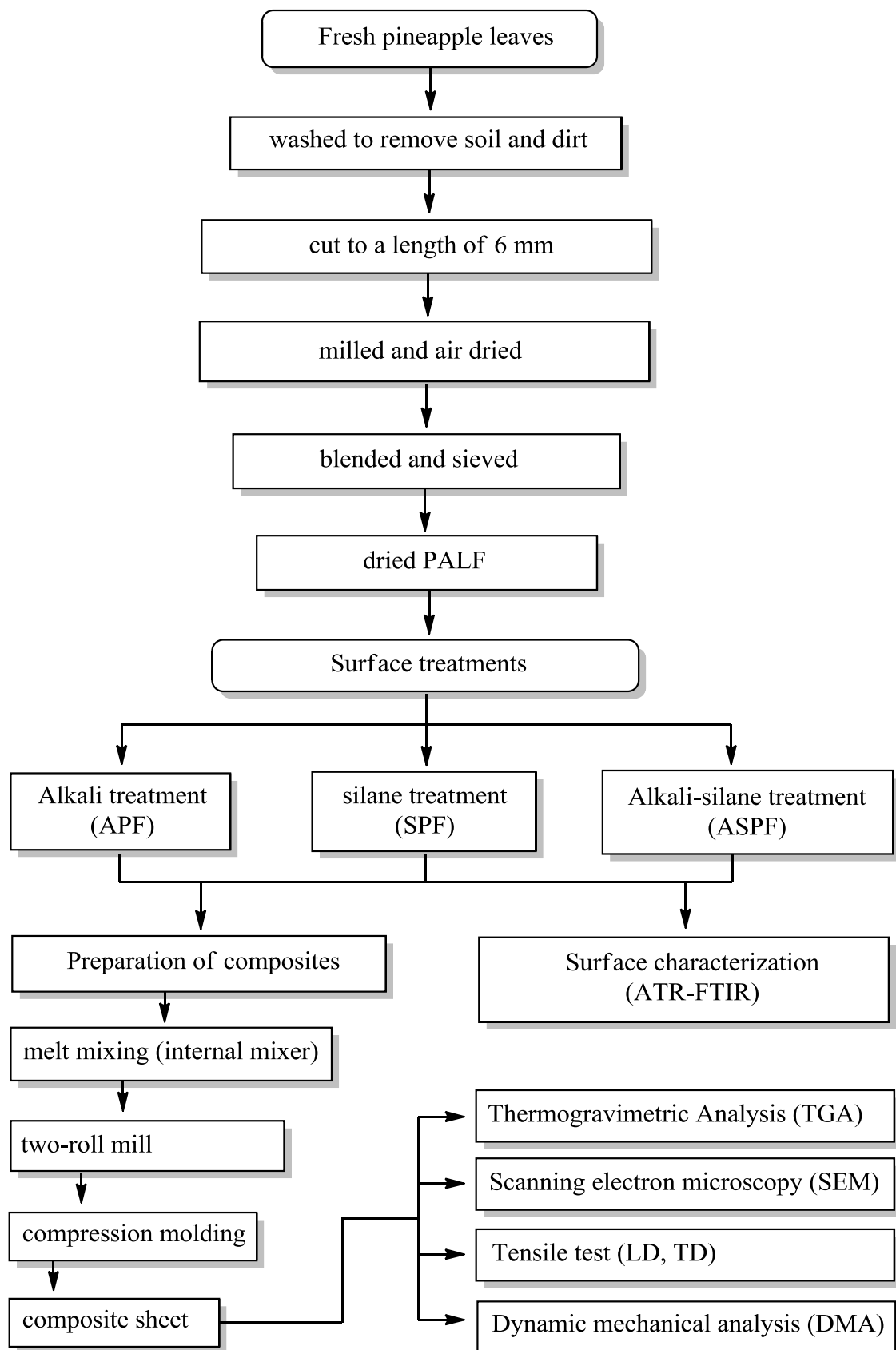


Figure 3.1 Flow charts of the whole experiments.



CHAPTER 4

RESULTS AND DISCUSSION

In this work, the thermoplastic elastomer composites based on SEBS reinforced with PALF was investigated. Before compounding, PALF surface was modified using alkali and silane treatments. The effects of surface treatments with and without compatibilizer (SEBS-g-MA) loading on mechanical, morphological and thermal properties of the elastomer composites were studied.

4.1 FTIR characterization of fiber surfaces

The FTIR spectra of untreated-, alkali-, silane- and alkali-silane- treated PALFs are shown in Figure 4.1. It is seen that the untreated fiber shows the band at 3300–3500 cm^{-1} and the band at 1034 cm^{-1} corresponding to -OH groups of cellulosic fiber. The peaks at 2910 cm^{-1} and 2850 cm^{-1} are attributed to methylene groups. The band at 1729 cm^{-1} belongs to pectin and wax. The wave number at 1630-1650 cm^{-1} is attributed to hemicellulose on the fiber. The bands at 1240-1247 cm^{-1} belong to phenolic and carbonyl group of lignin. For treated fiber, the peaks of pectin and wax at around 1729 cm^{-1} and the band at 1244 cm^{-1} belong to phenolic and carbonyl group of lignin are diminished. The increase in intensity for alkali treated fibers at 1034 cm^{-1} and 3300–3500 cm^{-1} is due to the increase in -OH groups on the fiber [31]. For silane treatment, the decrease in intensity for silane-treated fibers at 1638 cm^{-1} is due to removal of hemicellulose on fiber surface. Moreover, it can be seen that the band appeared at 1058 cm^{-1} involves the formation of Si-O-Si bonds, indicating the occurrence of chemical reaction between hydrolyzed silane and PALF, and the existence of polysiloxane network [30,31,126]. For alkali-silane treatment, the bands at 1729 and 1244 cm^{-1} as seen in the untreated fibers are not found after alkali-silane treatment, indicating that the hemicellulose, lignin and wax components in PALF were removed by alkali treatment. The details of the peak assignments for untreated-, alkali treated-, silane treated- and alkali-silane- treated pineapple leaf fibers are summarized in Table 4.1.



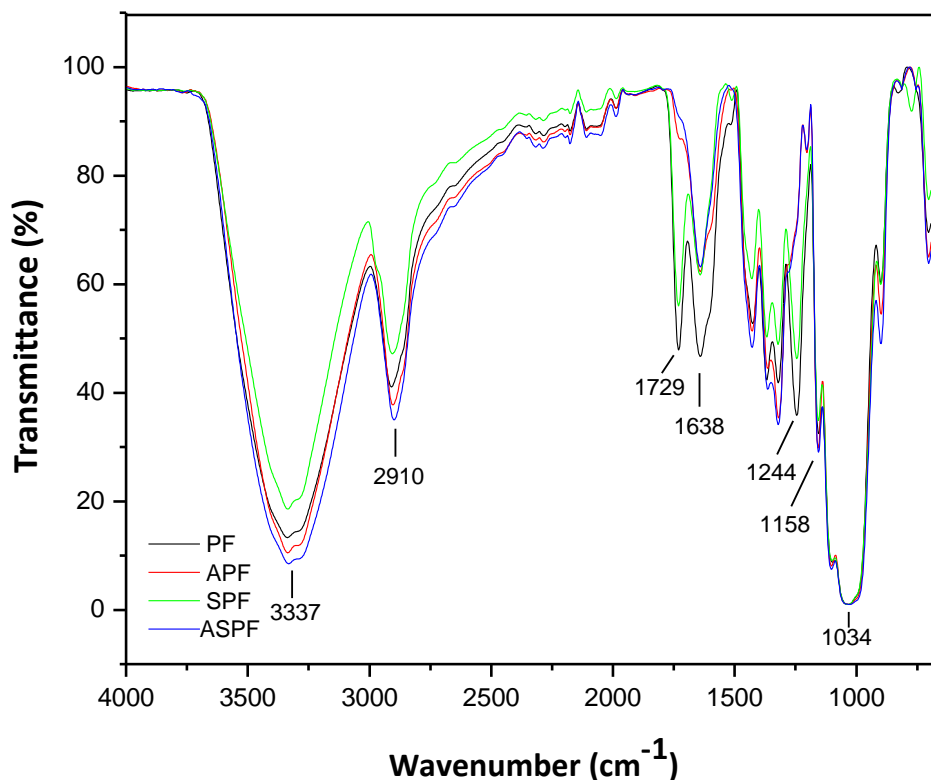


Figure 4.1 Normalized ATR-FTIR spectra of untreated (PF), alkali treated (APF), silane treated (SPF) and alkali-silane treated (ASPF) PALFs.

Table 4.1 Assignments of FTIR bands for untreated-, alkali treated-, silane treated- and alkali-silane treated pineapple leaf fibers.

Band wavelength (cm ⁻¹)	Associated chemical group	Untreated PALF	Alkali treated PALF	Silane treated PALF	Alkali-Silane treated PALF
3200-3600	-OH intensity	Low	High	Low	High
1240-1247	Lignin peak	Predominant	Removed	Reduced	Removed
1630-1650	Hemicellulose peak	Predominant	Reduced	Reduced	Reduced
1729	Pectin-Wax	Present	Removed	Present	Removed
2910, 2850	Methylene group	Present	-	Reduced	-
1058	Si-O-Si	-	-	Present	-



4.2 Thermal decomposition behavior of PALF and its composites

4.2.1 Effect of fiber treatments on thermal decomposition behavior

The thermogravimetric analysis (TGA) and derivative thermogravimetric (DTG) curves are used to determine decomposition behavior of materials. Non-isothermal TG and DTG curves for untreated, alkali treated, silane treated and alkali-silane treated PALF are shown in Figure 4.2a and 4.2b, respectively. It is seen that the curves for untreated and treated PALF showed a three-step weight loss. The initial weight loss observed below 100°C with PALF is due to evaporation of water. The second stage weight loss between 200°C and 350°C is due to decomposition of hemicelluloses [125]. The third stage weight loss between 400°C and 450°C corresponds to the thermal degradation of lignin and cellulose [125]. From non-isothermal TG and DTG curves of untreated and treated fibers, the thermal stability of alkali treated and silane treated fiber is better than that of the untreated fiber. This may be due to that the treated fibers have lower lignin content, wax and oil covering materials resulting in distension of crystalline cellulose order. The distension of the crystalline region would hinder the gas movement [125], resulting in better thermal stability. Figure 4.2c shows heat flow curves of untreated, alkali treated, silane treated and alkali-silane treated PALF. The results show that the degradation of all samples are exothermic process.

To compare effect of fiber treatments on thermal decomposition, the thermal decomposition data are summarized in Table 4.2. T_{onset} represents the onset degradation temperature. T_{max} represents the temperature at the maximum weight-loss rate, $(d\alpha/dt)_{\text{max}}$ represents the weight-loss rate at maximum temperature. T_d and ΔH_d represent the peak temperature and the enthalpy associated with the thermal degradation process, respectively. It is seen that T_{onset} and T_{max} of the treated fiber are higher than those of the untreated PALF. Oppositely, $(d\alpha/dt)_{\text{max}}$ and ΔH_d of PALF are higher than that of the treated fiber. Moreover, the thermal stability of APF and ASPF are comparable. APF seem to has the highest thermal stability among all sample examined.



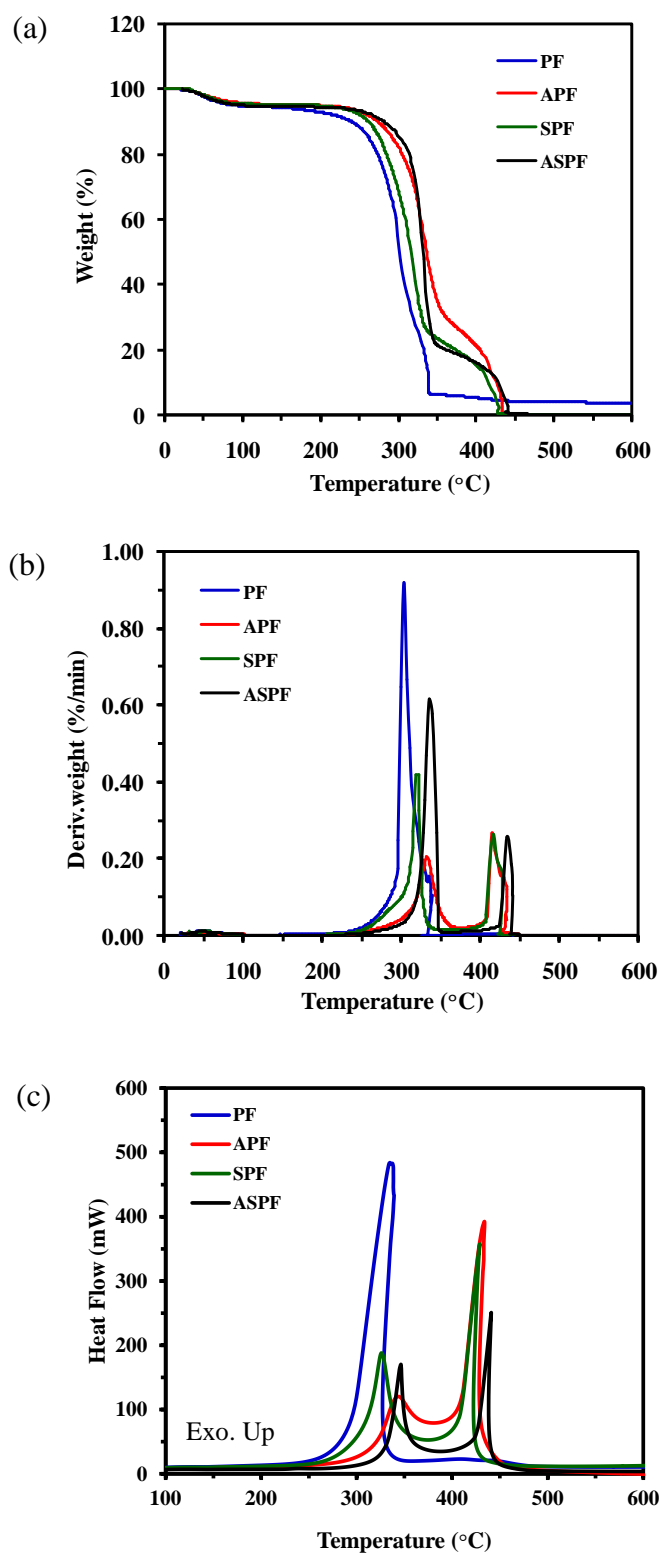


Figure 4.2 Non-isothermal TG (a), DTG (b) and heat flow (c) curves of untreated and treated fibers under heating rate of 10°C/min in air.



Table 4.2 Thermo-oxidative data for the first major weight-loss step of the untreated and treated fibers obtained from non-isothermal TG measurements.

sample	$T_{\text{onset}} (^{\circ}\text{C})$	$(\text{d}\alpha/\text{d}t)_{\text{max1}}$ (%/min)	$T_{\text{max}} (^{\circ}\text{C})$	ΔH_{dl} (kJ/g)	$T_{\text{d}} (^{\circ}\text{C})$
PF	277	64.5	300	7.36	335
APF	306	20.4	333	3.10	434
SPF	290	41.7	320	2.83	309
ASPF	319	61.9	332	4.95	440

4.2.2 Effect fiber loadings on thermal decomposition

Thermal degradation of composites with varied PALF loading is also studied. Non-isothermal TG and DTG curves for neat SEBS, PF10 and PF20 are presented in Figure 4.3a (TG) and 4.3b (DTG), respectively. As seen from TG curves, the non-isothermal TG profile of SEBS, PF10 and PF20 reveals only a single weight-loss step at the temperature range around 250–550°C. However, the thermal degradation of neat SEBS and the composites would undergo the complex mechanisms. This is due to the fact that the degradation mechanism in air involves both thermal and thermo-oxidative reactions [127]. Figure 4.3c shows heat flow curves of neat SEBS, PF10 and PF20. The results show that the degradation of all samples are exothermic process. The shapes of heat flow curve are clearly different depending on fiber loading.

To compare effect fiber loading on thermal decomposition, the thermal decomposition data summarized in Table 4.3. It is seen that T_{onset} values of the composites decrease with increasing fiber loading. In contrast, T_{max} and T_{d} of composites were increased with increases PALF content. As the fiber volume fraction increases in the composites, there is a decrease in thermal stability of the composites [31]. These results are logical since PALF has a much lower thermal stability than SEBS.



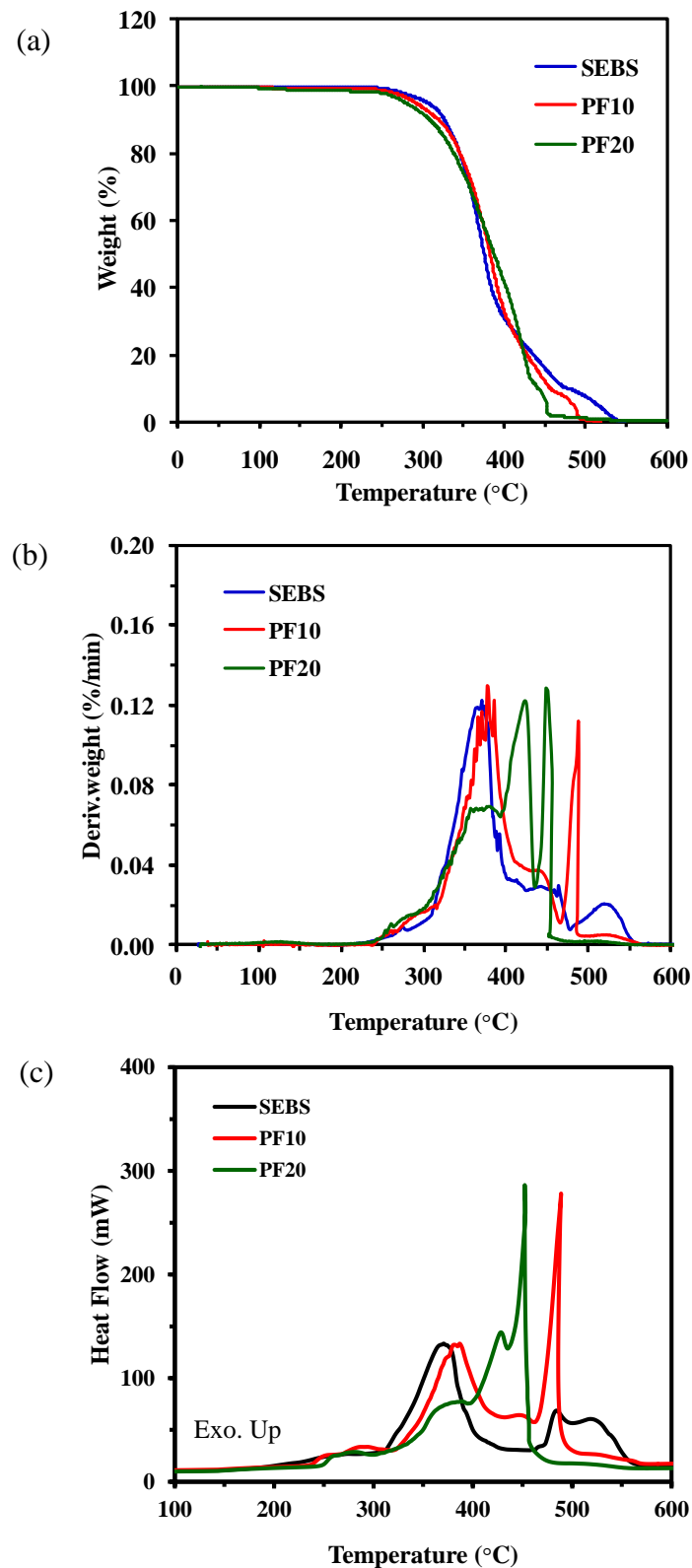


Figure 4.3 Non-isothermal TG (a), DTG (b) and heat flow (c) curves of neat SEBS and its composites containing of 10 and 20 wt% untreated PALF under heating rate of 10°C/min in air.



Table 4.3 Thermo-oxidative data for the first weight-loss step of neat SEBS, PF10 and PF20 obtained from non-isothermal TG measurements.

sample	T_{onset} (°C)	$(d\alpha/dt)_{\text{max1}}$ (%/min)	T_{max} (°C)	ΔH_{dt} (kJ/g)	T_{d} (°C)
SEBS	336	12.0	369	3.66	370
PF10	335	12.5	378	2.35	381
PF20	318	12.2	424	7.26	456

4.2.3 Effect of compatibilizer loading on thermal decomposition for silane treated fiber systems

In this work, the silane treated fiber system is selected to investigate effect of compatibilizer loading. Non-isothermal TG and DTG curves of SPF10-MA3, SPF10-MA5 and SPF10-MA7 are presented in Figures 4.4a and 4.4b, respectively. It is seen that, no significant change in the TG curves of the silane treated fiber composites with increase SEBS-g-MA content. This result is similar to those of the other compatibilized composite systems [127]. Moreover, it is seen that the DTG curves is likely the same for the composites. Figure 4.4c shows heat flow curves of SPF10-MA3, SPF10-MA5 and SPF10-MA7. The results show that the degradation of all samples are exothermic process. No significant change in heat flow curves is obviously observed.

Table 4.4 shows thermo-oxidative data for the first major weight-loss step of silane treated fiber composites with SEBS-g-MA loading. It is seen that T_{onset} , T_{max} and T_{d} values of the composites slightly increased with increasing SEBS-g-MA loading. Moreover, no significant change in other decomposition data are observed with varied compatibilizer loading.



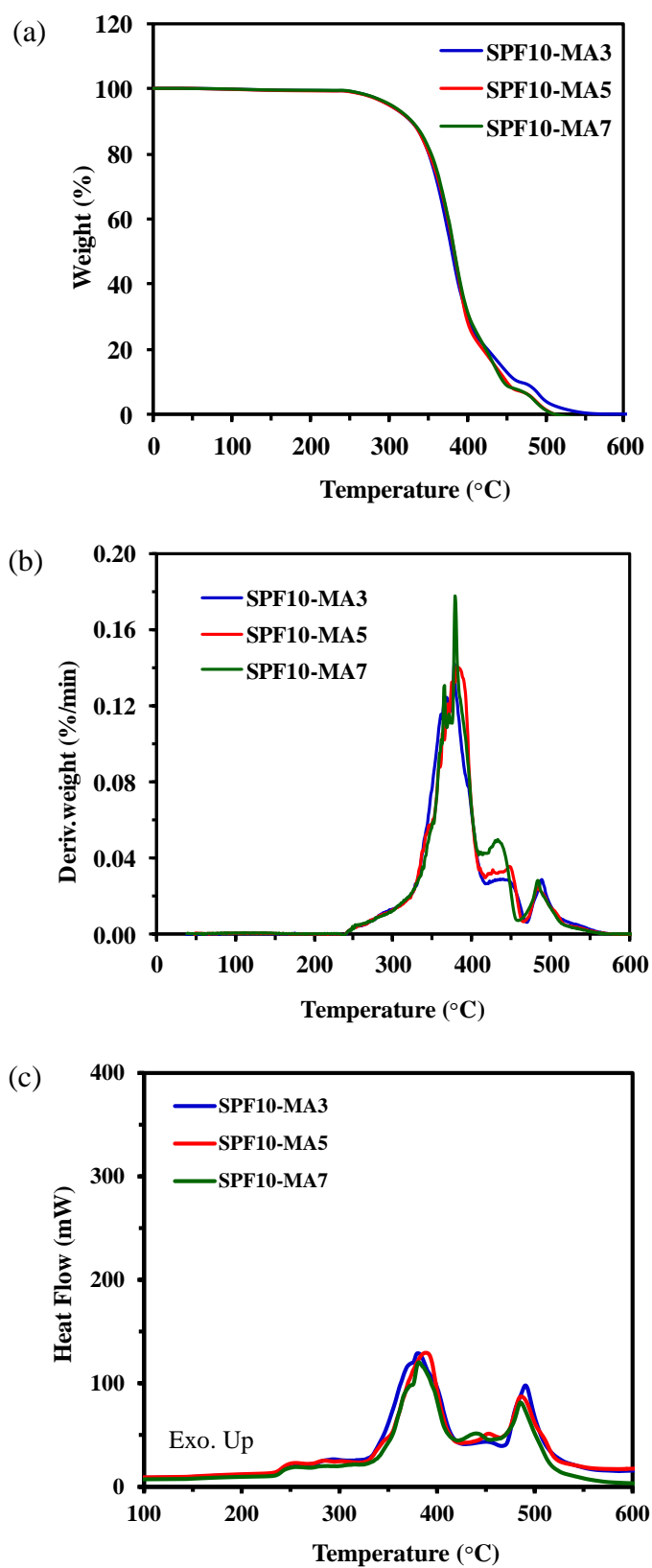


Figure 4.4 Non-isothermal TG (a), DTG (b) and heat flow (c) curves of SPF10-MA3, SPF10-MA5 and SPF10-MA7 under heating rate of 10°C/min in air.



Table 4.4 Thermo-oxidative data for the first weight-loss step of SPF10-MA3, SPF10-MA5 and SPF10-MA7 obtained from non-isothermal TG measurements.

sample	$T_{\text{onset}} (^{\circ}\text{C})$	$(\text{d}\alpha/\text{d}t)_{\text{max1}}$ (%/min)	$T_{\text{max}} (^{\circ}\text{C})$	ΔH_{dl} (kJ/g)	$T_{\text{d}} (^{\circ}\text{C})$
SPF10-MA3	339	12.3	382	2.86	380
SPF10-MA5	348	14.0	382	2.51	387
SPF10-MA7	348	13.2	383	2.11	381

4.2.4 Effect of fiber treatments and compatibilizer on thermal decomposition

Non-isothermal TG and DTG curves of untreated and treated fiber containing composites with 5 wt% SEBS-g-MA are shown in Figures 4.5a and 4.5b, respectively. It is seen that the thermal stability of composites is not largely different from that of neat SEBS. However, for the treated fiber composites, the samples show the higher thermal stability compared with the untreated fiber composites. Among the treated fiber composites, APF10-MA5 and ASPF10-MA5 show slightly higher thermal stability when compared to SPF10-MA5. Figure 4.5c shows heat flow curves of untreated and treated fiber containing composites with 5 wt% SEBS-g-MA. The results show that the degradation of all samples are exothermic process. At temperature $> 400^{\circ}\text{C}$, the shapes of heat flow curve are clearly depended on the surface treatment methods.

To compare the effect of fiber treatments on thermal decomposition of compatibilized composites, the thermal decomposition data in air are compared and summarized in Table 4.5. It is seen that the onset degradation temperature of APF10-MA5 are higher than those of composites. Furthermore, T_{max} and T_{d} of SPF10-MA5 are higher than that of the other treated fiber composites. The results suggests that surface treatment improves thermal resistance of PALF/SEBS composites due to the less amount of lignin present in the treated fiber composite than untreated fiber composite. Note that higher content of lignin in untreated fibers produces more char. Moreover, as the interaction between acid groups of the maleic anhydride groups and hydrophilic groups on the fiber surfaces increased, the thermal stability slightly increased for the treated fiber composites.



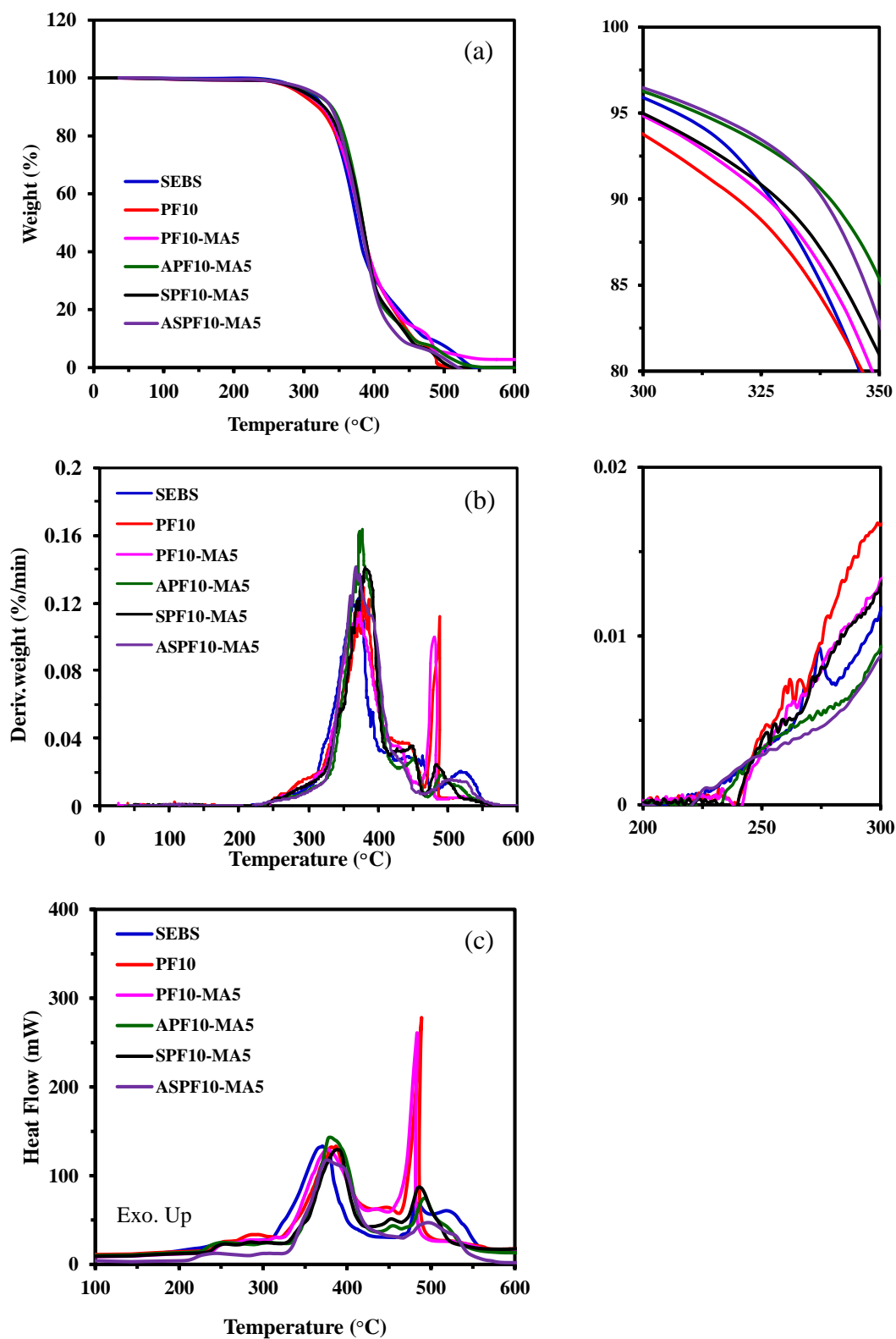


Figure 4.5 Non-isothermal TG (a), DTG (b) and heat flow (c) curves of neat SEBS, PF10, PF10-MA5, APF10-MA5, SPF10-MA5 and ASPF10-MA5 under heating rate of 10°C/min in air.



Table 4.5 Thermo-oxidative data for the first major weight-loss step of SEBS, PF10, PF10-MA5, APF10-MA5, SPF10-MA5 and ASPF10-MA5 obtained from non-isothermal TG measurements.

sample	$T_{\text{onset}} (^{\circ}\text{C})$	$(\text{d}\alpha/\text{d}t)_{\text{max1}}$ (%/min)	$T_{\text{max}} (^{\circ}\text{C})$	ΔH_{dl} (kJ/g)	T_{d} ($^{\circ}\text{C}$)
SEBS	336	12.0	369	3.66	370
PF10	335	12.5	378	2.35	381
PF10-MA5	334	11.1	373	2.07	375
APF10-MA5	350	15.8	376	3.25	379
SPF10-MA5	348	14.0	382	2.51	387
ASPF10-MA5	342	84.8	367	7.64	376



4.3 Tensile properties

4.3.1 Effect of fiber loadings on tensile properties

The stress-strain curves of neat SEBS and the composites containing 10 (PF10) and 20 (PF20) wt% untreated PALF in longitudinal (LD) and transverse (TD) direction are shown in Figures 4.6a and 4.6b, respectively. For longitudinal direction, it is seen that the elongation at break of SEBS is higher than those of the composites. SEBS exhibits high extensibility similar to the typical elastomer. For the composites, the stress is higher than that of the neat matrix and the stress is increased with fiber loading. At the strain $> 300\%$, the composites exhibit strain hardening effect. However, the strain hardening behavior is not observed for SEBS. In transverse direction, the stress-strain curves of neat SEBS and the composites show the same behavior as in LD. However, the tensile stress of PF10 and PF20 are nearly the same except for that the tensile strength of PF10 is higher than those of PF20. Moreover, the tensile stress of SEBS and the composites are higher in LD than in TD.

To compare the effect of fiber loadings on tensile properties for the composites both in LD and TD, the tensile properties data are compared and summarized in Table 4.6. It is interesting to note that the modulus at 50 and 100% of PF10 and PF20 are higher in LD than in TD. The young's modulus of composites in LD was increased with increased PALF loading. In contrast, the young's modulus of composites in TD was decreased with increased PALF loading. However, at the same fiber content, the composites show higher young's modulus in LD than in TD. The elongation at break of composites in LD and TD are decreased with increased PALF loading. Normally, the incorporation of cellulosic fibers into the polymer matrices decreases the elasticity and flexibility of the polymer chains. This arises from the loss of continuous connectivity of the matrix phase.



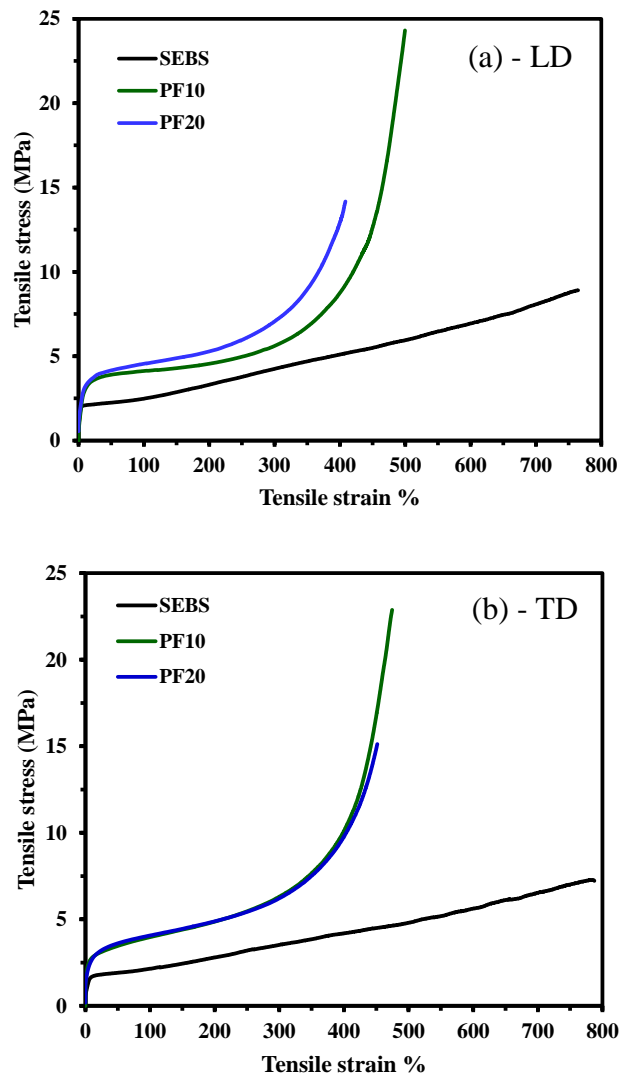


Figure 4.6 Stress-strain curves of neat SEBS, PF10 and PF20 in longitudinal (a) and transverse (b) direction.

Figure 4.7 shows the secant modulus at 1% strain of SEBS, PF10 and PF20 in LD and TD. For longitudinal direction, it is seen that the secant modulus of SEBS is slightly higher than that of PF10. The secant modulus in LD is slightly dependent on fiber loading. For transverse direction, the secant modulus progressive increases with fiber loading. Interestingly, the secant modulus of composites increased with increases PALF content. However, the secant modulus of SEBS is higher in LD than in TD, whereas secant modulus of the composites are higher than in TD than in LD.



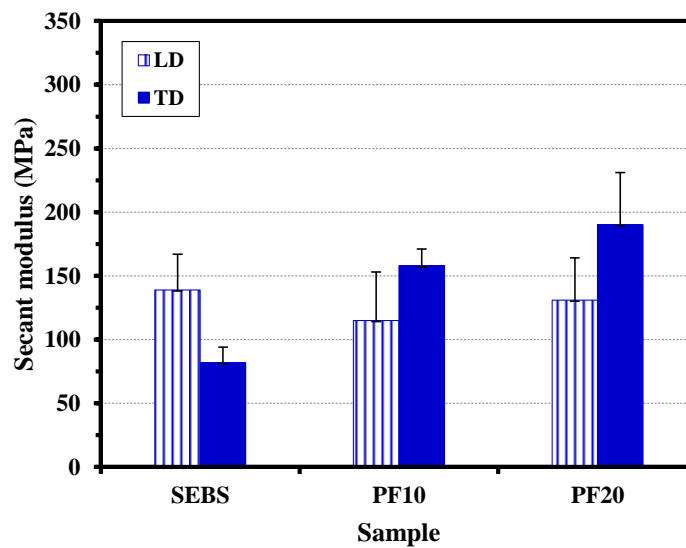


Figure 4.7 Effect of fiber loadings on secant modulus for the untreated fiber composites in LD and TD.

Table 4.6 Tensile properties of SEBS, PF10 and PF20 in LD and TD.

sample	Tensile strength (MPa)	Elongation at break (%)	Modulus at 50% (MPa)	Modulus at 100% (MPa)	Young's modulus (MPa)
LD					
SEBS	8.9 ± 0.8	764 ± 33	2.30 ± 0.12	2.56 ± 0.12	26.7 ± 13.1
PF10	22.8 ± 0.8	491 ± 9	3.85 ± 0.17	4.09 ± 0.14	28.8 ± 0.7
PF20	13.6 ± 0.5	409 ± 6	4.05 ± 0.24	4.37 ± 0.21	35.1 ± 7.2
TD					
SEBS	6.9 ± 0.3	736 ± 39	1.88 ± 0.08	2.11 ± 0.08	22.5 ± 4.5
PF10	21.9 ± 0.9	473 ± 2	3.35 ± 0.16	3.85 ± 0.18	26.2 ± 0.4
PF20	16.3 ± 0.4	461 ± 5	3.67 ± 0.05	4.12 ± 0.04	15.2 ± 1.1



4.3.2 Effect of fiber treatments on tensile properties of composites

The stress-strain curves of SEBS, untreated- and treated fiber composites in LD and TD are presented in Figures 4.8a and 4.8b, respectively. For stress-strain curves of composites in LD (Figure 4.8a), it is seen that the tensile stress of treated fiber composites are higher than those of SEBS and PF10. ASPF10 shows highest tensile stress when compared to APF10 and SPF10 at 50-300% strain. In TD, the tensile stress of PF10 (Figure 4.8b) is slightly higher than those of SEBS and the treated fiber composites. The obtained results suggest that the effect of fiber treatments slightly affect the tensile properties in TD.

To quantitatively compare the effect of fiber treatments on tensile properties for the composites in LD and TD, the tensile properties data are presented in Table 4.7. The young's modulus of the treated fiber composites are higher in LD than in TD. Interestingly, the young's modulus in TD of SPF10 in LD are about 5 times that of SPF10. Moreover, the modulus at 50 and 100% of treated fiber composites in LD is clearly higher in LD than in TD. Moreover, the tensile strength in LD and TD of treated fiber composites is not significantly different.

Figure 4.9 shows the effect of fiber treatments on secant modulus for the composites in LD and TD. In LD, the secant modulus of the composites increase with fiber loading. SPF10 shows highest secant modulus in LD. However, the addition of treated fiber is not significantly affect the secant modulus in TD.



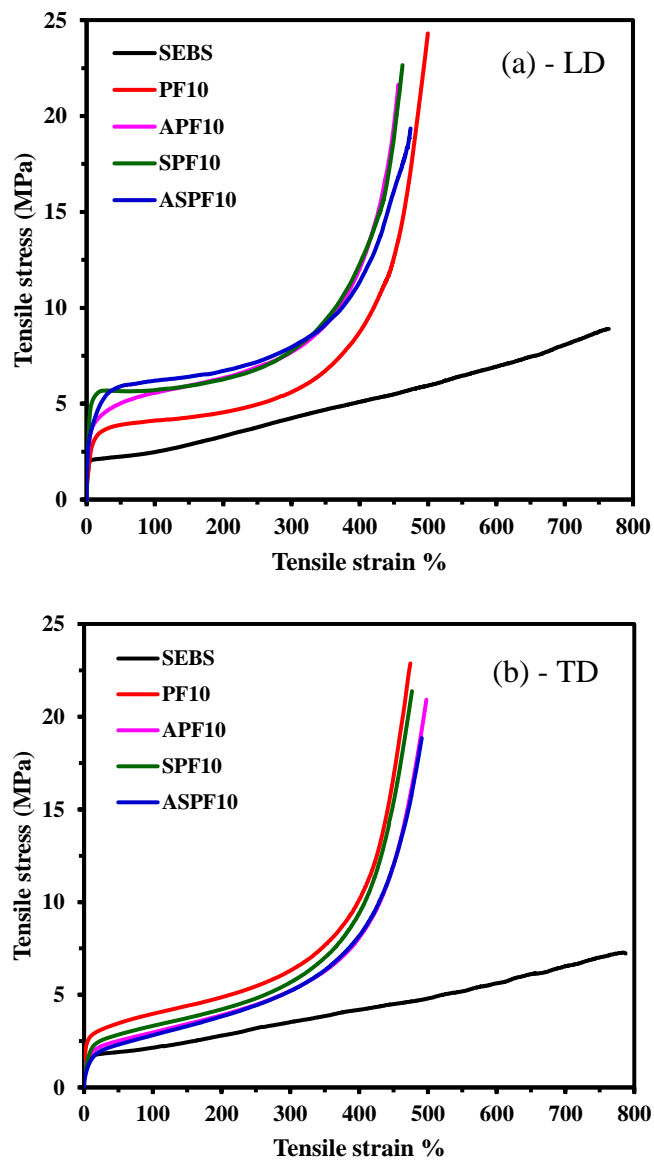


Figure 4.8 Stress-strain curves of neat SEBS, PF10, APF10, SPF10 and ASPF10 in longitudinal (a) and transverse (b) directions.



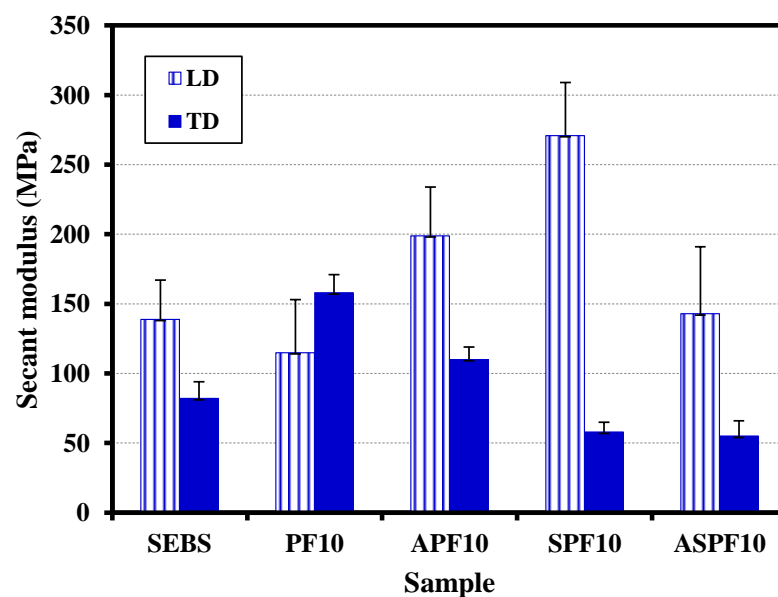


Figure 4.9 Secant modulus at 1% strain of neat SEBS, PF10, APF10, SPF10 and ASPF10 in longitudinal and transverse direction.

Table 4.7 Tensile properties of treated PALF composites in comparison with SEBS and PF10 in LD and TD.

sample	Tensile strength (MPa)	Elongation at break (%)	Modulus at 50% (MPa)	Modulus at 100% (MPa)	Young's modulus (MPa)
LD					
SEBS	8.9 ± 0.8	764 ± 33	2.30 ± 0.12	2.56 ± 0.12	26.7 ± 13.1
PF10	22.8 ± 0.8	491 ± 9	3.85 ± 0.17	4.09 ± 0.14	28.8 ± 0.7
APF10	20.0 ± 2.4	454 ± 8	5.22 ± 0.22	5.73 ± 0.18	42.7 ± 14.9
SPF10	21.6 ± 0.9	459 ± 11	5.52 ± 0.12	5.60 ± 0.11	135.5 ± 32.0
ASPF10	19.4 ± 1.0	485 ± 7	5.83 ± 0.21	6.14 ± 0.19	32.9 ± 6.4
TD					
SEBS	6.9 ± 0.3	736 ± 39	1.88 ± 0.08	2.11 ± 0.08	22.5 ± 4.5
PF10	21.9 ± 0.9	473 ± 2	3.35 ± 0.16	3.85 ± 0.18	26.2 ± 0.4
APF10	20.3 ± 0.8	487 ± 15	2.54 ± 0.05	3.00 ± 0.06	22.8 ± 1.2
SPF10	20.5 ± 0.7	476 ± 8	2.81 ± 0.04	3.30 ± 0.05	23.0 ± 0.6
ASPF10	18.12 ± 0.9	489 ± 6	2.30 ± 0.13	2.79 ± 0.12	18.9 ± 2.35



4.3.3 Effect of compatibilizer contents on tensile properties of untreated and treated fiber composites systems

The effect of compatibilizer loading on longitudinal tensile properties for untreated- and treated-fiber composites is shown in Figure 4.10. For the untreated fiber system, it is found that PF10-MA7 shows the highest tensile stress (Figure 4.10a) in the strain range of 10 – 300%. For alkali treated fiber systems (Figure 4.10b), the highest tensile stress of composites is observed for APF10-MA5. In the case of silane treated fiber systems (Figure 4.10c), it is seen that the tensile stress of SPF10-MA5 show highest value.

The effect of compatibilizer contents on tensile properties of untreated and treated fiber composites systems in LD are also quantitatively summarized in Table 4.8. In the case of untreated fiber system, it is seen that tensile data of the composites slightly change with increasing SEBS-g-MA loading. However, the modulus at 50 and 100% are found to slightly increase with SEBS-g-MA loading. Furthermore, the young's modulus of PF10-MA7 shows the highest value compared to those of PF10-MA3 and PF10-MA5.

For alkali treated fiber systems, it is interesting to note that the young's modulus of APF10-MA5 are much higher than neat SEBS and the other composites. Moreover, the modulus at 50 and 100% are increased with SEBS-g-MA loading compared to APF10.

In the case of silane treated fiber system, it is surprising to note that the young's modulus of SPF10 are much higher than silane treated fiber composites with compatibilizer. This effect may be due to the weakly interaction between alkyl groups in triethoxy vinyl silane with maleic anhydride linked SEBS, which lead to adhesion of fiber and SEBS matrix poorly. Moreover, the modulus at 50 and 100% shows no significant change with increasing SEBS-g-MA content, indicating that SEBS-g-MA had a little influence on the tensile properties of silane treated fiber composite systems. From the results, the use of the treated fibers along with SEBS-g-MA compatibilizer can be used to for improvement in tensile properties of the elastomer composites [131]. Therefore, the optimum compatibilizer loading used throughout this work is 5 wt%.



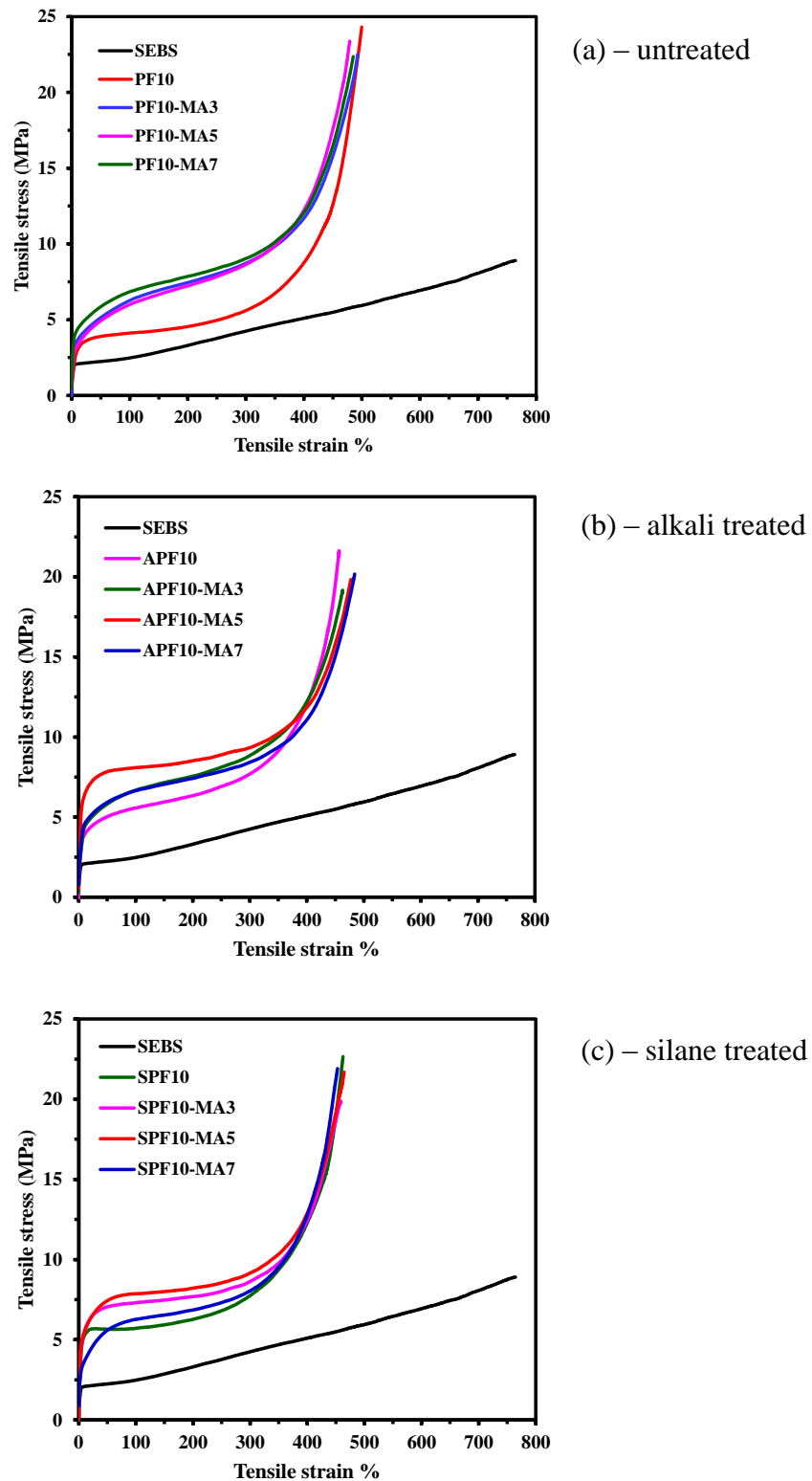


Figure 4.10 Effect of compatibilizer contents on stress-strain curves of (a) untreated-, (b) alkali- and (c) silane- treated fiber composite systems in longitudinal direction.



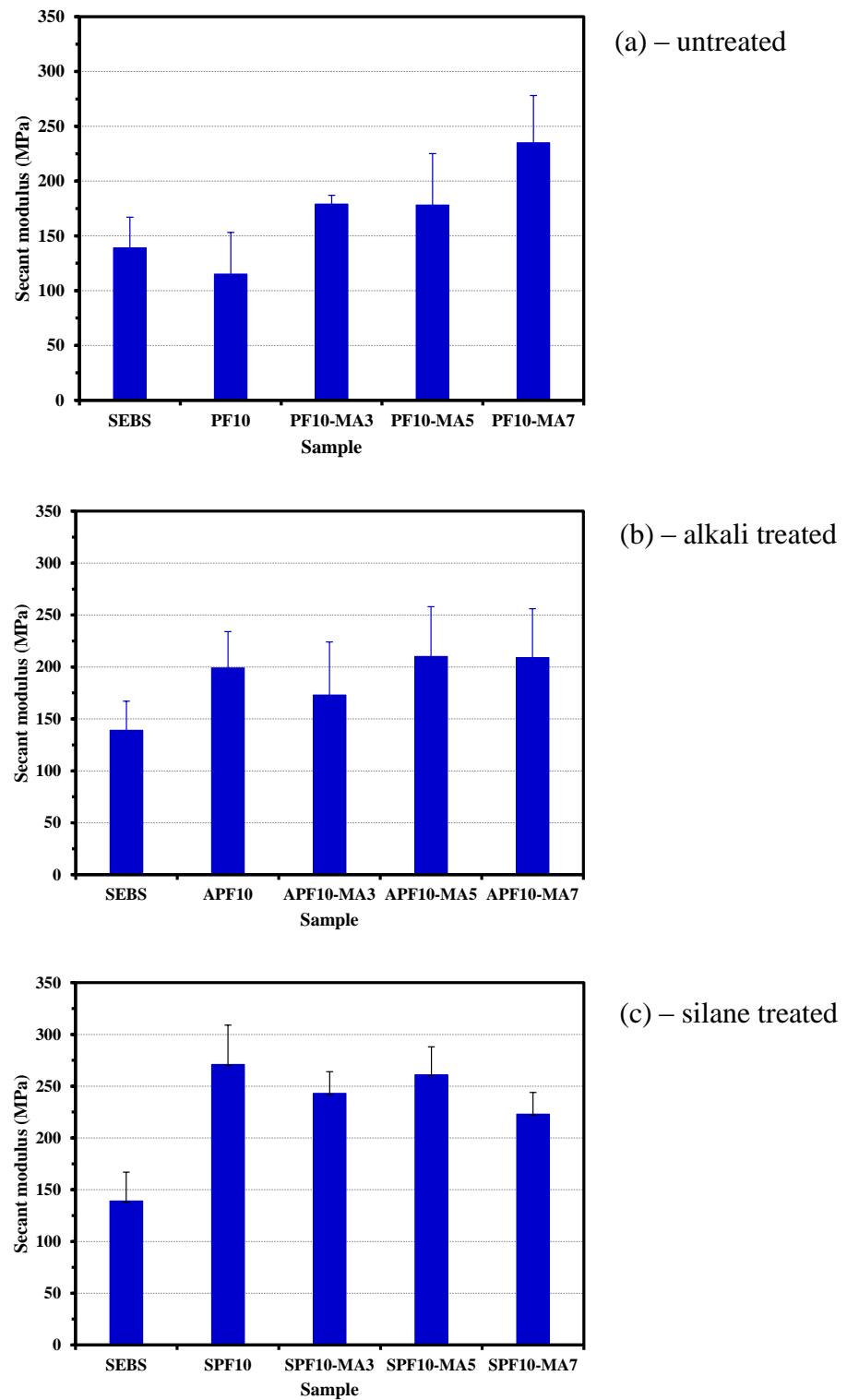


Figure 4.11 Effect of compatibilizer contents on secant modulus at 1% strain of (a) untreated-, (b) alkali- and (c) silane- treated fiber composite systems in longitudinal direction.



The effect of compatibilizer loading on secant modulus for untreated- and treated-fiber composites is shown in Figure 4.11. Similarly, the secant modulus of untreated and alkali treated composites systems mostly increase with increasing compatibilizer content. In the case of silane treated fiber system (Figure 4.11c), the secant modulus of composites are nearly the same with compatibilizer loading.

Table 4.8 Tensile properties of 10 wt% treated PALF with and without compatibilizer composites in comparison with SEBS and untreated fiber system in longitudinal direction.

sample	Tensile strength (MPa)	Elongation at break (%)	Modulus at 50% (MPa)	Modulus at 100% (MPa)	Young's modulus (MPa)
SEBS	8.9 ± 0.8	764 ± 33	2.30 ± 0.12	2.56 ± 0.12	26.7 ± 13.1
PF10	22.8 ± 0.8	491 ± 9	3.85 ± 0.17	4.09 ± 0.14	28.8 ± 0.7
PF10-MA3	20.3 ± 2.6	470 ± 18	5.11 ± 0.22	6.24 ± 0.22	26.3 ± 11.0
PF10-MA5	20.8 ± 1.9	474 ± 7	4.84 ± 0.66	6.02 ± 0.71	25.2 ± 13.9
PF10-MA7	21.6 ± 0.6	480 ± 4	5.87 ± 0.11	6.83 ± 0.08	49.8 ± 7.5
APF10	20.0 ± 2.4	454 ± 8	5.22 ± 0.22	5.73 ± 0.18	42.7 ± 14.9
APF10-MA3	18.4 ± 2.2	460 ± 16	6.15 ± 0.20	7.01 ± 0.19	57.0 ± 14.8
APF10-MA5	19.3 ± 0.7	475 ± 6	7.68 ± 0.13	7.99 ± 0.09	135.9 ± 18.5
APF10-MA7	19.3 ± 1.0	477 ± 7	6.16 ± 0.19	6.88 ± 0.18	82.4 ± 36.4
SPF10	21.6 ± 0.9	459 ± 11	5.52 ± 0.12	5.60 ± 0.11	135.5 ± 32.0
SPF10-MA3	18.0 ± 1.2	448 ± 9	6.93 ± 0.17	7.25 ± 0.14	93.9 ± 12.4
SPF10-MA5	20.7 ± 1.4	456 ± 14	7.35 ± 0.06	7.79 ± 0.06	98.4 ± 17.0
SPF10-MA7	20.0 ± 1.4	445 ± 6	5.73 ± 0.30	6.02 ± 0.29	24.2 ± 2.99



4.3.4 Effect of compatibilizer with fiber treatments on tensile properties of the composites

The tensile properties of neat SEBS, untreated- and treated-fiber composites with and without the presence of 5 wt% SEBS-g-MA in LD are shown in Figure 4.12 (column I). For alkali treated fiber composites (Figure 4.12Ia), It is seen that the tensile stress of composites clearly increases with addition of the treated fiber. Interestingly, the further improvement in tensile stress is observed in the alkali treated fiber composites with 5 wt% SEBS-g-MA.

In the case of silane treated fiber system (Figure 4.12Ib), It is seen that SPF10-MA5 also show the higher tensile stress when compared to PF10-MA5 and SPF10.

For the composites containing alkali-silane treated fiber (Figure 4.12Ic), It is seen that the tensile stress of ASPF10-MA5 in the strain range of 100-200% is higher than PF10-MA5 and ASPF10 composites.

To quantitatively compare the effect of compatibilizer loading on tensile properties of untreated- and treated-fiber composites, the comparative data of tensile properties are summarized in Table 4.9. It is seen that the tensile strength is not significantly different for alkali-, silane-, and alkali-silane treated fiber composites when compared to untreated sample. Furthermore, the modulus at 50 and 100% of alkali-, silane-, and alkali-silane treated PALF composites were increased compared to untreated fiber composites. It is interesting to note that the highest young's modulus was observed for APF10-MA5. The young's modulus of SPF10 are much higher than untreated fiber composites with and without compatibilizer. For alkali-silane treated fiber composites, the young's modulus of ASPF10 and ASPF10-MA5 is not largely different when compared to the untreated fiber composites.

Effect of compatibilizer loading on tensile properties of untreated- and treated-fiber composites in TD is also shown in column II of Figure 4.12. It is seen that the treated fiber and compatibilizer loading slightly affect the tensile properties in TD. Moreover, the tensile stress in TD are mostly lower in TD than in LD. The quantitative tensile data in TD are also shown in Table 4.9.



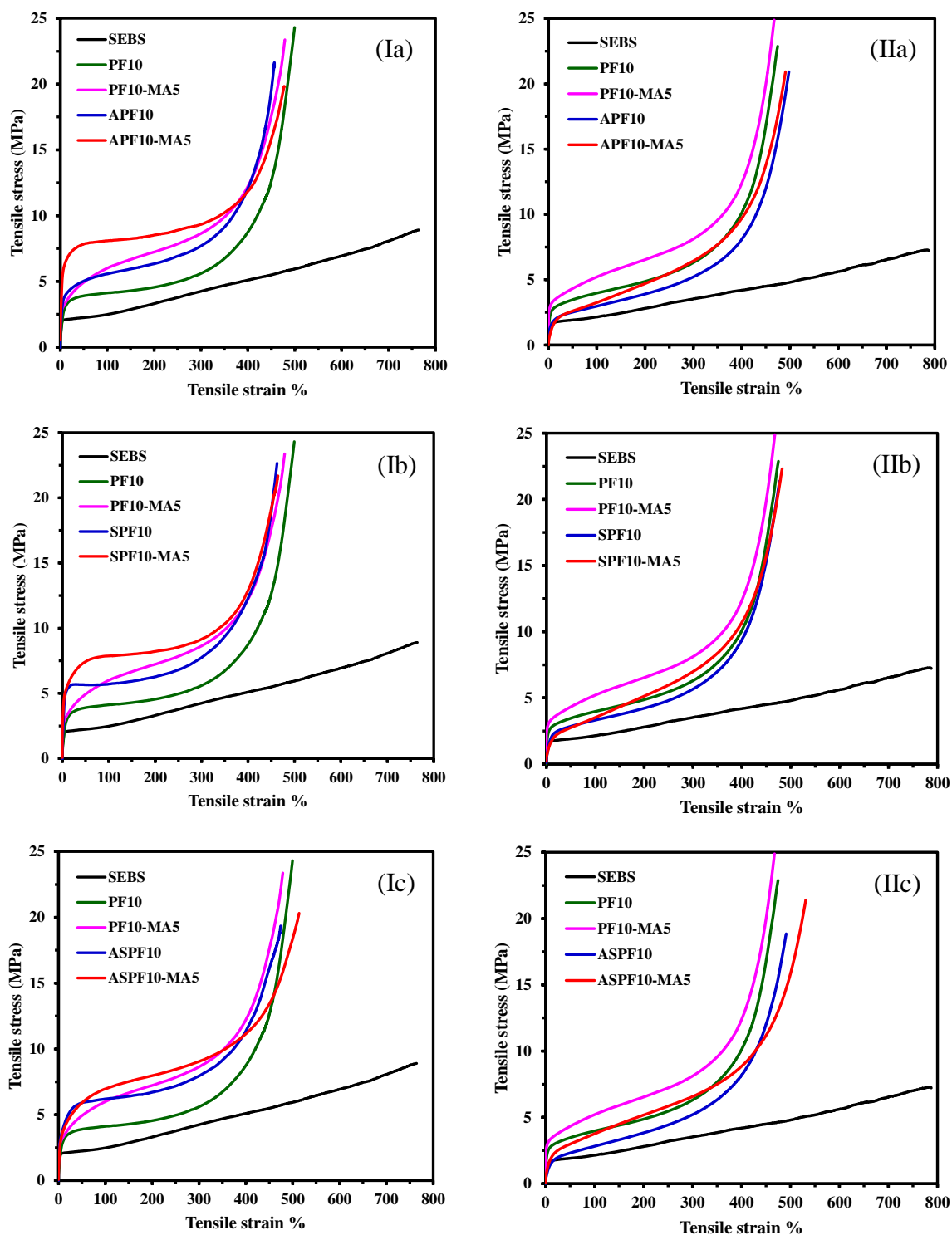


Figure 4.12 Effect of compatibilizer loading on stress-strain curves in longitudinal (I) and transverse (II) direction of the alkali-treated (a), silane-treated (b) and alkali-silane-treated (c) fiber composites systems.



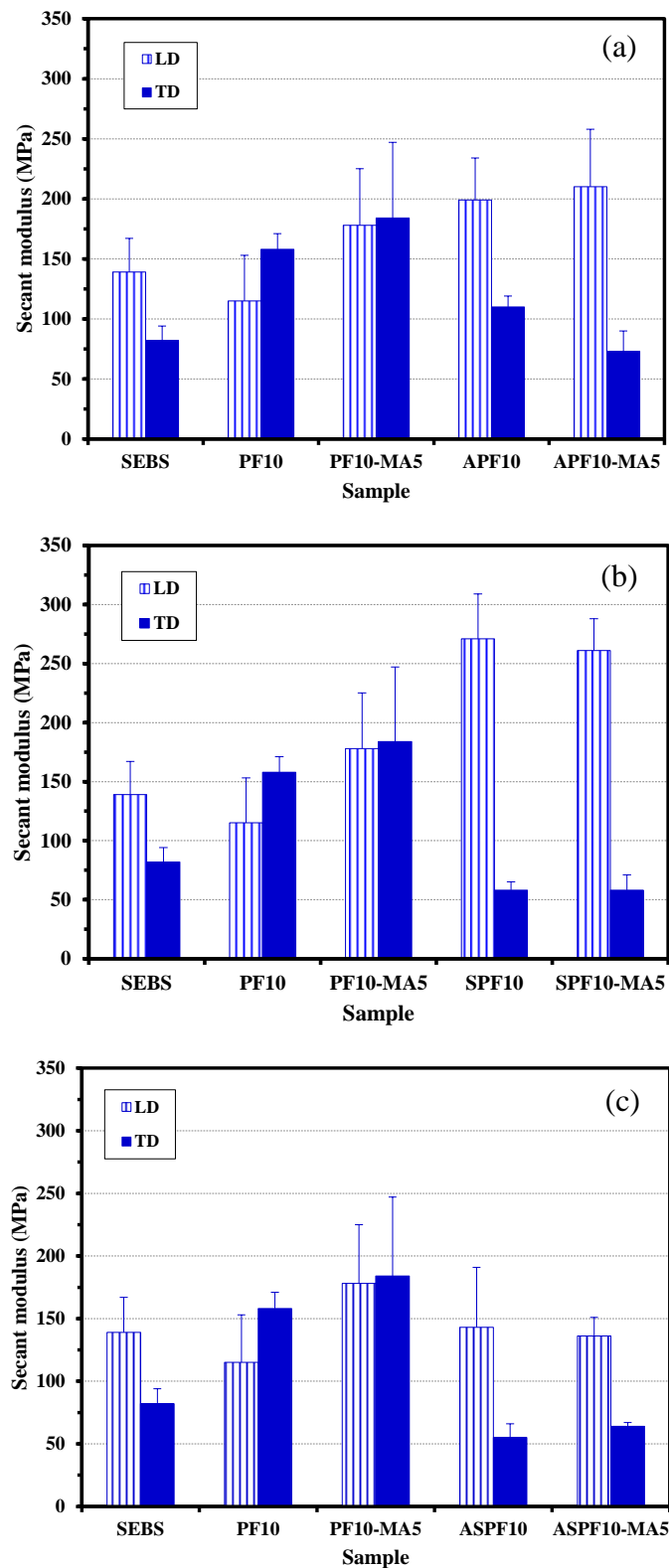


Figure 4.13 Effect of compatibilizer loading on secant modulus at 1% strain in longitudinal (LD) and transverse (TD) direction of the alkali-treated (a), silane-treated (b) and alkali-silane- treated (c) fiber composites systems.



Figure 4.13 shows the effect of compatibilizer with fiber treatments on secant modulus for the composites in LD and TD. The secant modulus for the untreated fiber system with and without compatibilizer is not significantly different in LD and TD. For alkali treated fiber composites (Figure 4.13a), it is seen that the secant modulus of composites in LD is much higher in LD than in TD. Similarly, the secant modulus are much higher in LD than in TD for APF10-MA5. In the case of silane treated fiber system (Figure 4.13b), it is seen that the similar trend of the secant modulus is observed for the treated system with and without compatibilizer. For the composites containing alkali-silane treated fiber (Figure 4.12Ic), it is seen that the secant modulus both in LD and in TD is much lower than the corresponding alkali- and silane-treated systems. However, the secant modulus is higher in LD than in TD.

Table 4.9 Tensile properties of treated fibers with 5 wt% compatibilizer composites in comparison with SEBS and untreated fiber system.

sample	Tensile strength (MPa)	Elongation at break (%)	Modulus at 50% (MPa)	Modulus at 100% (MPa)	Young's modulus (MPa)
LD					
SEBS	8.9 ± 0.8	764 ± 33	2.30 ± 0.12	2.56 ± 0.12	26.7 ± 13.1
PF10	22.8 ± 0.8	491 ± 9	3.85 ± 0.17	4.09 ± 0.14	28.8 ± 0.7
PF10-MA5	20.8 ± 1.9	474 ± 7	4.84 ± 0.66	6.02 ± 0.71	25.2 ± 13.9
APF10	20.0 ± 2.4	454 ± 8	5.22 ± 0.22	5.73 ± 0.18	42.7 ± 14.9
APF10-MA5	19.3 ± 0.7	475 ± 6	7.68 ± 0.13	7.99 ± 0.09	135.9 ± 18.5
SPF10	21.6 ± 0.9	459 ± 11	5.52 ± 0.12	5.60 ± 0.11	135.5 ± 32.0
SPF10-MA5	20.7 ± 1.4	456 ± 14	7.35 ± 0.06	7.79 ± 0.06	98.4 ± 17.0
ASPF10	19.4 ± 1.0	485 ± 7	5.83 ± 0.21	6.14 ± 0.19	32.9 ± 6.4
ASPF10-MA5	20.8 ± 0.9	514 ± 12	5.57 ± 0.37	6.66 ± 0.37	23.6 ± 7.6
TD					
SEBS	6.9 ± 0.3	736 ± 39	1.88 ± 0.08	2.11 ± 0.08	22.5 ± 4.5
PF10	21.9 ± 0.9	473 ± 2	3.35 ± 0.16	3.85 ± 0.18	26.2 ± 0.4
PF10-MA5	22.9 ± 1.5	469 ± 2	3.60 ± 0.52	4.41 ± 0.57	26.8 ± 2.0
APF10	20.3 ± 0.8	487 ± 15	2.54 ± 0.05	3.00 ± 0.06	22.8 ± 1.2
APF10-MA5	20.3 ± 0.9	496 ± 8	2.63 ± 0.07	3.28 ± 0.09	19.4 ± 1.7
SPF10	20.5 ± 0.7	476 ± 8	2.81 ± 0.04	3.30 ± 0.05	23.0 ± 0.6
SPF10-MA5	21.7 ± 0.7	487 ± 4	2.90 ± 0.13	3.71 ± 0.17	21.5 ± 1.0
ASPF10	18.12 ± 0.9	489 ± 6	2.30 ± 0.13	2.79 ± 0.12	18.9 ± 2.35
ASPF10-MA5	20.8 ± 0.9	517 ± 12	2.91 ± 0.11	3.67 ± 0.13	18.7 ± 0.7



4.3.5 Comparison of different fiber treatments effects on tensile properties of the compatibilized composites

In order to prepare the effects of different fiber treatments on tensile behavior, stress – strain curve of the compatibilized composites in LD and in TD for each fiber treatment systems are selected and compared in Figure 4.14. In LD (Figure 4.14I), it is seen that APF10-MA5 show the highest tensile stress compared to SPF10-MA5 and ASPF10-MA5. Moreover, it is interesting to note that the young's modulus for APF10-MA5 is about sixfold higher than that of SEBS matrix (Table 4.9). The obtained results indicate that the APF10-MA5 shows the best reinforcing performance compared among all of the samples examined.

In TD (Figure 4.14II), It is seen that the fiber treatments slightly affect the stress-strain behavior of the compatibilized composites. This indicates the predominant effect from fiber alignment.

Figure 4.15 shows the effect of different fiber treatment on secant modulus for the composites in LD and TD. In LD, it is seen that SPF10-MA5 show the highest secant modulus compared to APF10-MA5 and ASPF10-MA5. However, the effect of treated fiber and compatibilizer loading slightly affect the secant modulus in TD.



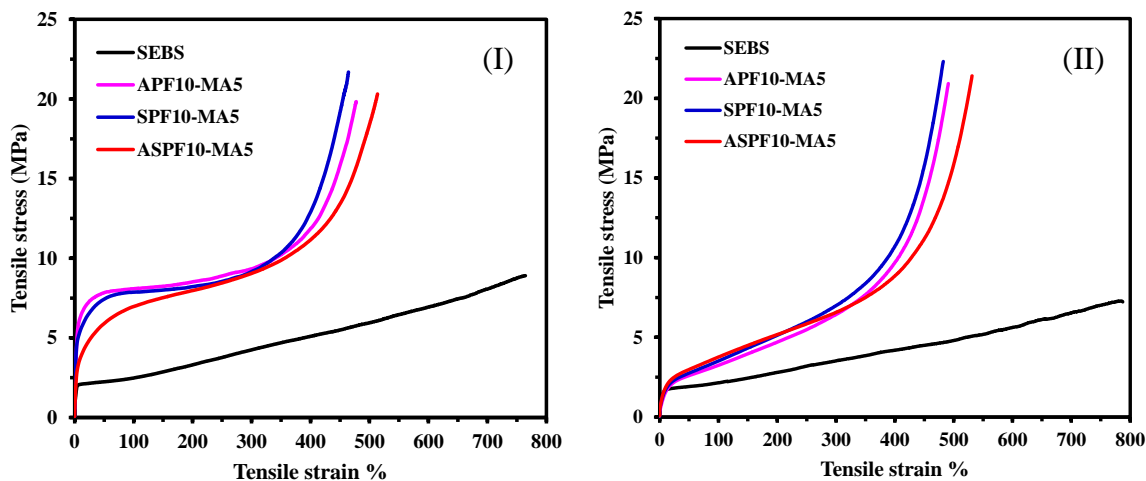


Figure 4.14 Comparison of stress-strain curves for neat SEBS, APF10-MA5, SPF10-MA5 and ASPF10-MA5 in longitudinal (I) and transverse (II) direction.

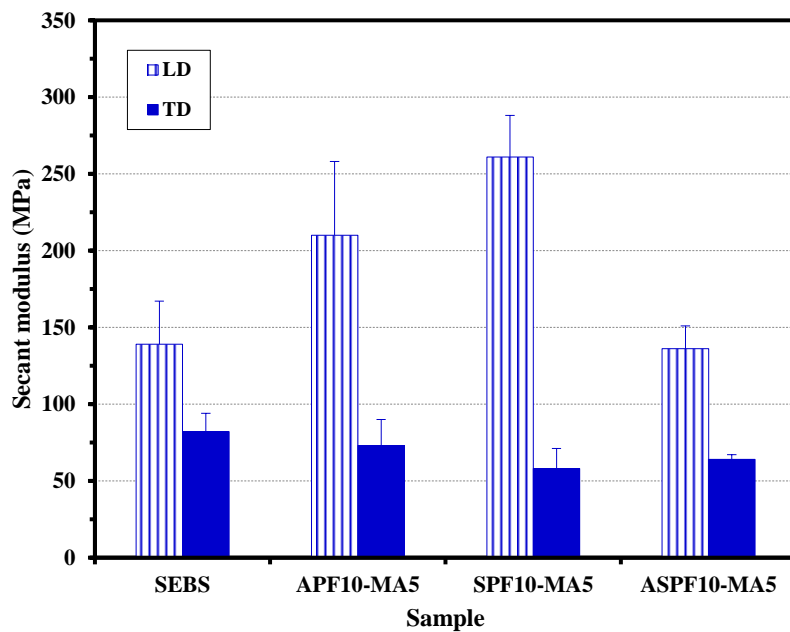


Figure 4.15 Comparison of secant modulus at 1% strain for neat SEBS, APF10-MA5, SPF10-MA5 and ASPF10-MA5 in longitudinal (LD) and transverse (TD) direction.

4.3.6 Comparison of stress ratios of the composites

In order to compare the reinforcing performance among the composites, the stress ratio (the stress of the composite to that of the neat matrix at the same strain) of the composites in LD are presented in Figure 4.16. For alkali treated fiber systems (Figure 4.16a), the stress ratios firstly increase at 0-50% strain and the highest stress ratio is observed for APF10-MA5. Beyond 300% strain, the stress ratios gradually decrease until 300% strain. After that, the stress ratio increase again as a result from the strain hardening effect.

For silane treated fiber composite systems (Figure 4.16b), the stress ratio increases and show the first maximum at ~ 50% strain. The highest reinforcing performance is observed for SPF10-MA5. At higher strain, the stress ratios gradually level off. Similarly to the alkali treated fiber system, the stress ratios again increase at the strain higher than 300%.

The stress ratios of alkali-silane treated fiber is also compared as shown in Figure 4.16c. It is seen that ASPF10-MA5 also show the higher stress ratio compared among all corresponding composite systems.

Moreover, the data of stress ratios are quantitatively summarized in Table 4.10. It is interesting to note that the improvement in reinforcing performance strongly depends on surface treatment and compatibility promotion. The highest reinforcing performance under stretching 0-200% is observed for APF10-MA5.



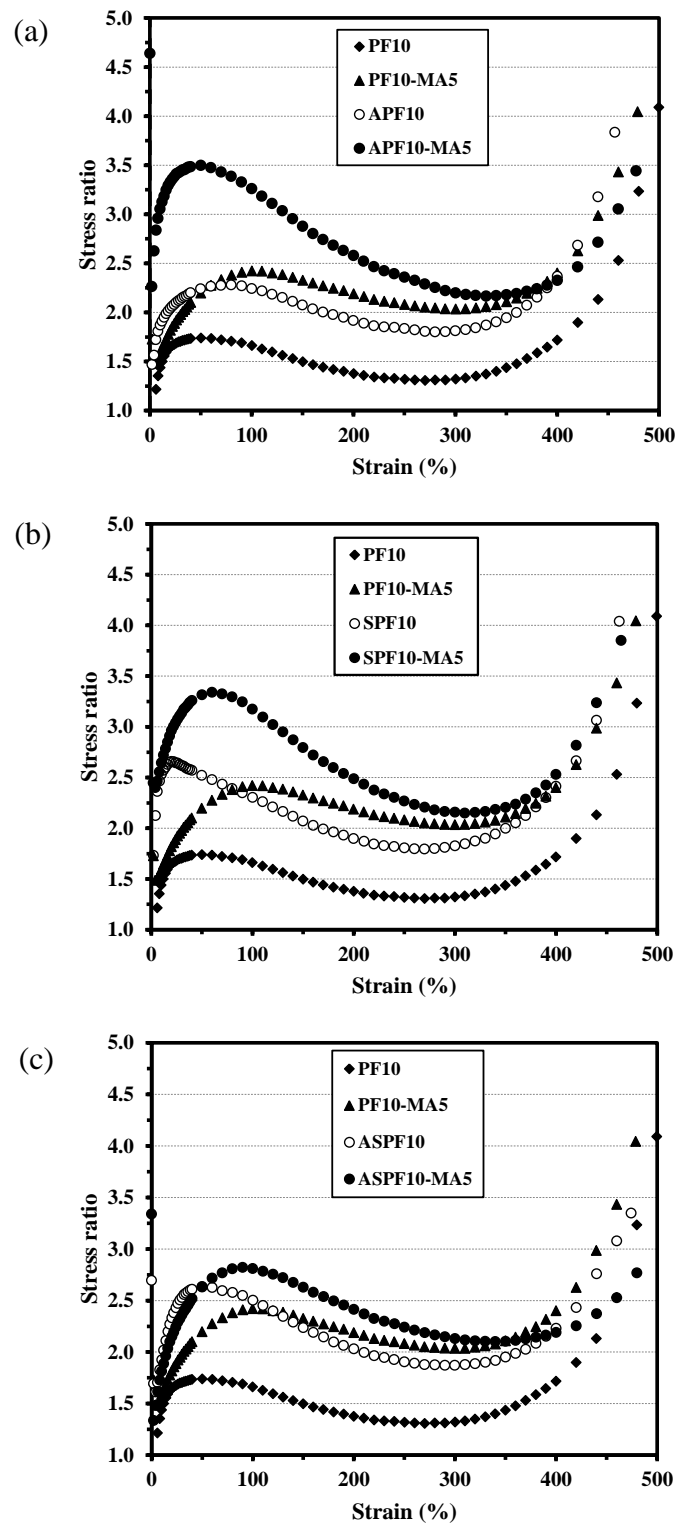


Figure 4.16 Longitudinal stress ratio (stress of the composites divided by stress of SEBS) in the strain region of 0-500% for the alkali-treated (a), silane-treated (b) and alkali-silane-treated (c) fiber composites systems.



Table 4.10 Values of stress ratio of untreated- and treated-fiber composites in longitudinal direction.

sample	stress ratio at 50% strain	stress ratio at 100% strain	stress ratio at break
PF10	1.74	1.66	4.09
APF10	2.24	2.24	3.83
SPF10	2.52	2.30	4.04
ASPF10	2.64	2.5	3.35
PF10-MA5	2.20	2.42	4.04
APF10-MA5	3.50	3.26	3.44
SPF10-MA5	2.64	2.50	3.35
ASPF10-MA5	2.63	2.81	3.35



4.4 Dynamic mechanical properties

As known that the reinforcing performance of the composite samples investigated in this work is effective in LD than in TD, the dynamic mechanical properties of neat SEBS and the composites were analyzed only in LD.

4.4.1 Effect of fiber loadings on dynamic mechanical properties

The dynamic storage modulus (E') as a function of temperature of neat SEBS, PF10 and PF20 are shown in Figure 4.17a. It is seen that as the fiber content increases, E' of composites increases. E' of the composites are higher than that of the neat SEBS at the whole states of transition. The results indicate an increase of material stiffness with fiber loading [31].

Figure 4.17b presents Tan δ curve for neat SEBS and untreated fiber composites with 10 and 20 wt% fiber loading, measured in the temperature range of -100°C to 140°C. Tan δ curves showed two damping (tan δ) peaks, corresponding to the glassy transition of the elastomer phase (EB-block) ($\approx -32^\circ\text{C}$) and thermoplastic phase (S-block) ($\approx -110^\circ\text{C}$), respectively. It is seen that the height of tan δ of EB-block slightly increases with the fiber loading. The tan δ of S-block reduced with the fiber loading in comparison to neat SEBS, which is mainly due to the dilution effect. The results indicated that after adding PALF fiber, the molecular mobility of the composites decreased and the mechanical loss to overcome inter-friction between molecular chains is reduced [129,130].

From DMA curve, the data of dynamic mechanical properties are summarized in Table 4.11. DMA results show that the storage modulus of composites is improved compared to neat SEBS. The $E'_{250^\circ\text{C}}$ and $E'_{1250^\circ\text{C}}$ of composites were increased with fiber loading. The storage modulus is high when molecular mobility is limited or restricted, which suggested a strong interaction between PALF and SBES matrix. T_g of EB-block (ethylene-co-butylene) and S-block (styrene) for neat SEBS were found to be -34°C and 109°C , respectively, at this temperature, the EB-block and S-block of SEBS change from glassy state to rubbery state. Moreover, T_g of EB-block of the composites slightly increases with fiber loading. With the presence of fiber in composite, the SEBS content is decreased, so does the amorphous phase of the SEBS was involved in the glass transition temperature. Therefore, the increases in T_g value shows the effectiveness



of the fiber as a reinforced composites. As the temperature approaches the glass transition temperature region, there is a large drop in the storage modulus values indicating the phase transition, from the rigid glassy state where molecular motions are restricted to a more flexible rubbery state where the molecular chains have greater freedom to move.

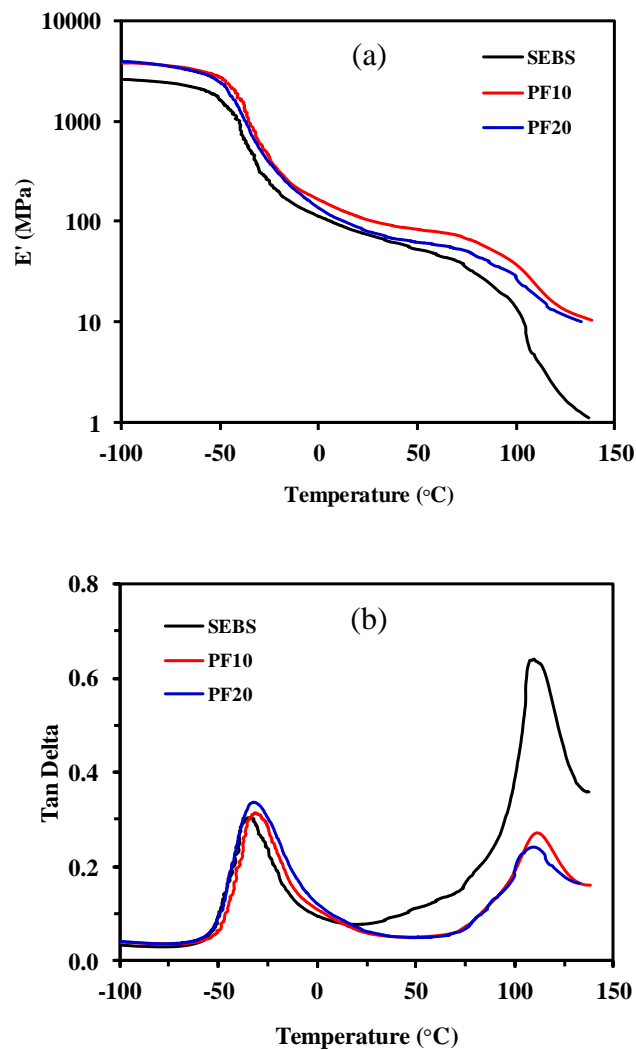


Figure 4.17 Dynamic storage moduli (E') (a) and $\tan \delta$ (b) as a function of temperature of neat SEBS, PF10 and PF20.



Table 4.11 Values of E' at 25°C and 125°C and T_g for the neat SEBS and its composites.

Sample	$E'_{25^\circ\text{C}}$ (MPa)	$E'_{125^\circ\text{C}}$ (MPa)	T_g (°C)	
			EB-block	S-block
SEBS	73	1.68	-34	109
PF10	104	13.3	-31	111
PF20	79	11.6	-32	110
APF10	131	11.9	-30	111
SPF10	198	22.1	-32	110
PF10-MA5	101	10.5	-31	111
APF10-MA5	208	29.6	-31	110
SPF10-MA5	175	18.7	-31	110



4.4.2 Effect of fiber treatments on dynamic mechanical properties

The E' as a function of temperature of neat SEBS, PF10, APF10 and SPF10 are shown in Figure 4.18a. It is seen that E' was improved for composites containing alkali- and silane-treated fiber. It is interesting to note that the highest E' value was observed for SPF10. The silane molecule forms covalent bond with the -OH group of the fiber and the organofunctional group of the molecule couples with the polymer [30]. Therefore, silane treated fiber composites has the highest stiffness compared among uncompatibilized treated-fiber composites. Furthermore, APF10 shows higher E' value compared to PF10. As known that alkali treatment can remove hemicellulose and lignin from the fiber [18]. In addition, it reduces fiber diameter and thereby increases the aspect ratio (length/diameter). This increases effective fiber surface area for good connection with the matrix through friction process. The results indicated that chemical treatments significantly affect the storage modulus of a composite.

The $\tan \delta$ curves for neat SEBS and treated fiber composites are shown in Figure 4.18b. These curves show that SEBS has two $\tan \delta$ peaks. The $\tan \delta$ peak height of EB-block are slightly lower than those for treated fiber composites compared to untreated fiber composites. However, the $\tan \delta$ peaks height of S-block are slightly higher for the treated fiber composites. Compared to untreated fiber composites, the $\tan \delta$ peaks of EB-block shifted to slightly higher temperature for APF10. This could be explained as the presence of strong fiber–matrix interface in the composite. Moreover, SPF10 shows the highest storage modulus at 25°C (198 MPa). T_g of EB-block also shifted slightly to the higher temperature (-30°C) for APF10 compared to the untreated fiber composites (Table 4.11), which indicates an decrease in molecular mobility of treated fiber composites.



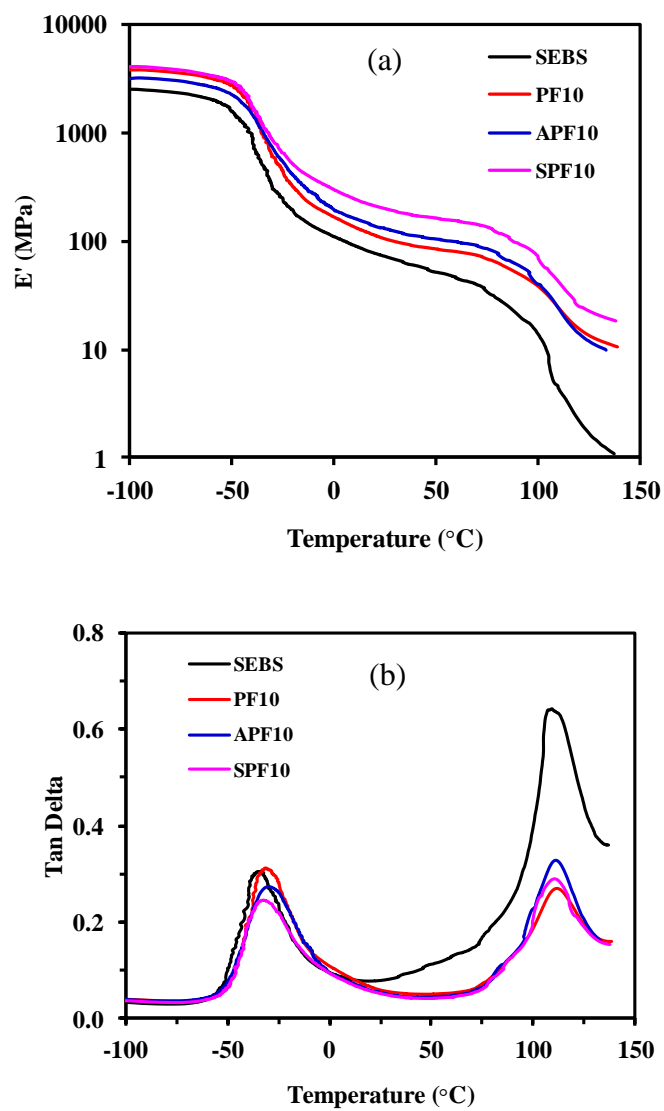


Figure 4.18 Dynamic storage moduli (E') (a) and $\tan \delta$ (b) as a function of temperature of neat SEBS, PF10, APF10 and SPF10.



4.4.3 Effect of fiber treatment and compatibilizer loadings on dynamic mechanical properties

The E' as a function of temperature of APF10, APF10-MA5, SPF10 and SPF10-MA5 are shown in Figure 4.19a. It's found that the E' of APF10-MA5 is clearly increase when compared to APF10. The compatibilizer may improve the adhesion between the fiber and SEBS matrix resulting in an increase in fiber reinforcement efficiency. For silane treated fiber composites, SPF10-MA5 has a lower storage modulus when compared with SPF10. However, the addition of compatibilizer does not significantly affect the storage modulus of the silane treated fiber system.

From Tan δ curves (Figure 4.19b), these curves show two tan δ peaks corresponding to the T_g s of EB-block ($\approx -30^\circ\text{C}$) and S-block ($\approx 110^\circ\text{C}$), respectively. APF10 show the highest peaks height of EB-block and S-block compared to the other composites. However, the tan δ profile is not different for silane treated fiber composites with and without the presence of 5 wt% SEBS-g-MA.

As seem from Table 4.11, it is interesting to note that $E'_{25^\circ\text{C}}$ and $E'_{125^\circ\text{C}}$ for APF10-MA5 show the highest value. Moreover, the addition of compatibilizer did not have a significant effect on T_g s of EB-block and S-block for the treated fiber composites.



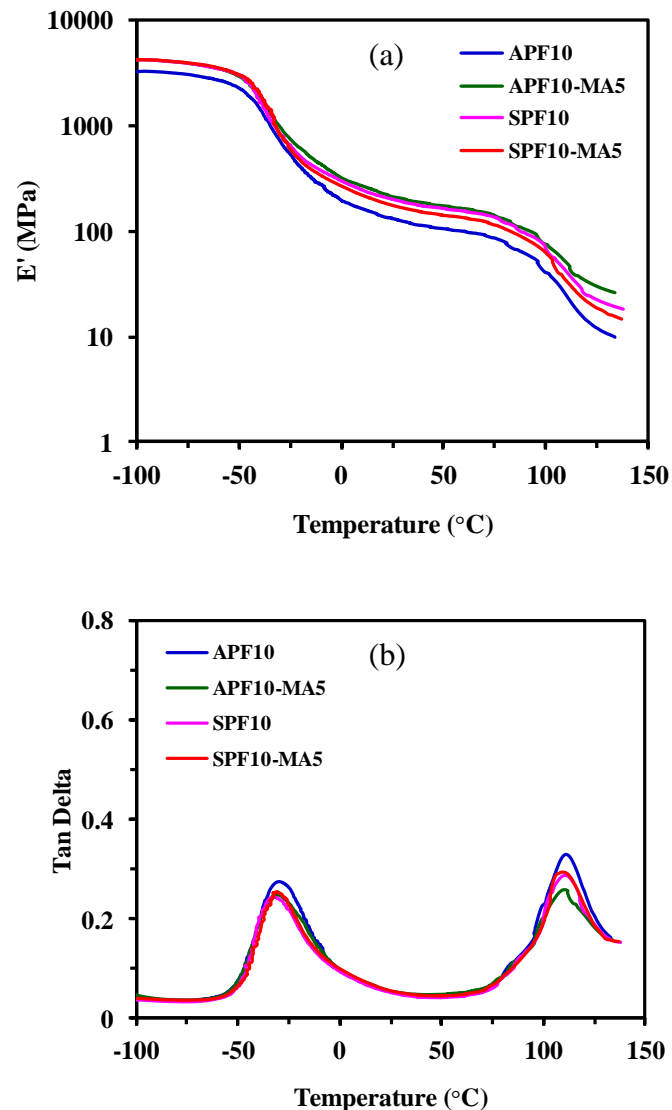


Figure 4.19 Dynamic storage moduli (E') (a) and $\tan \delta$ (b) as a function of temperature for APF10, APF10-MA5, SPF10 and SPF10-MA5.

4.4.4 Comparison of dynamic mechanical properties for the compatibilized treated-fiber composites

The E' as a function of temperature of SEBS, PF10, PF10-MA5, APF10-MA5 and SPF10-MA5 are compared in Figure 4.20a. It is seen that APF10-MA5 show the highest E' value compared to SPF10-MA5 and ASPF10-MA5. As seen from $\tan \delta$ of the compatibilized treated-fiber composites (Figure 4.20b), the composites shows two $\tan \delta$ peaks corresponding to T_g of EB-block (around -31°C) and T_g of S-block (near 110°C), respectively. Significant decrease in $\tan \delta$ peaks height at T_g of EB-block is



observed with fiber loading, the presence of PALFs and compatibilizer in the composites slightly affects the T_g of EB-block and S-block. The obtained results indicate that the addition of alkali- and silane- treated fibers with the presence of compatibilizer further improve the E' at room and high temperature.

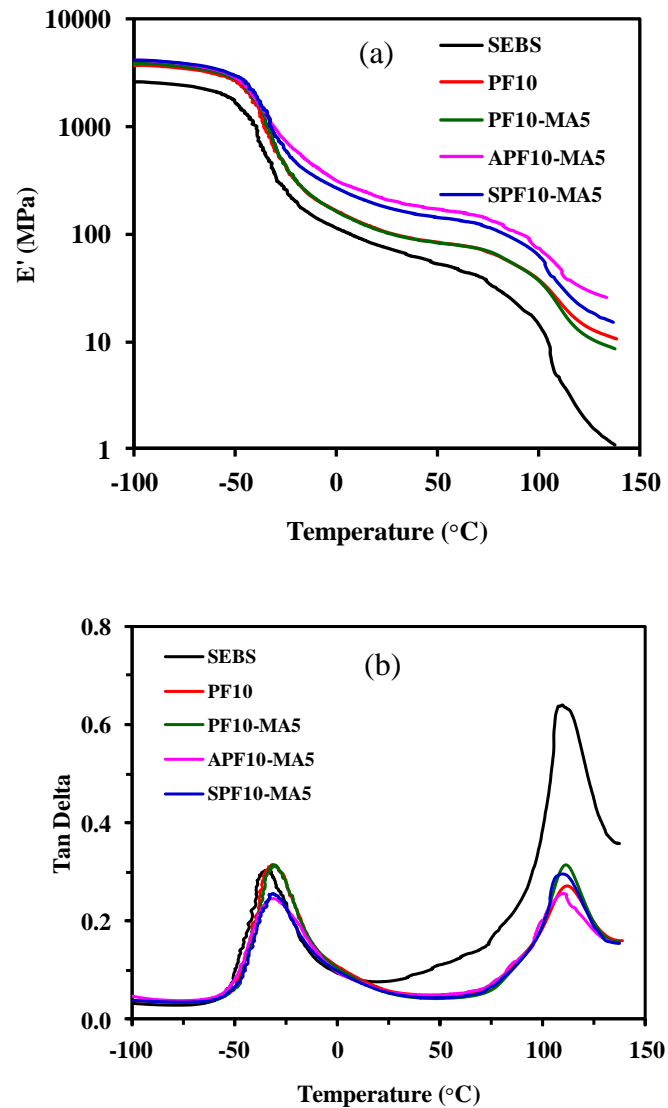


Figure 4.20 Dynamic storage moduli (E') (a) and Tan δ (b) as a function of temperature of neat SEBS, PF10, PF10-MA5, APF10-MA5 and SPF10-MA5.



4.5 Morphology of composites

4.5.1 SEM images of untreated- and treated- PALFs

The fiber surface morphology after treatments was observed using SEM. SEM images of untreated- and treated- fiber surfaces are shown in Figure 4.21. The roughened surface of the untreated fiber (PF) is observed because there are covering materials such as lignin, pectin and wax. The cleaner surface is observed with alkali treatment as seen from Figure 4.21b. This means that the covering materials are removed by alkali treatment. For the SPF (Figure 4.21c), the smooth surface is also observed. Moreover, the alkali-silane treated fiber shows a better smooth surface compared to those of the alkali- and silane- treated fibers.

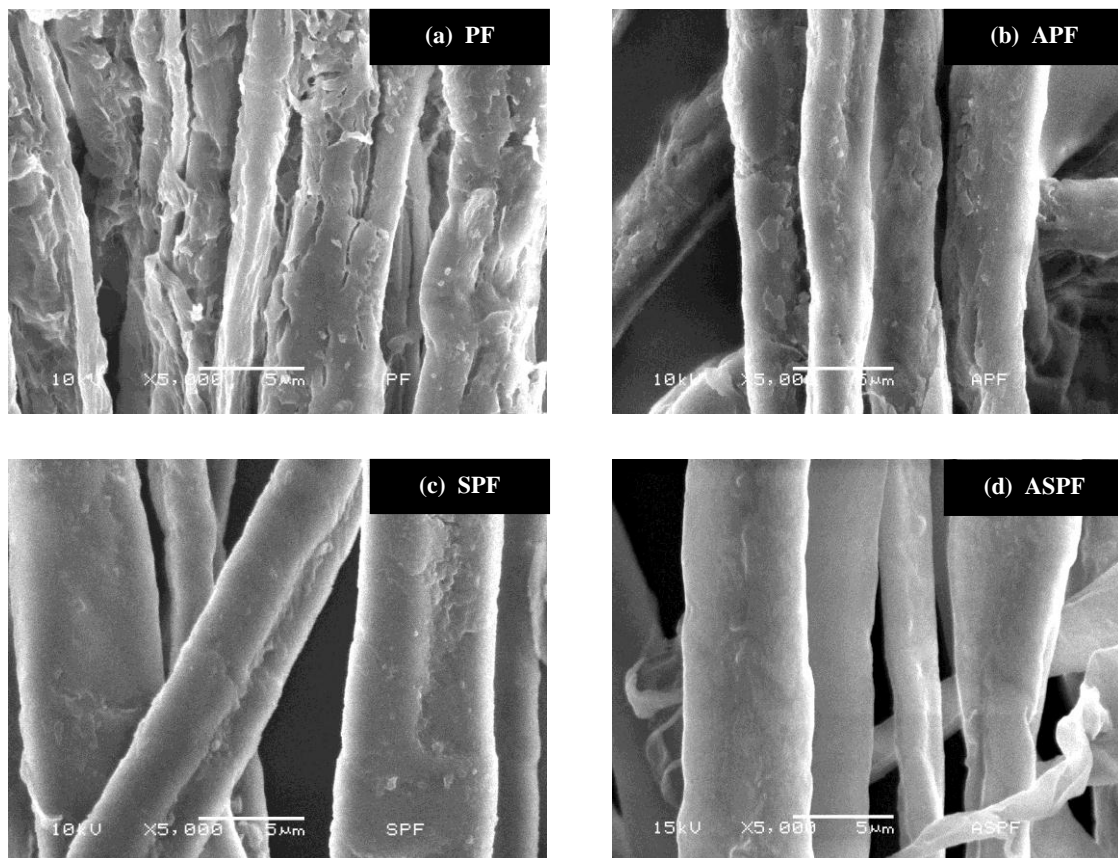


Figure 4.21 SEM images of untreated fiber (a), alkali treated fiber (b), silane treated fiber (c) and alkali-silane treated fiber (d).



4.5.2 SEM images of cryogenic fracture surface of composites

The SEM images of neat SEBS, PF10 and PF20 perpendicular to the fiber direction are shown in Figure 4.22. For PF10, some pull-out fibers are observed. With increasing of fiber content, large bundle of PALFs is observed (Figure 4.22c).

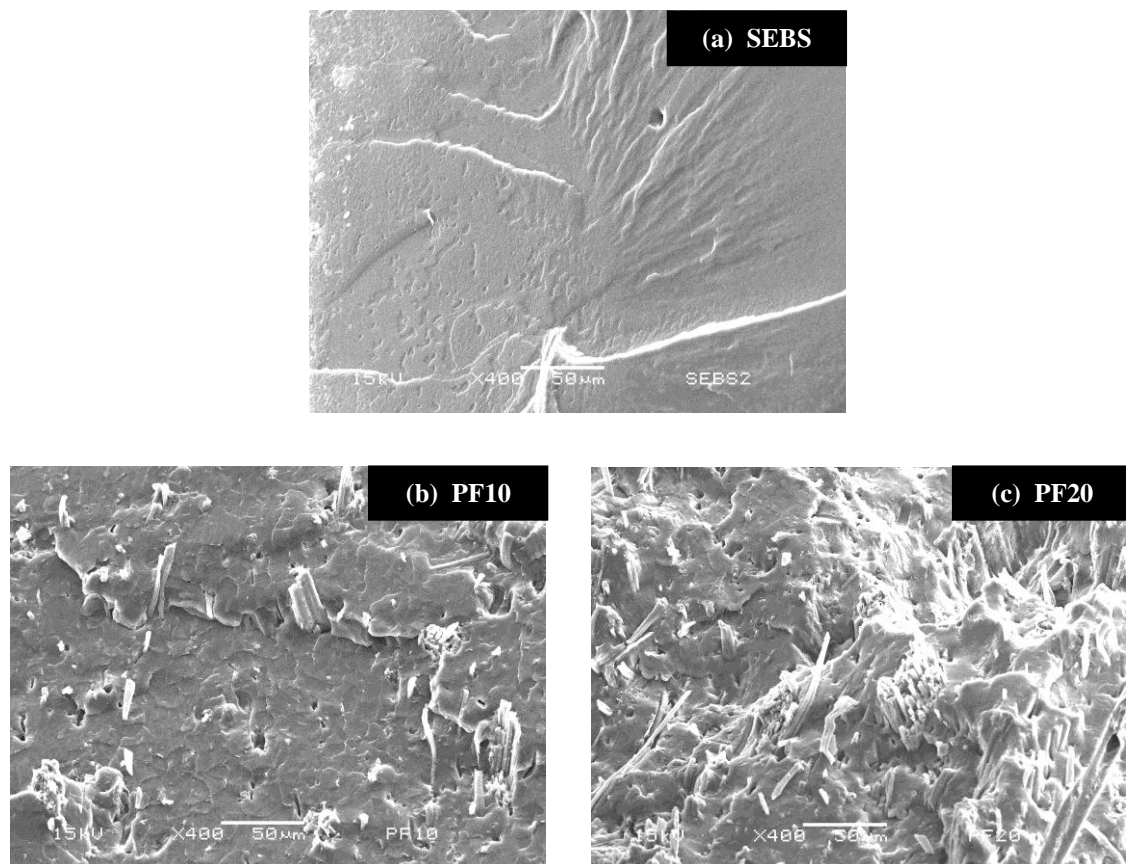


Figure 4.22 SEM images of cryogenic fracture surface perpendicular to the fiber direction for (a) neat SEBS, (b) PF10 and (c) PF20.

4.5.3 SEM images of cryogenic fracture surfaces parallel and perpendicular to the fiber direction for PALF/SEBS composites

The effect of fiber treatments on morphology of the interface between SEBS matrix and PALF filler are shown in Figure 4.23. In perpendicular to the fiber direction (column I), it is seen that the dispersion of PALFs in the treated-fiber composites is better than that in the untreated system. In parallel to the fiber direction (column II), the fiber alignment along the preferred direction is mostly observed. However, in case of SPF10 and ASPF10, the alignment of the fiber is not clearly observed.

The effect of compatibilizer loading on morphology of the composites are shown in Figure 4.24. With addition of compatibilizer, the treated fiber composites, especially for the APF10-MA5, show better dispersion when compared with untreated fiber composites.



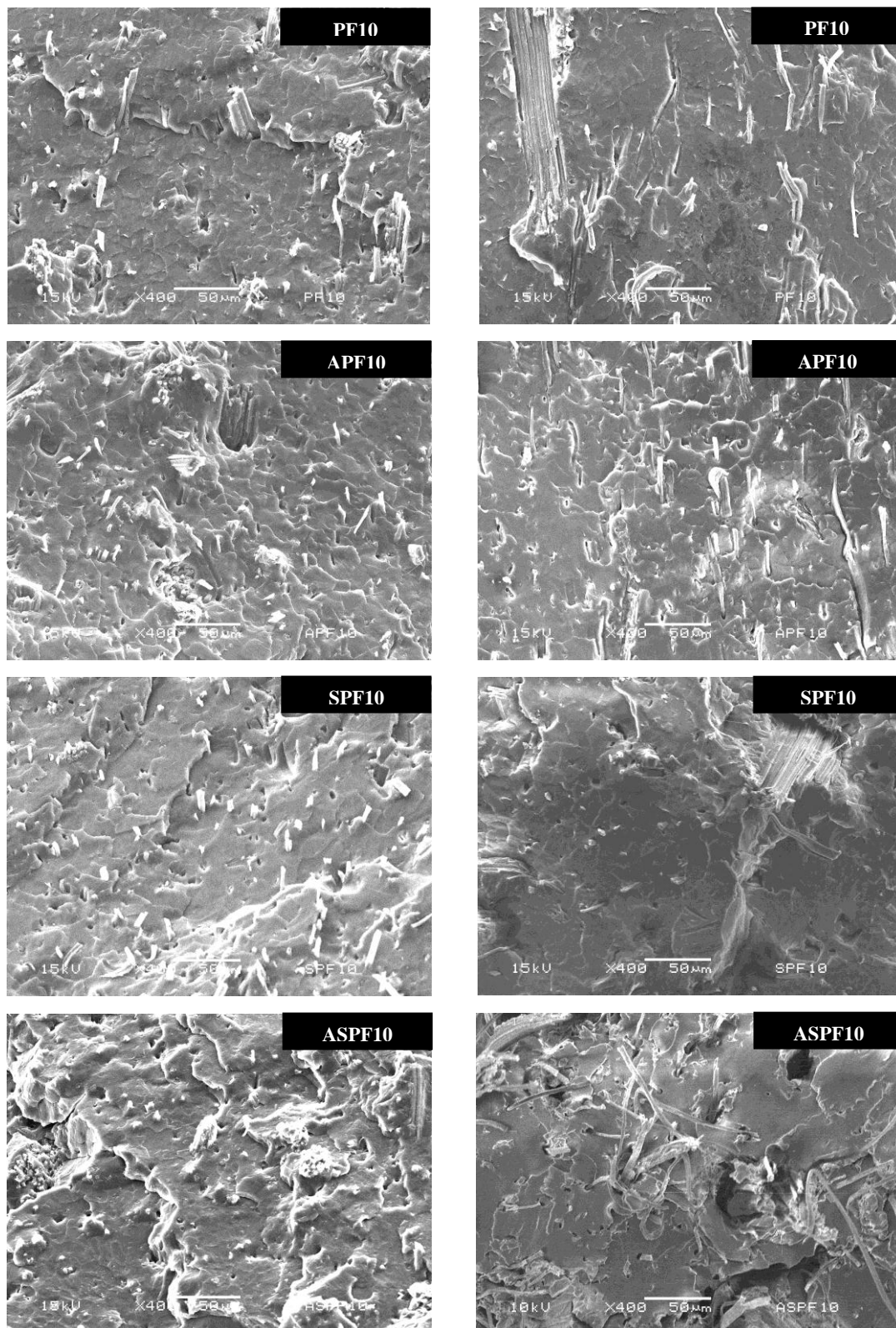


Figure 4.23 SEM images of cryogenic fracture surface perpendicular (column I) and parallel (column II) to the fiber direction for untreated- and treated-fiber composites.

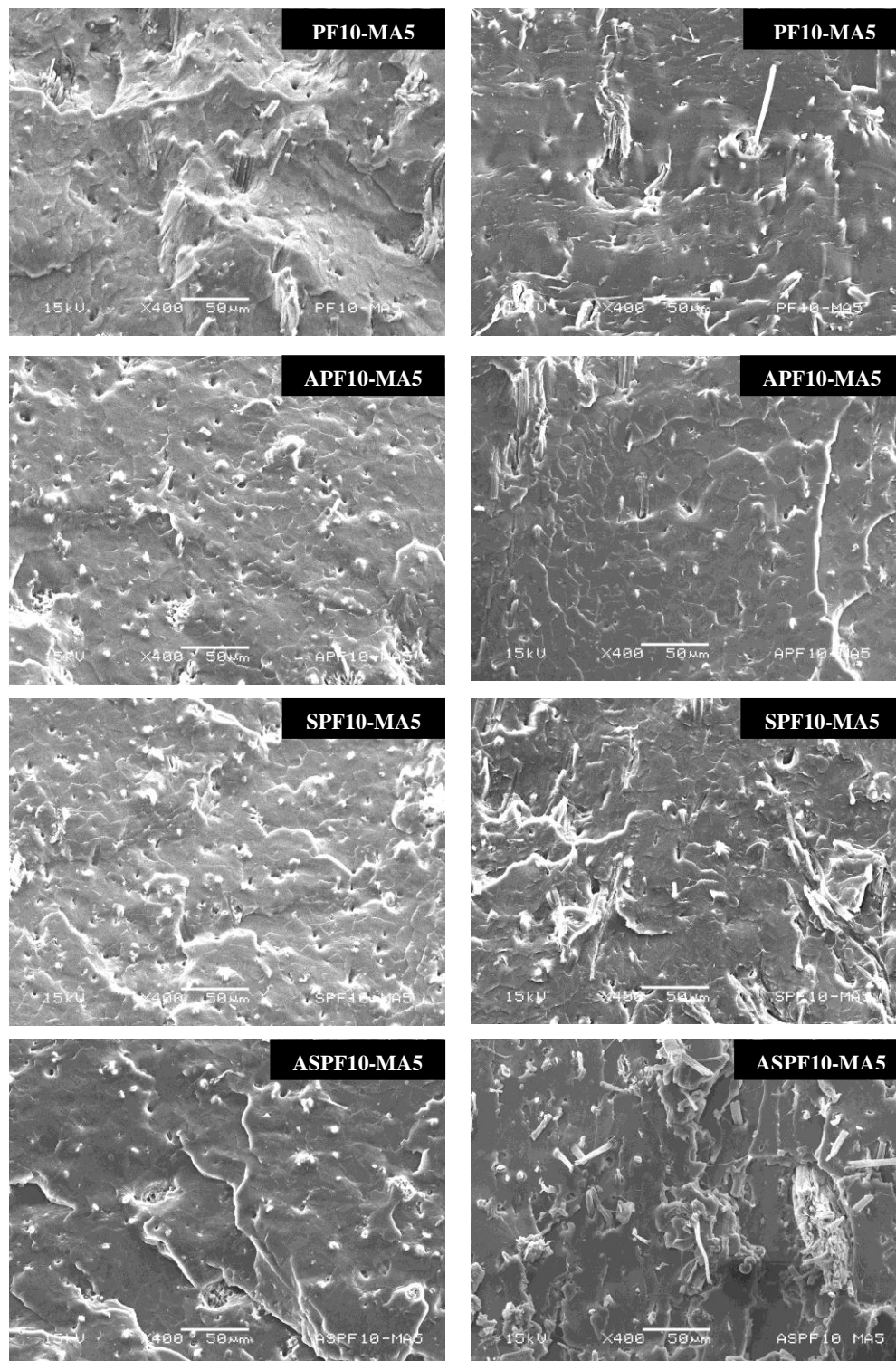


Figure 4.24 SEM images of cryogenic fracture surface perpendicular (column I) and parallel (column II) to the fiber direction for untreated- and treated-fiber composites with the presence of 5 wt% SEBS-g-MA.

4.5.4 SEM images of tensile fracture surfaces perpendicular to the fiber direction for PALF/SEBS composites

The effect of fiber treatment on morphology of the composites without and with compatibilizer after tensile test are shown in Figures 4.25 and 4.26, respectively. From Figure 4.25, it is indicated that poor interfacial adhesion between the fiber and SEBS matrix is observed, as evident by the gap at the interface and the pull-out fibers. After adding SEBS-g-MA (Figures 4.26), the better adhesion between fiber and polymer matrix is found. Especially in alkali treated PALF with compatibilizer loading, the compatibilizing phenomena strongly affects the mechanical properties of the elastomer composite. This may arise from the interaction between SEBS-g-MA and negative charge sites of the fiber as schematically proposed in Figures 4.28 [7]. For silane treated fiber composites system, pull-out fibers and smaller bundle of PALFs are observed. The interfacial interaction between PALFs and SEBS matrix are also improved by silane coupling agent, thereby, improving the tensile and dynamic mechanical properties composites. Interaction mechanisms of silane-treated fiber system were proposed in Figures 4.29. The interaction involves the reaction between silanol groups from silane agents and hydroxyl groups on fiber surface leading to a polysiloxane network at the PALF surface. The physical interaction between vinyl groups of the coupling agent and the non-polar SEBS matrix is expected to occur [128].



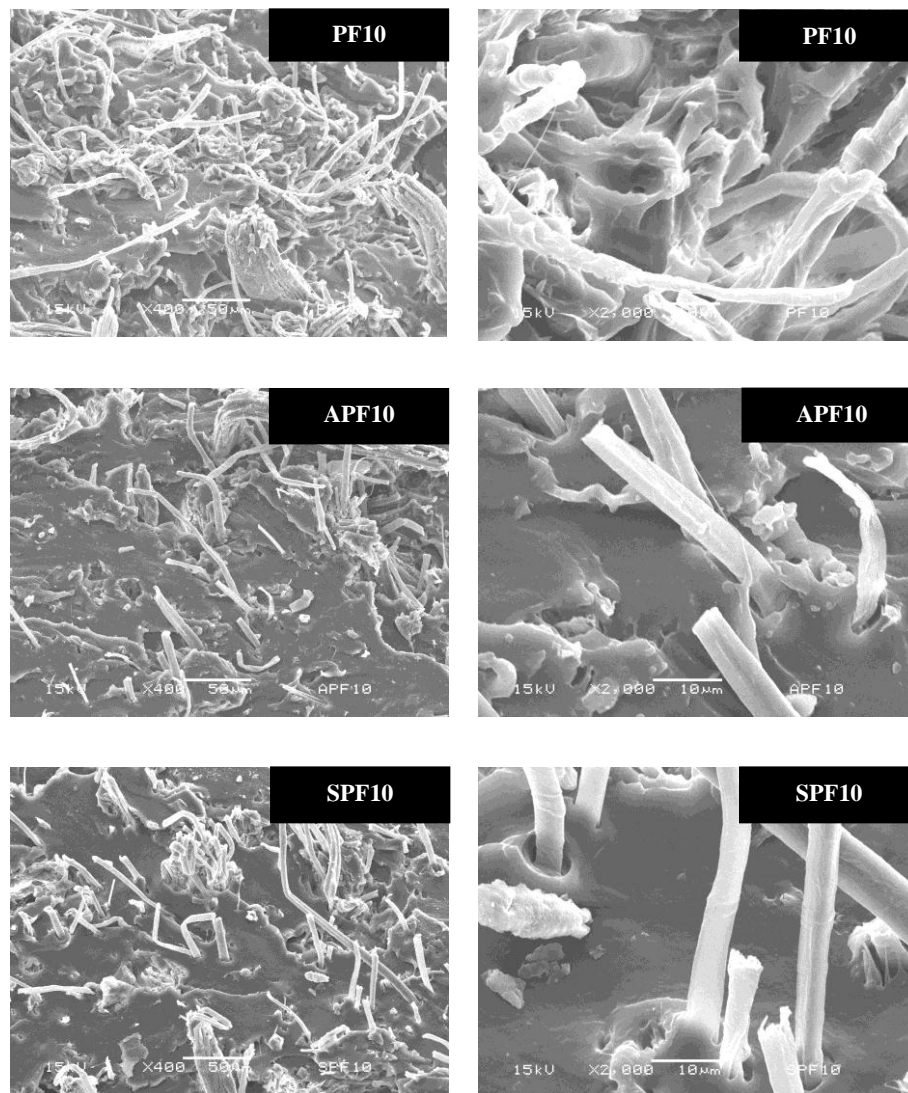


Figure 4.25 SEM images of tensile fracture surface perpendicular to the fiber direction for PF10, APF10 and SPF10 at magnifications of 400 \times (column I) and 2,000 \times (column II).

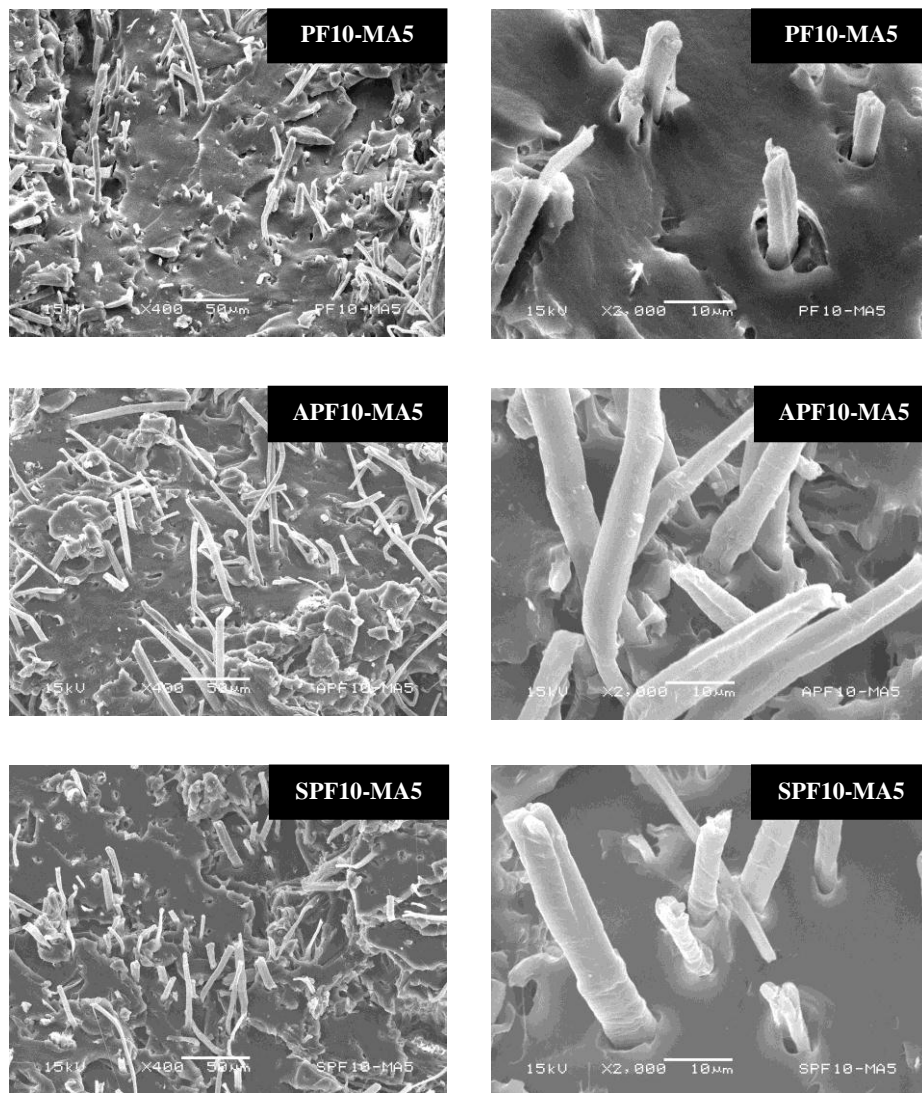


Figure 4.26 SEM images of tensile fracture surface perpendicular to the fiber direction for PF10-MA5, APF10-MA5 and SPF10-MA5 at magnifications of 400× (column I) and 2,000× (column II).

4.5.5 SEM images of pineapple fibers after extraction of the matrix

The effect of compatibilizer content on morphology of the extracted fibers are shown in Figures 4.27. It is found that the roughness of the fiber surface increases with increased compatibilizer contents. The similar trend of the results is observed for all composite systems.



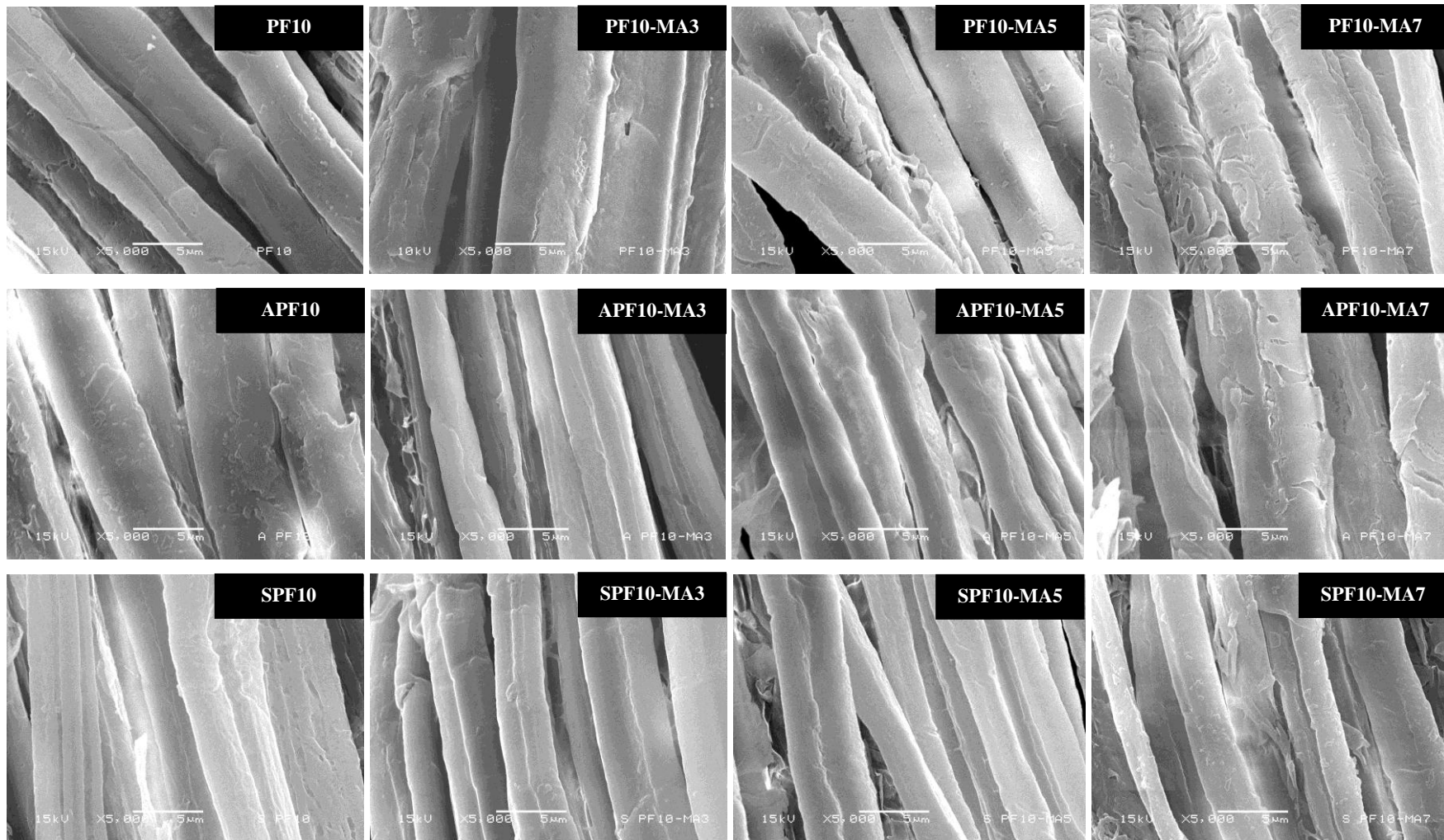


Figure 4.27 SEM images of pineapple fibers after extraction of the matrix.

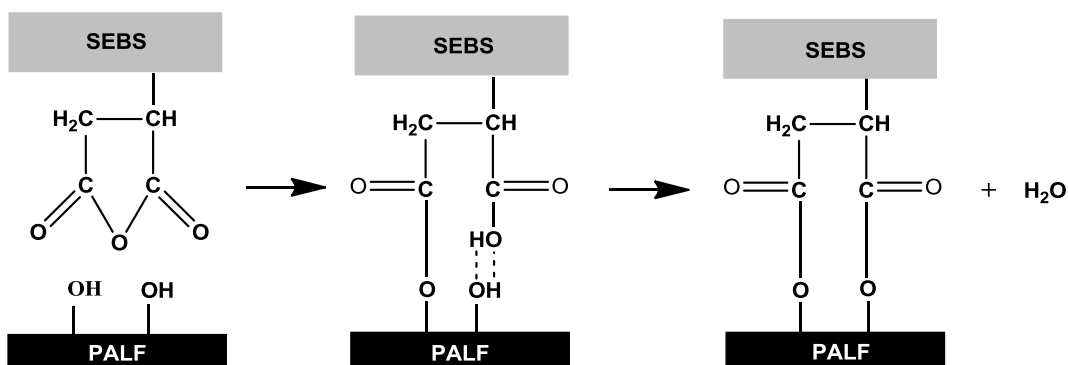


Figure 4.28 Scheme of interfacial interactions between SEBS-g-MA and the fiber surface.

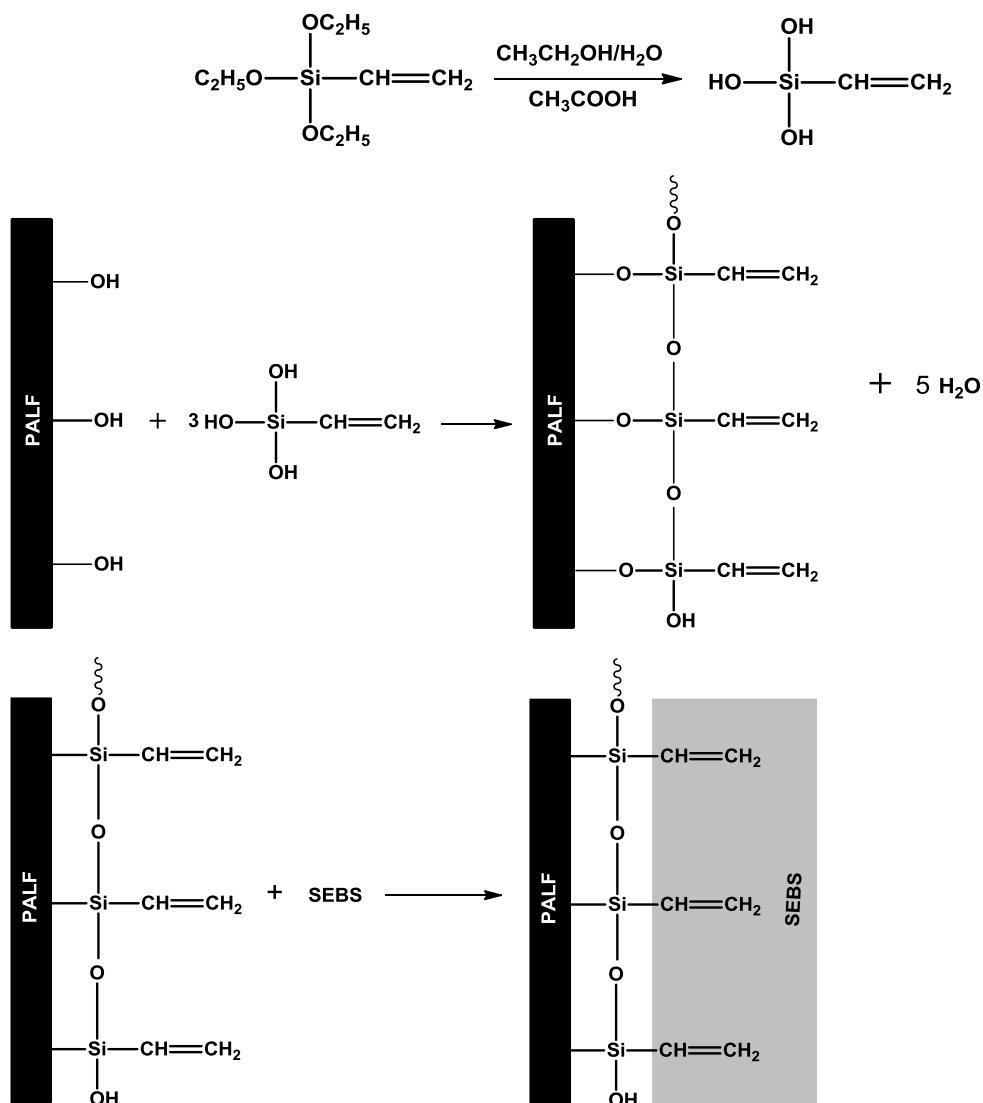


Figure 4.29 Interfacial interactions between SEBS matrix and the fiber surface for the compatibilized silane treated fiber composites [7,128].

CHAPTER 5

CONCLUSIONS

In this work, PALF reinforced elastomer composites were investigated. PALFs were treated using sodium hydroxide (alkali treatment) and triethoxy vinyl silane before compounding. The effects of fiber surface treatments and compatibilizer loading on thermal and mechanical properties of the elastomer were studied. The conclusion can be drawn as follows:

1. The alkali-treated fiber exhibited the highest thermal stability in air compared among all of the samples. For the composites, the highest thermal stability was observed for the composite containing alkali-treated fibers.

2. The enhancement in mechanical performance of the elastomer matrix was achieved by PALF loadings both in longitudinal and transverse directions.

3. The mechanical performance of composites with treated fibers and compatibilizers loading in longitudinal direction were better than that of composites with untreated fiber loading. No significant difference in mechanical performance of the treated fiber composites with and without compatibilizer is observed in transverse direction.

4. In longitudinal direction, the composite of alkali treated fiber with compatibilizer loading showed the best mechanical properties.

5. The dynamic mechanical results related well with the tensile data.



References



References

- [1] Sena Neto AR, Araujo MAM, Souza FVD, Mattoso LHC, Marconcini JM. Characterization and comparative evaluation of thermal, structural, chemical, mechanical and morphological properties of six pineapple leaf fiber varieties for use in composites. *Ind Crop Prod* 2013; 43: 529–537.
- [2] Leao AL, Machado IS, Souza SF, Soriano L. Production of curaua fibers for industrial applications: characterization and micropropagation. *Acta Hortic. João Pessoa* 2009; 822: 227–238.
- [3] Rout J, Misra M, Tripathy S, Nayak SK, Mohanty AK. The influence of fibre treatment on the performance of coir-polyester composites. *Compos Sci Technol* 2001; 61(9): 1303–1310.
- [4] Bledzki AK, Gassan J. Composites reinforced with cellulose based fibres. *Prog Polym Sci* 1999; 24(2): 221–274.
- [5] Abdelmouleh M, Boufis S, Belgacem MN, Dufresne A. Short natural-fibre reinforced polyethylene and natural rubber composites: effect of silane coupling agents and fibre loading. *Compos Sci Technol* 2007; 67(7–8): 1627–1639.
- [6] Tserki V, Zafeiropoulos NE, Simon F, Panayiotou C. A study of the effect of acetylation and propionylation surface treatments on natural fibres. *Compos Part A – Appl Sci Manuf* 2005; 36(8): 1110–1118.
- [7] Kabir MM, Wang H, Lau KT, Cardona F. Chemical treatments on plant-based natural fibre reinforced polymer composites: An overview. *Composites: Part B* 2012; 43: 2883–2892.
- [8] Mohanty AK, Misra M, Hinrichsen G. Biofibres, biodegradable polymers and biocomposites: an overview. *Macromol Mater Eng* 2000; 266–277(1): 1–24.
- [9] Uma Devi L, Bhagawan SS, Thomas S. Mechanical properties of pineapple leaf fiber-reinforced polyester composites. *J Appl Polym Sci* 1997; 64: 1739–1748.
- [10] George J, Bhagawan SS, Thomas S. Effects of environment on the properties of low-density polyethylene composites reinforced with pineapple leaf fibre. *Compos Sci Technol* 1998; 58: 1471–1485.



- [11] Arib RMN, Sapuan SM, Ahmad MMHM, Paridah MT, Khairul Zaman HMD. Mechanical properties of pineapple leaf fibre reinforced polypropylene composites. *Mater Des* 2006; 27: 391–396.
- [12] Lopattananon N, Panawarangkul K, Sahakaro K, Ellis B. Performance of pineapple leaf fiber–natural rubber composites: The effect of fiber surface treatments. *J Appl Polym Sci* 2006; 102: 1974–1984.
- [13] Liu W, Misra M, Askeland P, Drzal LT, Mohanty AK. ‘Green’ composites from soy based plastic and pineapple leaf fiber: fabrication and properties evaluation. *Polymer* 2005; 46: 2710–2721.
- [14] George J, Bhagawan SS, Thomas S. Thermogravimetric and dynamic mechanical thermal analysis of pineapple fibre reinforced polyethylene composites. *J Therm Anal* 1996; 47: 1121–1140.
- [15] Li X, Tabil LG, Panigrahi S. Chemical Treatments of Natural Fiber for Use in Natural Fiber-Reinforced Composites: A Review. *J Polym Environ* 2007; 15: 25–33.
- [16] Kabira MM, Wanga H, Laua KT, Cardona F. Effects of chemical treatments on hemp fibre structure. *Appl Surf Sci* 2013; 276: 13– 23.
- [17] Hill CAS. Wood–plastic composites: strategies for compatibilising the phases. *J Inst Wood Sci* 2000; 15: 140–146.
- [18] Daneault C, Kokta BV, Maldas D. Grafting of vinyl monomers onto wood fibers initiated by peroxidation. *Polym Bull* 1988; 20: 137–141.
- [19] Hong CK, Kim N, Kang SL, Nah C, Lee YS, Cho BH, Ahn JH. Mechanical properties of maleic anhydride treated jute fibre/polypropylene composites. *Plast Rubber Compos* 2008; 37: 325–330.
- [20] Hill CAS. Wood modification: chemical, thermal and other processes. John Wiley & Sons, Ltd. 2006; 19–44.
- [21] Lu JZ, Wu Q, McNaabb HS. Chemical coupling in wood fiber and polymer composites: a review of coupling agents and treatments. *Wood Fiber Sci* 2000; 32: 88–104.
- [22] Belgacem MN, Gandini A. The surface modification of cellulose fibres for use as reinforcing elements in composite materials. *Compos Interf* 2005; 24: 41–75.



- [23] Nam TH, Ogihara S, Tung NH, Kobayashi S. Effect of alkali treatment on interfacial and mechanical properties of coir fiber reinforced poly (butylenes succinate) biodegradable composites. *Compos Part B – Eng* 2011; 42: 1648–1656.
- [24] Joseph PV, Joseph K, Thomas S, Pillai CKS, Prasad VS, Groeninckx G, Sarkissova M. The thermal and crystallisation studies of short sisal fibre reinforced polypropylene composites. *Compos Part A – Appl Sci Manuf* 2003; 34(3): 253–266.
- [25] Rider AN, Arnott DR. Boiling water and silane pre-treatment of aluminium alloys for durable adhesive bonding. *Int J Adhes Adhes* 2000; 20: 209–220.
- [26] Wu HF, Dwight DW, Huff NT. Effects of silane coupling agents on the interphase and performance of glass–fiber-reinforced polymer composites. *Compos Sci Technol* 1997; 57: 975–983.
- [27] Clark HA, Plueddemann EP. Bonding of silane coupling agents in glass reinforced plastics. *Mod Plast* 1963; 40. p. 133–5, 137–8, 195–6.
- [28] Park JM, Subramanian RV, Bayoumi AE. Interfacial shear strength and durability improvement by silanes in single-filament composite specimens of basalt fiber in brittle phenolic and isocyanate resins. *J Adhes Sci Technol* 1994; 8: 133–150.
- [29] Favis BD, Blanchard LP, Leonard J, Prud’Homme RE. The interaction of a cationic silane coupling agent with mica. *J Appl Polym Sci* 2003; 28: 1235–1244.
- [30] Xie Y, Hill ASC, Xiao Z, Militz H, Mai C. Silane coupling agents used for natural fiber/polymer composites: A review. *Composites: Part A* 2010; 41: 806–819.
- [31] Lu N, Oza S. Thermal stability and thermo-mechanical properties of hemp-high density polyethylene composites: Effect of two different chemical modifications. *Compos B* 2013; 44: 484–490.
- [32] Jovanovic V, Javanovic SS, Simendic JB, Markovic G, Cincovic MM. Composites based on carbon black reinforced NBR/EPDM rubber blends. *Compos Part B Eng* 2013; 45(1): 333-340.



- [33] Markovic G, Marinovic-Cincovic M, Jovanovic V, Samarzija-Javanovic S, Budinski-Simendic J. NR/CSM/biogenic silica rubber blend composites. *Compos Part B Eng* 2013; 55: 368-373.
- [34] Kasgoz A, Akin D, Durmus A. Rheological and electrical properties of carbon black and carbon fiber filled cyclic olefin copolymer composites. *Compos Part B Eng* 2014; 62: 113-120.
- [35] Bledzki AK, Reihmane S, Gassan J. Thermoplastics reinforced with wood fillers: a literature review. *Polym Plast Technol Eng* 1998; 37(4): 451-468.
- [36] Nekkaa S, Chebira F, Haddaoui N. Effect of fiber treatment on the mechanical and rheological properties of polypropylene/broom fiber *sparitium junceum* composites. *J Eng Appl Sci* 2006; 1(3): 278-283.
- [37] Espet A, Vilapana F, Karlsson S. Comparison of water absorption in natural cellulosic fibres from wood and one-year crops in polypropylene composites and its influence on their mechanical properties. *Compos Part A Appl S* 2004; 35(11): 1267-1276.
- [38] Kazayawoko M, Balatinecz JJ, Matuana LM. Surface modification and adhesion mechanisms in wood fiber-polypropylene composites. *J Mat Sci* 1999; 34(24): 6189-6199.
- [39] Li Q, Matuana L. Surface of cellulosic materials modified with functionalized polyethylene coupling agents. *J Appl Polym Sci* 2003; 88: 278-286.
- [40] Belgacem MN, Gandini A. The surface modification of cellulose fibres for use as reinforcing elements in composite materials. *Compos Interface* 2005; 12(1-2): 41-75.
- [41] Wang X, Pang SL, Yang JH, Yang F. Structure and properties of SEBS/PP/OMMT nanocomposites. *Trans. Nonferrous Met. SOC. China* 2006; 16: 524-528.
- [42] Mistrali F, Proni A. Styrenic block copolymers. In: Whelan A, Lee KS, editors. *Developments in rubber technology*, vol. 3. London: Applied Science, 1982.
- [43] Haws JR, Wright RF. Block copolymers. In: Walker BM, editor. *Handbook of thermoplastic elastomers*. New York: Van Nos-trand Reinhold, 1979.
- [44] Mistrali F, Proni A. Styrenic block copolymers. *Applied Science* 1982; 3.



- [45] Allen NS, Luengo C, Edge M, Wilkinson A, Parellada MD, Barrio JA, Quiteria VRS. Photooxidation of styrene–ethylene–butadiene–styrene (SEBS) block copolymer. *J Photochem Photobiol A* 2004; 162: 41–51.
- [46] Juárez D, Ferrand S, Fenollar O, Fombuena V, Balart R. Improvement of thermal inertia of styrene–ethylene/butylene–styrene (SEBS) polymers by addition of microencapsulated phase change materials (PCMs). *Eur Polym J* 2011; 47: 153–161.
- [47] Chou TW, McCullough RL, Pipes RB. Composites materials. *Sci. Am.* 1986; 10: 193–203.
- [48] Friedrich K, Almajid AA. Manufacturing Aspects of Advanced Polymer Composites for Automotive Applications. *Appl Compos Mater* 2013; 20: 107–128.
- [49] Leonard YM, Martin PA. Chemical modification of hemp, sisal, jute and kapok fibres by alkalisation. *Appl Polym Sci* 2002; 84(12): 2222–2234.
- [50] Mwaikambo YM, Ansell MP. The effect of chemical treatment on the properties of hemp, sisal, jute and kapok fibres for composite reinforcement. *Angew Makromol Chem* 1999; 272: 108–116.
- [51] Abdelmouleh M, Boufis S, Belgacem MN, Dufresne A. Short natural-fibre reinforced polyethylene and natural rubber composites: effect of silane coupling agents and fibre loading. *Compos Sci Technol* 2007; 67(7–8): 1627–1639.
- [52] Wang B, Panigrahi S, Tabil L, Crerar W. Pre-treatment of flax fibres for use in rotationally molded biocomposites. *J Reinf Plast Compos* 2007; 26(5): 447–463.
- [53] Sgriecia N, Hawley MC, Misra M. Characterization of natural fibre surfaces and natural fibre composites. *Compos Part A – Appl Sci Manuf* 2008; 39(10): 1632–1637.
- [54] Taj S, Ali M, Khan S. Review: natural fibre reinforced polymer composites. *Proc Pak Acad Sci* 2007; 44(2): 129–144.
- [55] Fakirov S, Bhattacharyya D, editors. *Engineering biopolymers: homopolymers, blends and composites*. Munich Hanser Publishers; 2007, ISBN: 978-1-56990-405-3.



- [56] Bowles KJ, Frimpong S. Void effects on the interlaminar shear strength of unidirectional graphite–fiber-reinforced composites. *J Compos Mater* 1992; 26(10): 1487–1509.
- [57] Vaxman A, Narkis M, Siegmann A, Kenig S. Void formation in short-fiber thermoplastic composites. *Polym Compos* 2004; 10(6): 449–453.
- [58] Zakaria S, Poh LK. Polystyrene-benzoylated EFB reinforced composites. *Polym Plast Technol Eng* 2002; 41(5): 951–962.
- [59] Huda MS, Drzal LT, Mohanty AK, Misra M. Effect of chemical modifications of the pineapple leaf fiber surfaces on the interfacial and mechanical properties of laminated biocomposites. *Compos Interfaces* 2008; 15: 169–191.
- [60] Jawaid M, Abdul Khalil HPS. Cellulosic/synthetic fibre reinforced polymer hybrid composites: a review. *Carbohydr Polym* 2011; 86: 1–18.
- [61] Mwaikambo LY, Ansell MP. Chemical modification of hemp, sisal, jute and kapok fibres by alkalisation. *J Appl Polym Sci* 2002; 84(12): 2222–2234.
- [62] Saheb DN, Jog JP. Natural fibre polymer composites: a review. *Adv Polym Tech* 1999; 18(4): 351–363.
- [63] Madsen B. Properties of plant fibre yarn polymer composites. PhD thesis, BYG-DTU, Technical University of Denmark; 2004, ISBN: 87-7877-145-5.
- [64] Bledzki AK, Gassan J. Composites reinforced with cellulose based fibres. *Prog Polym Sci* 1999; 24(2): 221–274.
- [65] John MJ, Anandjiwala RD. Recent developments in chemical modification and characterization of natural fibre-reinforced composites. *Polym Compos* 2008; 29(2): 187–207.
- [66] Mohanty AK, Misra M, Hinrichsen G. Biofibres, biodegradable polymers and biocomposites: an overview. *Macromol Mater Eng* 2000; 266–277(1):1–24.
- [67] Dhakal HN, Zhang ZY, Richardson MOW. Effect of water absorption on the mechanical properties of hemp fibre reinforced unsaturated polyester composites. *Compos Sci Technol* 2007; 67(7–8): 1674–1683.
- [68] Hattallia S, Benaboura A, Ham-Pichavant F, Nourmamode A, Castellan A. Adding value to alfa grass (*Stipa tenacissima* L.) soda lignin as phenolic resins. 1. Lignin characterization. *Polym Degrad Stab* 2002; 76: 259–264.



- [69] Hoareau W, Trindade WG, Siegmund B, Castellan A, Frollini E. Sugar cane bagasse and curaua lignins oxidized by chlorine dioxide and reacted with furfuryl alcohol: characterization and stability. *Polym Degrad Stab* 2004; 86: 567–657.
- [70] Mahdavi S, Kermanian H, Varshoei A. Comparison of mechanical properties of date palm fibre-polyethylene composite. *Bioresources* 2010; 5: 2391–2403.
- [71] Rozman HD, Tay GS, Kumar RN, Abusamah A, Ismail H, Mohd Ishak ZA. Polypropylene–oil palm empty fruit bunch–glass fibre hybrid composites: a preliminary study on the flexural and tensile properties. *Eur Polym J* 2001; 37: 1283–1291.
- [72] Thwe MM, Liao K. Effects of environmental aging on the mechanical properties of bamboo–glass fiber reinforced polymer matrix hybrid composites. *Compos Part A – Appl S* 2002; 33: 43–52.
- [73] Bendahou A, Kaddami H, Sautereau H, Raihane M, Erchiqui F, Dufresne A. Short palm tree fibers polyolefin composites: effect of filler content and coupling agent on physical properties. *Macromol Mater Eng* 2008; 293: 140–148.
- [74] Kim HS, Kim HJ, Lee JW, Choi IG. Biodegradability of bio-flour filled biodegradable poly(butylene succinate) bio-composites in natural and compost soil. *Polym Degrad Stabil* 2006; 91: 1117–1127.
- [75] Contat-Rodrigo L, Greus AR. Biodegradation studies of LDPE filled with biodegradable additives: morphological changes. *I J Appl Polym Sci* 2002; 83: 1683–1691.
- [76] Tserki V, Matzinos P, Panayiotou C. Novel biodegradable composites based on treated lignocellulosic waste flour as filler Part II. Development of biodegradable composites using treated and compatibilized waste flour. *Compos Part A – Appl S* 2006; 37: 1231–1238.
- [77] Sena Neto AR, Araujo MAM, Souza FVD, Mattoso LHC, Marconcini JM. Characterization and comparative evaluation of thermal, structural, chemical, mechanical and morphological properties of six pineapple leaf fiber varieties for use in composites. *Ind Crop Prod* 2013; 43: 529– 537.
- [78] Faruka O, Bledzka AK, Finkb HP, Sain M. Biocomposites reinforced with natural fibers: 2000–2010. *Prog Polym Sci* 2012; 37: 1552– 1596.



- [79] Mwaikambo LY, Tucker N, Clark AJ. Mechanical properties of hemp fibre reinforced euphorbia composites. *Macromol Mater Eng* 2007; 292(9): 993–1000.
- [80] Ray D, Sarkar BK, Rana AK, Bose NR. Effect of alkali treated jute fibres on composite properties. *Bull Mater Sci* 2001; 24(2): 129–135.
- [81] Wang B, Panigrahi S, Tabil L, Crerar W. Pre-treatment of flax fibres for use in rotationally molded biocomposites. *J Reinf Plast Compos* 2007; 26(5): 447–463.
- [82] Huda MS, Drzal LT, Mohanty AK, Misra M. Effect of chemical modifications of the pineapple leaf fiber surfaces on the interfacial and mechanical properties of laminated biocomposites. *Compos Interface* 2008; 15: 169–191.
- [83] Salon MCB, Gerbaud G, Abdelmouleh M, Bruzzese C, Boufi S, Belgacem MN. Studies of interactions between silane coupling agents and cellulose fibers with liquid and solid-state NMR. *Magnet Reson Chem* 2007; 45: 473–483.
- [84] Arkles B, Steinmetz JR, Zazyczny J, Mehta P. Factors contributing to the stability of alkoxy silanes in aqueous solution. *J Adhes Sci Technol* 1992; 6: 193–206.
- [85] Xu Y, Kawata S, Hosoi K, Kawai T, Kuroda S. Thermomechanical properties of the silanized-kenaf/polystyrene composites. *Express Polym Lett* 2009; 3: 657–664.
- [86] Sapuan SM, Mohamed AR, Siregar JP, Ishak MR. Pineapple Leaf Fibers and PALF-Reinforced Polymer Composites. *Cellulose Fibers: Bio- and Nano-Polymer Composites* 2011: 325-343.
- [87] Mwaikambo LY. Review of the history, properties and application of plant fibres. *Afr J Sci Technol* 2006; 7: 120–133.
- [88] Ahmed OH, Husni MH, Anuar AR, Hanafi MM. Effect of residue management practice on yield and economic viability of Malaysian pineapple production. *J Sustain Agric* 2002; 20: 83–94.
- [89] Ahmed OH, Husni MH, Anuar AR, Hanafi MM. Towards sustainable use of potassium in pineapple waste. *Sci World J* 2004; 4: 1007–1013.
- [90] Goering HK, Van Soest PJ. (1970). *Forage Fiber Analyses (Apparatus, Reagents, Procedures, and Some Applications)*. Agric. Handbook No. 379. Washington, DC: U.S. Government Printing Office.



- [91] Prachyalak P, Puipanthavong P, Boonsriri J. The utilization of pineapple leaves for fattening cattle In: Animal Nutrition Division, Ministry of Agriculture and Cooperatives. Annual Research Report 1998, Bangkok, 1998, p. 49–61.
- [92] Van Soest PJ. Nutritional Ecology of The Ruminant. Portland: Durham & Downey Inc.; 1982.
- [93] Kellems RO, Wayman O, Nguyen AH, Nolan Jr JC, Campbell CM, Carpenter JR, et al. Post-harvest pineapple plant forage as a potential feedstuff for beef cattle: evaluated by laboratory analyses In Vitro and In Vivo digestibility and feedlot trials. *J Anim Sci* 1979; 48: 1040–1048.
- [94] Kengkhetkit N, Amornsakchai T. A new approach to “Greening” plastic composites using pineapple leaf waste for performance and cost effectiveness. *Mater Des* 2014; 55: 292–299.
- [95] Paul D, Bhattacharyya SK, Banik S, Basu MK, Mukherjee AB. Extracting pineapple leaf fibre. *Appropriate Technol* 1998; 24(4): 27.
- [96] Ghosh SK, Sinha MK. Assessing textile value of pineapple fibre. *Ind. Text. J.* 1977; 88: 111-115.
- [97] Sinha MK. A- review of processing technology for the utilization of agro-waste fibers. *Agricult Wastes* 1982; 4(6): 461-475.
- [98] Mohamed AR, Sapuan SM, Shahjahan M, Khalina A. Characterization of pineapple leaf fibers from selected Malaysian cultivars. *J Food Agric Environ* 2009; 7: 235–240.
- [99] Basu A, Chellamani KP, Kumar PR. Jute and pineapple leaf fibres for the manufacture of technical textiles. *Asian Text J* 2003; 12: 94–96.
- [100] Hayavadana J, Jacob M, Sampath G. Diversified product of pine apple leaf fibres. *Man Made Text India* 2003; 46: 301–305.
- [101] Kumar KBK, Prabhakaran G, Muruganandam R, Raghu P, Namasivayam N, Rajendran K, Durairaj V, Kannan G. Study on pineapple fiber processing. *Colourage* 1997; 44: 27–30.
- [102] Anon. A guide to unusual natural fibers: pineapple leaf fiber (PALF). *Textiles* 1992: 21; 21.



- [103] George J, Janardhan R, Anand JS, Bhagawan SS, Sabu T. Melt rheological behaviour of short pineapple fibre reinforced low density polyethylene composites. *Polymer* 1996; 37: 5421–5431.
- [104] Abu-Sharkh BF, Hamid H. Degradation study of date palm fibre/polypropylene composites in natural and artificial weathering: mechanical and thermal analysis. *Polym Degrad Stab* 2004; 85: 967–973.
- [105] Threepopnatkul P, Kaerkitcha N, Athipongarporn N. Effect of surface treatment on performance of pineapple leaf fiber-polycarbonate composites. *Compos B* 2009; 40: 628–632.
- [106] Bledzki AK, Mamun AA, Volk J. Barley husk and coconut shell reinforced polypropylene composites: the effect of fibre physical, chemical and surface properties. *Compos Sci Technol* 2010; 70: 840–846.
- [107] Luo S, Netravali AN. Mechanical and thermal properties of environment-friendly “green” composites made from pineapple leaf fibres and poly(hydroxybutyrate-co-valerate) resin. *Polym Compos* 1995; 57: 843–854.
- [108] Mukhopadhyay S, Srikanta R. Effect of ageing of sisal fibres on properties of sisal: polypropylene composites. *Polym Degrad Stab* 2008; 93: 2048–2051.
- [109] Antich P, Vazquez A, Mondragon I, Bernal C. Mechanical behavior of high impact polystyrene reinforced with short sisal fibers. *Compos A* 2006; 37: 139–150.
- [110] Kim SJ, Moon JB, Kim GH, Ha CS. Mechanical properties of polypropylene/natural fiber composites: Comparison of wood fiber and cotton fiber. *Polym Test* 2008; 27: 801–806.
- [111] Nair MKC, Thomas S, Groeninckx G. Thermal and dynamic mechanical analysis of polystyrene composites reinforced with short sisal fibres. *Compos Sci Technol* 2001; 61: 2519–2529.
- [112] George J, Bhagawan SS, Prabhakaran, Thomas S. Short pineapple-leaf-fibre-reinforced low-density polyethylene composites. *J Appl Polym Sci* 1995; 57: 843–854.
- [113] Threepopnatkul P, Kaerkitcha N, Athipongarporn N. Polycarbonate with pineapple leaf fiber to produce functional composites. *Adv Mater Res* 2008; 47–50: 674–677.



- [114] John MJ, Anandjiwala RD, Thomas S. Hybrid composites. In: Thomas S, Pothan LA (eds) Natural fiber reinforced polymer composites: macro to nanoscale. Old City, Philadelphia, pp 315-328.
- [115] Mishra S, Mohanty AK, Drzal LT, Misra M, Parija S, Nayak SK, Tripathy SS. Studies on mechanical performance of biofibre/glass reinforced polyester hybrid composites. *Compos Sci Technol* 2003; 63: 1377–1385.
- [116] Idicula M, Boudenne A, Umadevi L, Ibos L, Candau Y, Thomas S. Thermophysical properties of natural fibre reinforced polyester composites. *Compos Sci Technol* 2006; 66: 2719–2725.
- [117] Zhou Y, Fan M, Chen L, Zhuang J. Lignocellulosic fibre mediated rubber composites: An overview. *Compos B* 2015; 76: 180-191.
- [118] Bledzki AK, Reihmane S, Gassan J. Thermoplastics reinforced with wood fillers: a literature review. *Polym Plast Technol Eng* 1998; 37(4): 451-468.
- [119] Nekkaa S, Chebira F, Haddaoui N. Effect of fiber treatment on the mechanical and rheological properties of polypropylene/broom fiber *sparitium junceum* composites. *J Eng Appl Sci* 2006; 1(3): 278-283.
- [120] Espet A, Vilapana F, Karlsson S. Comparison of water absorption in natural cellulosic fibres from wood and one-year crops in polypropylene composites and its influence on their mechanical properties. *Compos Part A Appl S* 2004; 35(11): 1267-1276.
- [121] Kalapakdee A, Amornsakchai T. Mechanical properties of preferentially aligned short pineapple leaf fiber reinforced thermoplastic elastomer: Effects of fiber content and matrix orientation. *Polym Test* 2014; 37: 36–44.
- [122] Wisittanawat U, Thanawan S, Amornsakchai T. Mechanical properties of highly aligned short pineapple leaf fiber reinforced – Nitrile rubber composite: Effect of fiber content and Bonding Agent. *Polym Test* 2014; 35: 20–27.
- [123] Wisittanawat U, Thanawan S, Amornsakchai T. Remarkable improvement of failure strain of preferentially aligned short pineapple leaf fiber reinforced nitrile rubber composites with silica hybridization. *Polym Test* 2014; 38: 91-99.
- [124] KRATON™ Polymers Inc. (2012). KRATON® G1650 M Polymer. Retrieved from http://www.kraton.com/products/Kraton_G_SEBS_SEPS.php



- [125] Methacanon P, Weerawatsophon U, Sumransin N, Prahsarn C, Bergado DT. Properties and potential application of the selected natural fibers as limited life geotextiles. *Carbohydr Polym* 2010; 82: 1090–1096.
- [126] Shih YF, Huang CC, Chen PW. Biodegradable green composites reinforced by the fiber recycling from disposable chopsticks. *Mater Sci Eng A* 2010; 527: 1516–1521.
- [127] Attharangsarn S, Saikrasun S. Kinetic analysis of thermal and thermo-oxidative decomposition of recycled PE/PALF bio-based composites. *Int J Plast Technol* 2013; 17(1): 94-110.
- [128] Panaitescu MD, Vuluga Z, Ghiurea M, Iorga M, Nicolae C, Gabor R. Influence of compatibilizing system on morphology, thermal and mechanical properties of high flow polypropylene reinforced with short hemp fibers. *Composites: Part B* 2015; 69: 286–295.
- [129] Rezaei F, Yunus R, Ibrahim NA. Effect of fiber length on thermomechanical properties of short carbon fiber reinforced polypropylene composites. *Mater Des* 2009; 30: 260–263.
- [130] Harris B, Braddel O, Almond D, Lefebure C, Verbic J. Study of carbon fiber surface treatment by dynamic mechanical analysis. *J Mater Sci* 1993; 28: 3353–3366.
- [131] Cantero G, Arbelaiz A, Llano-Ponte R, Mondragon I. Effects of fiber treatment on wettability and mechanical behavior of flax/polypropylene composites. *Compos Sci Technol* 2003; 63: 1247–1254.



Appendices



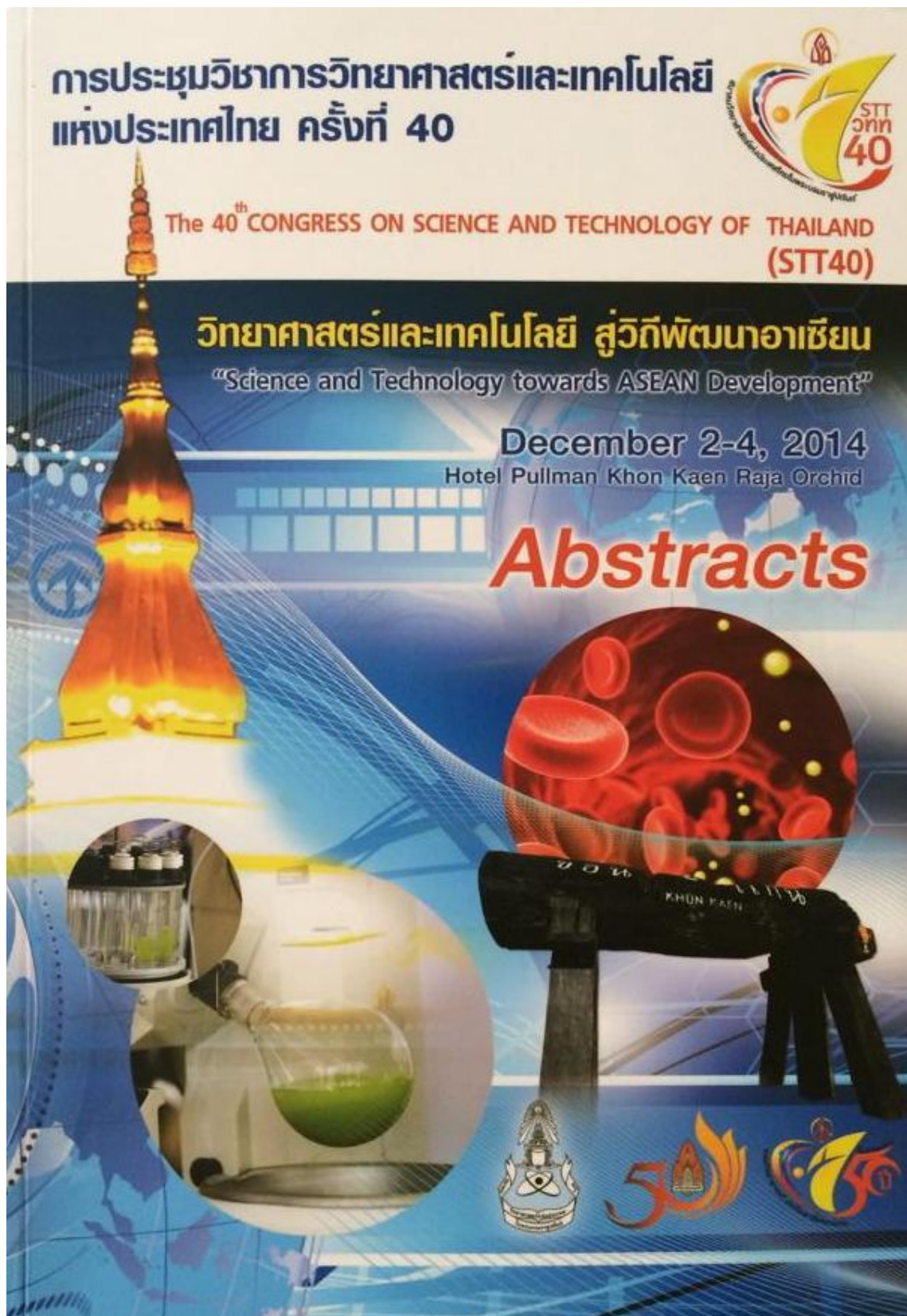
Appendix
Supporting paper



Table A1 Comparison of secant modulus at 1% strain for neat SEBS and the composites in longitudinal (LD) and transverse (TD) direction.

Sample	Secant Modulus		S.D.	
	LD	TD	LD	TD
SEBS	139	82	28	12
PF10	115	158	38	13
PF20	131	190	33	41
PF10-MA3	179	-	8	-
PF10-MA5	178	184	47	63
PF10-MA7	235	-	43	-
APF10	199	110	35	9
APF10-MA3	173	-	51	-
APF10-MA5	210	73	48	17
APF10-MA7	209	-	47	-
SPF10	271	58	38	7
SPF10-MA3	243	-	21	-
SPF10-MA5	261	58	63	13
SPF10-MA7	223	-	21	-
ASPF10	143	55	48	11
ASPF10-MA5	136	64	15	3





D_D0018: TENSILE AND DYNAMIC MECHANICAL PROPERTIES OF MODIFIED PINEAPPLE LEAF FIBER/STYRENIC BASED THERMOPLASTIC ELASTOMER COMPOSITES

Darawan Yuakkul,¹ Taweechai Amornsakchai,² Sunan Saikrasun^{1,*}

¹Creative Chemistry and Innovation Research Unit, Department of Chemistry and Center of Excellence for Innovation in Chemistry, Faculty of Science, Maharakham University, Maha Sarakham 44150, Thailand

²Center for Alternative Energy, Department of Chemistry and Center of Excellence for Innovation in Chemistry, Faculty of Science, Mahidol University, Nakhon Pathom 73170, Thailand

*e-mail: sunan.s@msu.ac.th

Abstract: In this work, pineapple leaf fibers (PALFs) were chemically treated by alkaline solution and a silane coupling agent (triethoxy vinyl silane). The elastomeric composite based on styrene-(ethylene butylene)-styrene (SEBS) triblock copolymer and PALFs with and without the presence of maleic anhydride grafted SEBS (SEBS-g-MA) were prepared using melt mixing on a two-roll mill and compression molding. Thermal decomposition, tensile and dynamic mechanical properties of the neat matrix and its composites were evaluated. Among the treated and untreated fibers, the alkali-treated fiber, exhibited the

138

© The 40th Congress on Science and Technology of Thailand (STT40)

highest thermal stability in air. For the composites, the highest thermal stability was observed for the composite containing alkali-treated fibers. The enhancement in mechanical performance of the elastomer matrix was achieved by PALF loadings. The further improvement in tensile stress, over those of SEBS matrix and untreated-fiber composite, was observed for composites containing alkali- and silane-treated fibers. Interestingly, the use of the treated fibers along with SEBS-g-MA compatibilizer remarkably improved the reinforcing performance of the composites as revealed by very high maximum stress ratio (up to ≈ 3.25 - 3.30). The compatibilized composite of alkali -treated fiber showed better reinforcing performance than that of the silane-treated fiber. The dynamic mechanical results related well with the tensile data. The obtained results indicated that both fiber treatments and compatibilizing promotion are mainly necessary factors for elevation of the material reinforcing performance. (abstract only)





**โครงการนำเสนอผลงานของนิสิตชั้นปีที่ 4
และวิทยานิพนธ์ระดับบัณฑิตศึกษา ครั้งที่ 14 ประจำปี 2557
ในวันที่ 8 พฤษภาคม 2558 ณ ห้อง SC1-200**



**คณะวิทยาศาสตร์ มหาวิทยาลัยมหาสารคาม
ปีการศึกษา 2557**



โครงการนำเสนอผลงานของนิสิตชั้นปีที่ 4 และวิทยานิพนธ์นิสิตระดับบัณฑิตศึกษา ครั้งที่ 14 วันที่ 8 พฤษภาคม 2558

P - 19

- ชื่อเรื่อง : สมบัติการทนต่อแรงดึงและสมบัติเชิงกลพลวัตของวัสดุเชิงประกอบเทอร์โมพลาสติกแบบหยุ่นประเภทไฮโดรเจลที่เติมเส้นใยจากใบสับประรดที่ผ่านการตัดแปรเชิงเคมี
- : Tensile and dynamic mechanical properties of modified pineapple leaf fiber/styrenic based thermoplastic elastomer composites
- ผู้นำเสนอ : น.ส.ศารารวรรณ หยกกุล นิสิตหลักสูตร วท.ม. เคมี
- อาจารย์ที่ปรึกษา : รศ.ดร.สุนันท์ สายกระสุน
- ที่ทำงาน : ภาควิชาเคมี คณะวิทยาศาสตร์ มหาวิทยาลัยมหาสารคาม

บทคัดย่อ

ในงานวิจัยนี้ได้ทำการตัดแปรผิวเส้นใยจากใบสับประรด (PALFs) ด้วยวิธีอัลคาไลและสารคัพปลิงซิลิโคน (triethoxy vinyl silane) และนำเส้นใยไปใช้เสริมแรงในวัสดุเชิงประกอบแบบหยุ่น สไตรีน-(เอทิลีน-บิวทิลีน)-สไตรีน (SEBS) ที่เติมและไม่เติมสารเสริมสภาพเข้ากันได้ SEBS-g-MA ทำการเตรียมวัสดุโดยผสมในเครื่อง internal mixer two-roll mill และ compression molding จากนั้นนำไปวิเคราะห์สมบัติการทนต่อแรงดึงและสมบัติเชิงกลพลวัต พบว่า ค่าการความทนต่อแรงดึงของวัสดุเชิงประกอบที่เติมเส้นใยที่ตัดแปรผิวด้วยวิธีอัลคาไลและสารคัพปลิงซิลิโคนมีค่าสูงกว่า SEBS และวัสดุเชิงประกอบที่มีเส้นใยที่ไม่ผ่านการตัดแปรผิวเส้นใย การใช้เส้นใยที่ผ่านการตัดแปรผิวและใช้สารเสริมสภาพเข้ากันได้ SEBS-g-MA ร่วมกันจะช่วยเพิ่มประสิทธิภาพการเสริมแรงของวัสดุเชิงประกอบได้มากขึ้น การเติมสารเสริมสภาพเข้ากันได้ในวัสดุเชิงประกอบที่มีเส้นใยที่แปรผิวด้วยวิธีอัลคาไลให้ประสิทธิภาพการเสริมแรงดีกว่าเส้นใยที่แปรผิวด้วยสารคัพปลิงซิลิโคน

Abstract

In this work, pineapple leaf fibers (PALFs) were chemically treated by alkaline solution and a silane coupling agent (triethoxy vinyl silane). The elastomeric composite based on styrene-ethylene butylene-styrene (SEBS) triblock copolymer and PALFs with and without the presence of maleic anhydride grafted SEBS (SEBS-g-MA) were prepared using melt mixing in an internal mixer, melt blending on a two-roll mill and compression molding. Tensile and dynamic mechanical properties of the neat matrix and its composites were evaluated. The improvement in tensile stress, over those of SEBS matrix and untreated-fiber composite, was observed for composites containing alkali- and silane-treated fibers. The use of the treated fibers along with SEBS-g-MA compatibilizer remarkably improved the reinforcing performance of the composites. The compatibilized composite of alkali-treated fiber showed better reinforcing performance than that of the silane-treated fiber.

References

- Charangsan S., Saikrasun S. (2013) Kinetic analysis of thermal and thermo-oxidative decomposition of recycled PE/PALF bio-based composites. *Int J Plast Technol.* 17(1): 94-110.
- Ngkhetkit N, Amornsakchai T. (2014) A new approach to "Greening" plastic composites using pineapple leaf waste for performance and cost effectiveness. *Mater. Des.* 55: 292-299.





Biography



Biography

Name Miss Darawan Yuakkul

Date of birth July 20, 1991

Place of birth Udonthani, Thailand

Institution attended

2012 Bachelor of Science degree in Chemistry Maharakham University

2016 Master of Science degree in Chemistry Maharakham University

Position and Work Place

Maharakham University

Contact address

174 Moo. 5, Tambon Somyiam, Amphoe Namsom, Udonthani, 41210

